AN ANALYSIS OF PROPOSED MITOTIC DEFECTS IN THE *TOYS ARE US* MUTANT AND *DROSOPHILA* HYBRIDS

A Dissertation

Presented to the Faculty of the Graduate School

of Cornell University

in Partial Fulfillment of the Requirements for the Degree of

Doctor of Philosophy

By

Bonnie Jean Bolkan

January 2008

AN ANALYSIS OF PROPOSED MITOTIC DEFECTS IN THE *TOYS ARE US* MUTANT AND *DROSOPHILA* HYBRIDS

Bonnie Jean Bolkan, Ph.D.

Cornell University 2008

Animals homozygous for mutations in the *toys are us* (*trus*) gene are developmentally stunted and third instar lethal. The phenotype was initially proposed to stem from a mitotic defect, but has since been associated with a defect in the ecdysone pathway. In addition *trus*^{1} mutants lack optic lobes, have malformed imaginal discs, and are often missing the imaginal cells of the salivary glands, all of which are known hallmarks of ecdysone deficient mutants.

Trus is primarily expressed in the prothoracic cells of the ring gland, which is the main location of ecdysone synthesis. To test if Trus might play a role in ecdysone synthesis, I fed larvae 20HE precursors, all of which are able to overcome the developmental delay. I have tested the effects of the *trus*^{1} mutant on expression levels of ecdysone pathway genes by constructing double mutants with *trus*^{1} and members of the ecdysone pathway.

Recent results of TAP-tagging experiments indicate that Trus is in a tight complex with the products of the *string of pearls* gene, which is the S2 subunit of the small ribosomal subunit, and Elongation Factor 1-α. My findings are consistent with a model that Trus acts downstream of PTTH but upstream of the *ecdysoneless* gene to promote the translation in the ring gland of mRNAs for genes in the ecdysone pathway.

Matings between *D. melanogaster* females and males of sibling species in the *D. melanogaster* complex yield males that are also developmentally devalyed and die at a stage similar to the *trus*^{1} mutation (prior to pupal differentiation). I have re-examined a previous report suggesting that the developmental defects in hybrid males may be the consequence of problems in mitotic chromosome condensation. I found in contrast that the frequencies of mitotic figures, as well as cells in S phase in the brains of hybrid male larvae are extremely low. The cells in hybrid male brains appear to be particularly sensitive to environmental stress; my results indicate that certain in vitro incubation conditions induce widespread cellular necrosis in these brains, causing an abnormal nuclear morphology noticed by previous investigators.

BIOGRAPHICAL SKETCH

Bonnie Jean Bolkan started "life" as a ball of undifferentiated cells. After rounds of mitosis, cell differentiation, and growth she entered the world showing her sense of humor, self-determination, and spunk from the moment she decided to be born in 1979. To this day she claims that she chose to be nearly a month premature because the night before her brother claimed, "…at least she won't be an April Fool's baby…" In actuality being an April Fool sounded good to her and really, who can pass up making a liar out of their older brother?

In 1997 she graduated as valedictorian from Hilo High School in Hilo, Hawaii. She then attended Willamette University in Salem, Oregon where she received a BS in biology. During the summers she returned home and worked as a teacher and tutor for the Upward Bound Program as well as spending a summer doing research on Hawaiian "Picture Wing" *Drosophila* in the lab of Dr. Donald Price at the University of Hawaii at Hilo. During her semester abroad she attended the University of Oulu in Northern Finland and completed her senior research project on chromosomal inversions between isolated populations of *Drosophila virilis,* in the laboratory of Dr. Janna Liimatainen.

In 2001 she entered the Genetics and Development PhD program at Cornell University where she joined the lab of Dr. Michael Goldberg, and completed the research described in this thesis.

ACKNOWLEDGEMENTS

A Ph.D. is not a solitary achievement and I have received support from many that deserve my thanks and acknowledgement.

I would first like to thank my advisor, Dr. Michael Goldberg, for advice, financial support, and allowing me to follow where my projects took me, even though it was outside the scope of the lab. Mike is also a talented scientific writer and his comments have greatly helped me in my writing.

I would also like to acknowledge my committee members. I collaborated with Dr. Daniel Barbash on the hybrid incompatibility project that composes chapter 3 of this thesis. His scientific expertise and enthusiasm for the research and results were instrumental to that project and a great advantage to me.

My additional committee members: Dr. Anthony Bretscher and Dr. Timothy Huffaker provided me with valuable advice both during and outside of committee meetings though out my Ph.D. career. I greatly appreciated Dr. David Lin and Dr. Kathleen Whitlock who served as special committee members for my A-exam. Dr. Whitlock and Dr. John Ewer also deserve a big thanks for their assistance in finding protocols, reagents, and understanding when my project took me outside the scope of our lab. I also thank them both deeply for their friendship.

I believe that those who provided me with emotional support to be as important to my success as a graduate student as those who provided the intellectual support. First and foremost I thank my parents whom have always supported and believed in me. To my brother Raymond who often called to remind me that, “there is more to life than maggot brains,” such as sci-fi TV.

and books. And to all of the other family members who have expressed their support of my endeavors, thank you.

I also thank Maegan Harden, who wonderfully filled the roles of friend, coffee buddy, intellectual sounding board, fellow cake decorator, collaborator on PDCD2, and even purveyor of roommate. To said roommate and friend, Karen Hoffman, I will always value your friendship. I thank Wendy Hoose who provided me with much needed help on ecdysis, a host random fly techniques, and friendship. I would also like to thank all of my other friends and lab mates whom if I listed their assistance would take up too many pages of this thesis: Jackie Creque, Casey Jager, Jin Li, Jym Ochbina, Karla Stucker, Christopher Wolyniak, Byron Williams, Erika Williams, Jiangtao Yu, Adam Zahand, and Yong Zhao. And also, much thanks to my canine friends: Lily D' Dog, Murphy, and Swifty Brown, who provided hours of fun, exercise, and doggie kisses.

The extensive support staff of the Biotech Building and MBG department also deserve acknowledgement as they filled the roles of custodian, glassware washer, fly food maker (and cleaner of dirty fly vials), filer of paperwork, building care manager, and the multiple others behind the scenes. Kevin Tadock and Mick LoPinto deserve an extensive thank you in the role of "computer guys" with my multiple computer "mishaps", and for rescuing the completed figures of this thesis from a "dead" computer.

Finally I would like to thank the sources that funded me and my research; NIH training grant (Issued to the field of Genetics and Development, Cornell University), NIH grant,# 5R01GM048430-14 (Issued to Michael Goldberg) and The Cornell Graduate School Travel Grant.

Dedicated to those who believed…

TABLE OF CONTENTS

BIOGRAPHICAL SKETCH……iii

ACKNOWLEDGEMENTS……iv

DEDICATION……..…vi

TABLE OF CONTENTS……vii

LIST OF FIGURES……..…xii

LIST OF TABLES……..xvi

LIST OF ABBREVIATIONS……xvii

CHAPTER 1: INTRODUCTION……..……1

I. Review of *Drosophila* development, mitosis, and classical mitotic mutants……..1

Developmental stages of *Drosophila melanogaster*……...1

Mitosis……3

Drosophila and mitosis……4

II. *Toys are us* and ecdysone signaling……6

Ecdysone signaling……..6

Physical and developmental cues to trigger ecdysone synthesis……6

Synthesis of ecdysone……7

Ecdysone early response……11

Secondary ecdysone responses: tissue competence and late ecdysone gene regulation……..…13

Phenotype of mutants in the ecdysone pathway……14

III. Hybrid incompatibility in *Drosophila* ……15

Hybrids in the *Drosophila melanogaster* clade……16

Genetic basis of *Drosophila* hybrid incompatibility……...19

Mitotic defect proposed as a cause of hybrid lethality……20

IV. Organization of thesis……22

LITERATURE CITED……..……25

CHAPTER 2:TOYS ARE US: A NOVEL PROTEIN INVOLVED IN ECDYSONE SIGNALING……31

INTRODUCTION……31

MATERIALS AND METHODS……32

Flies……..32

Mapping of the *trus*^{1} mutation……..33

Transgenic rescue of the *trus*^{1} mutation ……33

Antibody production and purification……..36

Cytology……..37

Western Blots……..38

Purification of protein complexes containing Trus……39

Ecdysone feeding……..39

Sucrose gradient fractionation of S2 cell extracts……40

RESULTS……40

Identification of the *trus* gene as CG5333……40

Trus is expressed cytoplasmically in relevant ecdysis tissues……43

Defective proliferation of *trus*^{1} neuroblasts……43

Defects in some *trus*^{1} mutant salivary glands……46

Trus mutants exhibit developmental delay and arrest……50

Heterozygotes for *trus*^{1} are partially temperature-sensitive for eclosion……..50

The larval lethality of *trus*^{1} mutants can be rescued by an ecdysone-enriched diet ……...55

Second-site noncomplementation of *trus*^{1} with mutations in known ecdysone pathway genes……58

Expression levels of proteins up-regulated by ecdysone are low in *trus*^{1} mutants……58

Trus forms one or more complexes with String of Pearls and perhaps with Elongation Factor 1 alpha……61

Trus fails to co-sediment with ribosomes or polysomes……..63

The mouse homologue of *trus,* (*pdcd2l*) is expressed in discrete areas of the brain in developing embryos……66

DISCUSSION……69

LITERATURE CITED……72

CHAPTER 3: DEVELOPMENTAL AND CELL CYCLE PROGRESSION DEFFECTS IN *DROSOPHILA* HYBRID MALES……..75

ABSTRACT……75

INTRODUCTION……75

MATERIALS AND METHODS……77

Fly strains and cultures……77

Cytology for Analysis of Mitosis ……..78

Determination of S Phase using Bromodeoxyuridine ……79

Cell Death Assays ……79

Ecdysone Feeding ……80

Larval staging and brain-size estimation……81

RESULTS……81

Developmental Delays in Hybrid Males ……81

Defects in Ecdysone-Induced Behavior ……88

Low Mitotic Frequencies in Hybrid Male Larvae ……..……96

DISCUSSION……...104

ACKNOWLEDGEMENTS……..107

LITERATURE CITED……..108

CHAPTER 4: CONCLUSIONS AND FUTURE DIRECTIONS……..……111

I. TOYS ARE US (TRUS) AND ECDYSONE SYNTHESIS…..……..111

A model for ecdysis including a potential role for Trus……..111

Trus, Ecdysone and PTTH titers……...115

trus[1] as a possible tool in studying the ecdysone pathway…...116

Ring gland-specific rescue……116

Insights into the function of Trus through interactors.……117

Studying Trus homologs in mammals……..119

II. HYBRID INCOMPATIBILITY……120

Mitotic defects in hybrid females and rescued hybrid males…120

Chromosome condensation defects as a potential explanation for hybrid incompatibility……121

Exploring hybrid incompatibility through interactors of Hmr and Lhr……..122

Determination of timing of the cell cycle arrest……..……122

When do the proliferation defects begin? ……...123

Greater implications of hybrid incompatibility in *Drosophila*.…123

LITERATURE CITED……..124

APPENDIX 1: THE *DROSOPHILA* LKB1 KINASE IS REQUIRED FOR SPINDLE FORMATION AND ASSYMETRIC

NEUROBLAST DIVISION……..127
ABSTRACT……...127
INTRODUCTION……..128
MATERIALS AND METHODS……...130
Fly strains and genetic manipulations……..130
Antibodies and immunoblotting……130
Cytology……131
RESULTS……132
Isolation and characterization of mutations in the *dlkb1* gene……..132
Mutations in the *dlkb1* gene affect spindle formation……133
dlkb1 mutations disrupt the asymmetry of NB division leading to a reduction in NB size……..138
dlkb1 mutations affect Mira and Baz/Par-6/DaPKC but not Pins/Gαi localization in dividing Nbs……145
Dlkb1 and Pins function in different pathway controlling NB division ……153
DISCUSSION……...163
Dlkb1 controls the stability of spindle Mts……163
Dlkb1 controls the asymmetry of NB division……..165
Dlkb1 is not required for NB spindle rotation……..168
Conclusions and perspectives……...169
ACKNOWLEDGEMENTS……..170
LITERATURE CITED……..171

APPENDIX 2:CHARACTERIZATION OF SIX CELL CYCLE MUTATIONS IN *DROSOPHILA*……175
INTRODUCTION……175

Drosophila and mitosis……176

MATERIALS AND METHODS……...177

Wild Type Flies……..…..177

Cytology of brains for analysis of mitosis……179

RNAi……..180

Cytology for analysis of Kc cells and RNAi…….180

RESULTS AND DISCUSSION……..181

The B38 mutant phenotype is caused by mutations in the *Drosophila* homologue of *cell division cycle 6 (dcdc6)* ……..181

The MA41 mitotic phenotype is likely caused by a mutation in *DNA polymerase-delta*……..188

The M374 mutation causes high levels of polyploidy…..……..192

MA9 mutants have small fragile brains with very few cells in mitosis ……..195

Mit1174 and M370x are likely alleles of Polo kinase…….198

CONCLUSION…….198

LITERATURE CITED……..199

LIST OF FIGURES

Figure 1.1 Synthesis of Ecdysone.....9

Figure 1.2 Evolution of *Drosophila*, *Hmr* and the results.....17

Figure 1.3 Hybrid male mitotic phenotype as previously described.....21

Figure 2.1 Identification of CG5333 as the gene responsible for the *trus* phenotype.....34

Figure 2.2 Expression of the Trus protein.....44

Figure 2.3 *trus* larvae fail to develop and divide neuroblasts properly.....47

Figure 2.4 Development of imaginal ring cells of the salivary glands.....49

Figure 2.5 Rate of development in *trus* mutants is delayed.....51

Figure 2.6 *trus*^{1} mutants spend an extended period as third instar larvae.....53

Figure 2.7 Expression of EcR and BrC is significantly decreased in *trus* mutants. 60

Figure 2.8 Tap tagging reveals stable binding of Trus with Sop and Ef1-α.....62

Figure 2.9 Sucrose gradients show Trus does not associate with intact ribosomes.....64

Figure 2.10 Mouse Trus (PDCD2L) localizes to specific regions of the brain in 8.5e and 10.5e embryos.....67

Figure 3.1. Developmental progress of hybrid males.....85

Figure 3.2. Progress of mitosis based on age of the larvae.....91

Figure 3.3. Chromosome morphology in hybrid brains.....92

Figure 3.4 Hybrid male larval brains lack cells in S phase.....95

Figure 3.5 Cells with aberrant nuclear morphology seen in the cultured brains of hybrid males are not in mitosis.....97

Figure 3.6 Cell death is increased in 0.7% NaCl cultured third instar hybrid male brains.....101

Figure 3.7 Naturally forming melanotic tumors from third instar hybrid males.....103

Figure 4.1 Model for Ecdysis including Trus 113

Figure 4.2 Cross scheme for ring gland specific rescue.....118

Figure A1.1. Mutations in the *dlkb1* gene disrupt spindle organization of both NBs and GMCs.....134

Figure A1.2. Mutations in *pins* affect aster formation without altering the density of spindle MTs.....140

Figure A1.3. Mutations in *dlkb1* disrupt unequal cytokinesis and reduce the average size of NB population within mutant brains.....142

Figure A1.4. Mutations in the *dlkb1* gene affect centrosome size during NB division.....146

Figure A1.5. Mutations in the *dlkb1* gene affect Mira localization at the NB basal pole 148

Figure A1.6. Mutations in the *dlkb1* gene disrupt Baz/Par-6/DaPKC but not Pins/Gαi localization at the NB apical pole.....151

Figure A1.7. Mud localization in wild type and *dlkb1* mutant NBs. Cells were stained for Mud, tubulin (Tub) and DNA (blue). 154

Figure A1.8. Expression and intracellular localization of the Dlkb1 kinase. 157

Figure A1.9. *dlkb1* and *pins* function in different pathways controlling the stability of spindle MTs.....160

Figure A2.1 Phenotype of wild type brains.....178

Figure A2.2 B38 map and mitotic phenotype.....182

Figure A2.3 Homologs of *cdc6* and the structure of the mutation.....184

Figure A2.4 *cdc6* RNAi causes under-condensation in Kc cells.....187

Figure A2.5 MA41 map and mitotic phenotype.....190

Figure A2.6 M374 map and mitotic phenotype.....194

Figure A2.7 MA9 map and mitotic phenotype.....197

LIST OF TABLES

Table 2.1 Eclosion phenotypes at 25˚C and 30˚C.....54

Table 2.2 Percentage eclosion based on sterol additions to media.....57

Table 2.3 Double heterozygote phenotype with *trus*.....59

Table 3.1. Days post egg deposition taken to reach indicated stage of development.....83

Table 3.2. Lethality during indicated developmental stage.....84

Table 3.3. Brain sizes.....87

Table 3.4. Percentage of mitotic figures in pure species and hybrid third instar larvae.....89

Table 3.5 Mitotic indices of larval brain cells before and after colchicine treatment.....93

Table 3.6 Percentage of aberrant cells in larval brains.....98

Table A1.1 Mitotic parameters in larval brains from *dlkb1* mutants.....137

LIST OF ABBREVIATIONS

-	Deficient
˚C	degrees Celsius
+	wild type
*µ*g	micrograms
20HE	20-Hydroxyecdysone
7dC	7,7-dehydrocholesterol
ABB	annexin binding buffer
AMP	adenosine monophosphate
AMPK	AMP-activated kinase
asl	asterless
Baz	Bazooka
B-ftz	*beta-fushi tarazu*
BrC	Broad complex
BrDU	5-bromo-2-deoxyuridine
cAMP	cyclic AMP
cdc #	cell division cycle protein number __
cDNA	complimentary DNA
Cnn	Centrisomin
Cy	*Curly* (dominant marker on the 2nd chromosome)
Cy	Cyano (Fluorocene used in Cy2 and Cy3 conjugated antibodies)
D. mel	*Drosophila melanogaster*
D. sim	*Drosophila simulans*
DAPI	4',6-Diamidino-2-Phenylindole (double stranded DNA staining)
DaPKC	Drosophila atypical protein kinase C
Df	Deficiency
dlkb1	Drosophila lkb1
DNA	Deoxyribose nucleic acid
DNApol-δ	DNA polymerase-delta
Dpn	Deadpan
E74	Ecdysone-induced protein 74
E75	Ecdysone-induced protein 75
ecd	*ecdysoneless*
ECL	Enhanced chemiluminescence (HRP Western blot detection Solution)
EcR	Ecdysone Receptor
EF-1a	Elongation Factor 1 alpha
EMS	Ethyl methanesulfonate
F1	First generation descendants

FITC	Fluorescein Isothiocyanate
FM7i	X-Chromosome balancer
FucTA	Fucosylation Protein TA
g	grams
G1	Gap 1 stage of the cell cycle
G2	Gap 2 stage
Gαi	subunit αi of the G protein
GAL4	galactose-induced protein 4
GFP	Green Fluorescent Protein
gmc	ganglion mother cell
hmr	*hybrid male rescue*
HP1	Heterochromatic protein 1
hr	hour
Hu	*Humeral* (Dominant marker on the 3rd chromosome)
IgG	Immunoglobulin G
Insc	Inscuteable
IPTG	isopropyl-beta-D-thiogalactopyranoside
Kb	kilobases
Kc	Embryonically derived *Drosophila* cell culture line
kD	kilodalton
l	lethal
LB	Lutrient Broth (1% w/v Bactotryptone, 0.5%w/v yeast, 0.17M NaCl)
LC	loading control
lhr	*lethal hybrid rescue*
M	molar
MALDI	matrix assisted laser adsorption ionization
MARK	Microtubule affinity regulating kinase
MCM	mini chromosome maintenance
MI	Mitotic Indices
Mira	Miranda
ml	milliliters
mM	millimolar
mRNAs	messenger RNA
MTs	microtubules
Mud	Mushroom body defect
MYB	myeloblastosis
NaCl	Sodium Chloride
NBs	neuroblasts
NTAP	(see Tap) with tag on N-terminus of protein
ORC	Origin recognition complex
PAGE	PolyAcrylamide Gel Electrophoresis

PBS	Phosphate Buffered Saline
PBT	PBS + 1% Triton X
PBX	PBS + 3% Triton X
PDCD2	Putative Domain Cell Death 2
PDCD2L	Putative Domain Cell Death 2 Like
Pfk	Phosphofructo Kinase
PH3	Phosphohistone H3
pins	*partner of inscuteable*
Pon	Partner of Numb
Pros	Prospero
PTTH	Prothoracicotrophic hormone
RNA	Ribonucleic acid
RNAi	RNA interference
Rps6	Ribosomal protein subunit 6
RXR	Retinoic acid receptor
S	DNA Synthesis stage of the cell cycle
S6	Subunit 6
SDS	sodium dodecyl sulfate
Ser	Serine
sgs3	*salivary gland secretion 3*
Sop	String of pearls
TAP	Tandem Affinity Purification
Tb	*Tubby* (Dominant marker on the 3rd chromosome)
TBS	Tris Buffed Saline (20mM Tris-HCl, 137mM NaCl)
TBST	TBS + 0.02% Tween 20
TCA	Trichloroacetic acid
TM6B	3rd Chromosome *Drosophila* balancer
TRITC	Tetrarhodamineisothiocyanate
trus	*toys are us*
Tub	Tubulin
USP	Ultraspirical
v	*vermilion*
w	*white*
w/v	weight to volume
wt	wild type
X	fold (increase or decrease)
Y	Y chromosome
y	*yellow*
Zfrp8	Zinc finger protein RP-8

CHAPTER 1

INTRODUCTION

I. Review of *Drosophila* development, mitosis, and classical mitotic mutants
II. Ecdysone signaling
III. Hybrid incompatibility in the *Drosophila melanogaster* clade
IV. Organization of thesis

I. Review of *Drosophila* development, mitosis, and classical mitotic mutants

Development of all multi-cellular eukaryotic organisms requires a complex and regulated series of events controlling cell differentiation, shape, movement, and division. Scientists often focus their studies on these topics by obtaining mutations in a gene encoding a particular protein product that controls the division or development of a single cell type.

Developmental stages of *Drosophila melanogaster*

Development of *Drosophila melanogaster* embryos begins when oocytes are fertilized internally in the female, and then laid immediately thereafter. During their 26 hours as embryos, the organisms undergo multiple rounds of replication and cell differentiation. After hatching, larvae undergo additional rounds of replication, cell differentiation and growth to prepare to undergo metamorphosis after the third instar larval molt.

In order for *Drosophila* to enter successive stages of development, they must complete essential tasks at each stage, including achieving a minimum

size and weight, and producing certain tissues needed for the next stage of development (Demerec, 1950). After these tasks have been completed, Prothoracicotrophic hormone (PTTH) is synthesized, which triggers a protein cascade allowing the synthesis of ecdysone, which then triggers the molt to the next stage of development. The transition of embryos into first instar larvae by hatching is still considered a molt because of its dependence on ecdysone.

After hatching, the first instar larva begins to feed, allowing the larval tissues and the imaginal tissues (those that will subsequently metamorphose into adult tissues) to increase in size and further differentiate. Although cells in tissues such as the salivary glands are all the same size at the beginning of the first instar they show characteristic size and shape differentiation by second instar. During the second instar stage the larva continues to feed and grow. The imaginal discs also continue to grow, differentiate, and begin to move and evaginate themselves into tissue shapes that will aid in them becoming adult structures.

The beginning of the third instar stage is similar to the earlier two larval stages, with a continuation of feeding and growth. However, at 24 hours post molt a small ecdysone peak is produced, which commits the animal to undergo the molt to pupariation (Richards, 1981; Riddiford, 1993). After this peak the larvae stop feeding and enter the wandering stage, during which they undergo the physical and chemical changes need to pupariate and undergo metamorphosis.

At approximately 96 hours post hatching the larvae will pupariate (Demerec, 1950). During this 4-hour stage the larvae become immobile and form a pupal case that tans and hardens. A small ecdysone peak at 100

hours post hatch allows the puparia to undergo the prepupal molt to become pupae. During pupation the larval tissues are broken down by apoptosis or rearranged to form adult tissues. The imaginal discs and other imaginal tissues also now begin to quickly differentiate, move, divide, and develop into adult structures. By 192 hours the pupa is ready for a final ecdysone pulse that will allow it to eclose (emerge) as an adult fly a few hours later.

Mitosis

Cell division is an essential, highly regulated process that in multicellular organisms allows cell numbers to increase, providing the raw material for differentiation. The cell cycle is usually described as containing four stages: G1 (gap 1 phase), S (DNA synthesis), G2 (gap 2), and M (mitosis). In total, the cell cycle allows the DNA replicated during S phase as well as other cellular components within the parental cell to become equally divided among the two daughter cells that are produced at the end of mitosis. The three stages prior to mitosis (G1, S, and G2) are often grouped together under the term interphase when discussing mitosis.

Mitosis itself can be subdivided into more specific stages. Cells exit interphase and first enter **prometaphase**, which is characterized by nuclear envelope breakdown, condensation of the chromosomes and the attachment of microtubules to the kinetochores of the chromatids (the two newly replicated copies of each chromosome). Of interest later to this thesis, prometaphase is also the time at which histone H3 is phosphorylated at serine 10 by aurora A kinase (Prigent and Giet, 2003). The phosphorylation state of Ser10 also regulates proper condensation of chromatin in during the cell cycle (Prigent and Dimitrov, 2003). **Metaphase** is considered to have begun when the

chromosomes align along the metaphase plate due to the attachment of sister kinetochores to spindle microtubules emanating from opposite poles. A checkpoint exists which monitors the tension arising from these bioriented attachments, so as to hold a cell in metaphase until the kinetochores of all chromatids are properly connected to the spindle, ensuring that all chromosomes are aligned properly and kinetochore microtubules have a proper amount of tension. During **anaphase**, the sister chromatids separate and move along the kinetochore microtubules to opposite poles of the cell. When the chromatids are fully separated, the cell enters **telophase**. The nuclear envelopes are reformed during this stage, while the chromosomes decondense. The two daughter cells are physically separated during **cytokinesis**, which occurs by the formation of a cleavage furrow at a position between the asters of the daughter cells. With mitosis complete the cells then re-enter interphase. The length of time spent in interphase depends on the cell type and developmental stage of the organism, but it can range from a couple of minutes as is the case in the rapid divisions of *Drosophila* embryogenesis (Foe and Alberts, 1983), or alternatively, the cell may in some extreme cases remain quiescent for the rest of the life of the organism.

Drosophila and mitosis

Drosophila is an ideal model organism for studying mitosis because mutants in genes encoding proteins important for many aspects of mitosis die at characteristic stages, allowing cell division to be observed at high cytological resolution. By comparing mitosis and the development of tissues containing these cells in mutants and wild type flies, the role of individual proteins can be elucidated.

Drosophila melanogaster mitotic mutants characteristically die at one of two developmental stages, although there are some exceptions. Several rounds of syncytial mitoses occur in early embryos immediately after fertilization. Since these mitoses are extremely rapid and occur before the zygotic genome is transcribed, they depend on maternally supplied mRNAs and proteins. Mutations in such mitotic genes will therefore act as maternal effect lethal mutations: mothers homozygous for the mutations will produce embryos that die soon after fertilization (Foe, 1989). Since the maternal stores of many proteins are sufficient to allow develop to the third instar larval stage, zygotes homozygous for mutants in the corresponding genes will develop to this stage, but will then die as third instar larvae or during the larval-to-pupal transition (Baker et al., 1982). These larval lethal mutants show defects in the three tissue types mitotically active in larvae: the imaginal discs, the abdominal histoblasts and the neuroblasts (Gatti and Goldberg, 1991). Cytologically, the most advantageous tissue in which to view these defects is the larval brain. Neuroblasts in various mutants can show a wide variety of mitotic abnormalities, including an increase or decrease in the mitotic index, unusual patterns in chromosome condensation, and aneuploidy or polyploidy (Gatti and Goldberg, 1991).

Hypomorphic mutations that are less severe or mutations in genes that are less essential for mitosis can result in the sterility of homozygous mutant flies. These homozygous mutants are able to complete cell division for their own development, but are unable to provide the needed proteins for meiosis and/or the mitotic proliferation of their germline. As a result, these animals cannot produce viable gametes. As mentioned previously, some female sterile mutants can produce apparently normal gametes, but if these females

are unable to provide sufficient maternal contributions of proteins needed for early mitotic divisions of the zygote, early embryonic lethality will result.

II. *Toys are us* and ecdysone signaling

Ecdysone signaling

Ecdysone signaling can be thought of in five major steps: (1) physical/developmental cues that the animal is ready to progress to the next stage of development; (2) synthesis of ecdysone; (3) the ecdysone early response; (4) secondary responses (ecdysone transcription factors providing competence for target tissues through the activation/repression of ecdysone late genes and the repression of ecdysone early genes); (5) and finally ecdysis. Each of these steps contains multiple components and levels of regulation. These components can differ depending on developmental stage, and in later steps, the components and targets are often tissue specific (Riddiford et al., 2003).

Physical and developmental cues to trigger ecdysone synthesis

In *Drosophila* each larval stage produces an increase in the size of the animal; in fact, the main function of the larval molts is to allow for these increases of size. In other holometabolous insects it has been shown that a minimum or critical weight must be achieved to undergo a molt (Nijhout, 1994). In *O. fasciatus* for example, larvae continue to eat until an optimum weight is achieved; however, this signal can be bypassed by injecting saline into the abdomen, causing an equal expansion of the animal which transmits a ”ready to molt” message to the brain. This critical mass requirement may explain why wild type larvae raised on ecdysone-augmented food do not undergo

premature molts, since the animals are not competent to respond to the ecdysone until they have reached the critical weight. It has been shown that the critical mass "checkpoint" is not absolute and can be overcome by time, such that even small larvae can continue to the next molt. In *Tineola bisselliella* researchers have even been able to get starved larvae to molt time and time again while losing weight each time (Titschack, 1926).

Synthesis of ecdysone

When a particular stage of development is complete, some unknown mechanism triggers Prothoracicotrophic Hormone (PTTH) to be synthesized in the dorsal lateral region of the developing brain hemispheres (Mizoguchi et al., 2001). Much of what is understood of PTTH is derived from studies in the silk worm, *Bombyx mori*. After its synthesis, a further cue causes PTTH to travel to the prothoracic cells of the ring gland, via neurons that connect the two cell types. This system allows for quick delivery of PTTH from a site of neural activity to the prothoracic cells, where ecdysone is synthesized (Riddiford, 1993). Ecdysone is then released and modified from alpha-ecdysone to the chemically active 20-Hydroxyecdysone (Thummel, 2001). The direct target(s) of PTTH which trigger this cascade of events are unknown, but PTTH causes an increase in extracellular calcium and cAMP (Smith et al., 1984; Birkenbeil, 1998; Birkenbeil, 2000; Gilbert et al., 2000; Birkenbeil and Dedos, 2002). This increase in cAMP activates S6 Kinase, which phosphorylates and activates Ribosomal Protein Subunit 6 (Rps6) (Gilbert et al., 2000; Smith et al., 2003), a subunit of the 40s ribosome subunit. What proteins are translated by this presumed up-regulation is also currently unknown. One likely target, however, is the Halloween family of cytochrome p450 proteins, which are involved in

various chemical conversions in ecdysteroid production. As shown in Figure 1.1, these Halloween proteins and the steps they govern include: 7,7-Dehydrogenase (Cholesterol to 7-Dehydrocholesterol); 5ß-Reductase (Δ4-Diketol to Diketol); 3-Dehydroecdysteriod-3ß-Reductase (Diketol to Ketodiol); Phantom (Ketodiol to Ketotriol); Disembodied (Ketotriol to 2-Deoxyecdysone); Shadow (2-Deoxyecdysone to Ecdysone); and finally Shade, which converts Ecdysone to 20-Hydroxyecdysone (20HE) after the Ecdysone has been released from the prothoracic cells into the hemolymph.

The phenotype of a mutant in the aptly named *ecdysoneless* (*ecd*) gene defines the effects on the organism of a lack of ecdysone. The *ecdysoneless*^{1} phenotype was described in 1977 after researchers discovered that the ring gland of these larvae failed to make ecdysone (Garen et al., 1977). The *ecd*^{1} third instar larval lethal phenotype is rescued by feeding 20HE to the larvae, which are then able to pupate. *ecd*^{1} is a conditional temperature sensitive allele, so that phenotypes including larval lethality and female sterility are exhibited only when the animals are shifted to a restrictive temperature of 29˚C. The female sterility can be rescued by shifting back down from 29˚C to a permissive 20˚C. While these phenotypes have been known for a number of decades, the gene responsible was not identified until 2004 (Gaziova et al.); the role of the gene product in the ecdysone synthesis pathways is still unknown.

Figure 1.1 Synthesis of Ecdysone

Modified from K.F Rewitz *et al*. (Rewitz et al.). Ecdysone is synthesized from cholesterol in multiple steps by cytochome proteins. The majority of these steps occur in the prothoracic cells of the ring gland. The final step of modifying ecdysone to the active form 20-hydroxyecdysone occurs in the hemolymph and tissues where the ecdysone will be utilized.

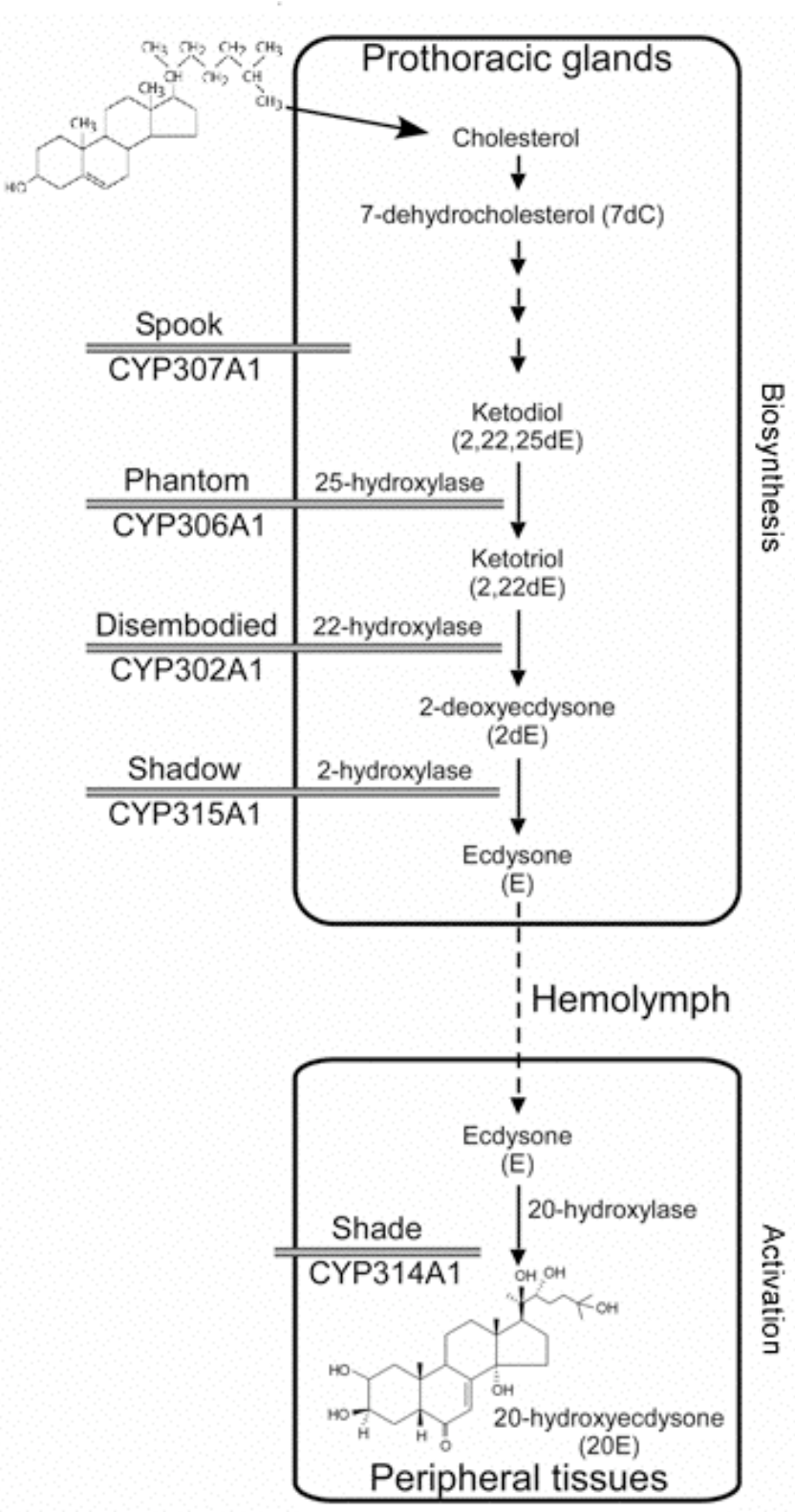
Prothoracic glands
Cholesterol
7-dehydrocholesterol (7dC)
Spook
CYP307A1
Ketodiol
(2,22,25dE)
Phantom
25-hydroxylase
CYP306A1
Ketotriol
(2,22dE)
Disembodied
22-hydroxylase
CYP302A1
2-deoxyecdysone
(2dE)
Shadow
2-hydroxylase
CYP315A1
Ecdysone
(E)
Biosynthesis
Hemolymph
Ecdysone
(E)
20-hydroxylase
Shade
CYP314A1
20-hydroxyecdysone
(20E)
Peripheral tissues
Activation

Ecdysone early response

The ecdysone early response (also known as the ecdysone immediate response) is defined as the transcription of genes that are immediately up-regulated by the presence of ecdysone. The early genes belong to a family of thirteen nuclear receptors with both ligand and DNA binding domains (Thummel, 1995). This allows them to function both as hormone receptors and transcriptional activators. The first acting, and arguably most important, of these early ecdysone genes is *ecdysone receptor*, whose protein product, when it is coupled with Ultraspirical, the fly homologue of the vertebrate Retinoid-X-receptor (RXR), directly binds ecdysone. This trimeric complex then up-regulates the Broad Complex (BrC, which is composed of the four isoforms of the *broad* gene), *E74*, and *E75*. These genes, first studied in the salivary glands, were also the first studied downstream responses of ecdysone. The polytene chromosomes of *Drosophila* salivary glands are highly endoreplicated and so are much larger than chromosomes in other cell types. When ecdysone pulses reach the salivary gland cells, these genes (*BrC, E74, E75*, and others) are transcribed so quickly and at such a high level that puffs can be visualized on the chromosomes at the bands corresponding to their genetic location (Ashburner, 1974; Becker, 1959).

Ecdysone Receptor and Ultraspirical effect this control by forming a heterodimeric complex that is capable of binding ecdysone that up-regulates the ecdysone early transcription factors. EcR contains both a DNA-binding-domain and ligand-binding domain, and is the only of the seventeen known nuclear receptors in *Drosophila* where the ligand is known (Bender et al., 1997). Three functionally separable isoforms of EcR have been identified, which result from differential splicing of a single gene (King-Jones and

Thummel, 2005; Thummel, 1995). The isoforms differ from each other by the tissue type in which they are expressed. Isoform EcR-A is the predominant form in imaginal discs, imaginal rings, prothoracic cells, and the neurons innervating from the brain into the prothoracic cells. EcR-B1 is found in the abdominal epithelium and in the imaginal histoblasts that will form the adult gut. Because of the subset of tissues in which EcR-B1 is expressed, null mutants in this isoform are third instar lethal. The localization of EcR-B2 is restricted mainly to the larval epithelium and fat bodies (Cherbas et al., 2003). Null mutants of EcR that fail to express all three isoforms are embryonic lethal, and homozygous mutant female germline clones are incapable of progressing past mid-oogenesis (Buszczak et al., 1999; Carney and Bender, 2000). This same phenotype is also seen in animals homozygous for mutant alleles of genes encoding the ecdysone early proteins BrC, E74 and E75 (Bayer et al., 1997; Bialecki et al., 2002).

Ultraspirical (USP) is a single polypeptide and a member of the nuclear hormone binding superfamily. In structure and function it is homologous to RXR, the vertebrate receptor for the vitamin A derivative, retinoic acid. Like RXR, USP in conjunction with various cofactors can bind numerous hormones. In addition to ecdysone, it binds the receptor for Juvenile Hormone (JH), which is also involved in molting and developmental signaling. Other functions of Usp include dimerizing with hormone receptor 38 to bind an unknown hormone, and binding with Seven-up inhibits USP's function in the orphan R7 photoreceptor pathway (Zelhof et al., 1995).

The **Broad Complex** (BrC) is made up made up of four different isoforms of Broad that are transcribed from one of two ecdysone inducible promoters. All four isoforms share an N-terminal BTB domain (Bric-a-brac,

Tramtrack, Broad Complex Domain), while the C-terminal regions formed by differential splicing result in C-terminal regions with one of four zinc finger domains. Most tissues express all isoforms of the BrC, however, relative levels of each isoform are tissue and stage dependant. Mutants disrupting isoform specific regions are not complemented by mutations affecting other isoforms (Bayer et al., 1997), suggesting that each isoform has unique functions. The products of the Broad Complex are transcription factors that not only up-regulate ecdysone late genes but are also involved in the rapid up-regulation of the early genes *E74* and *E75*.

E74 and **E75** are both considered orphan nuclear receptors. Similar to EcR and BrC, they encode multiple isoforms that share an N-terminal region. Despite being identified early as essential ecdysone immediate genes, little is known about the function of either protein. E74 functions primarily in the salivary glands and triggers autophagic cell death when the animal enters metamorphosis (Bayer et al., 1996). Mutants in *E75* uncouple molting from metamorphosis and are pupal-to-adult lethal depending on the isoform (Bialecki et al., 2002).

Secondary ecdysone responses: tissue competence and late ecdysone gene regulation

It is interesting to note that each ecdysone pulse signals a major developmental transition, yet each of those transitions is different. The mid-embryonic ecdysone pulse is the least well understood, but Chavez and colleagues (Chavez et al.) proposed that it plays a role in morphogenesis and cuticle deposition. The first and second instar pulses trigger molts of epithelial tissue (Riddiford, 1993), which allow larvae to grow despite their chitinous

cuticle. The mid-third instar pulse of ecdysone commits the animal to undergo metamorphosis. The animal stops feeding, begins to "wander" in search of a place to pupate, and up-regulates genes such as *salivary gland secretion 3 (sgs3*), which produce proteins needed early in the pre-pupal stage (Warren et al., 2006). The late third instar ecdysone peak triggers massive cell and tissue breakdown and rearrangement, which continue through pupation. Strictly larval tissues such as the salivary glands now undergo histolysis even though they turned on gene expression in response to ecdysone peaks at earlier molts (Bodenstein, 1943). Imaginal cells (discs, rings, and histoblasts) undergo equally dramatic changes and begin to form adult structures including eyes, wings, and internal tissues (Fristrom et al., 1993). Even larval tissues that remain and retain their general function in adults undergo cellular and morphological rearrangements during metamorphosis. The pupal peak triggers eclosion from the pupal case, and finally the early adult peak completes the remaining transitions to adulthood, including extension of the wings through control of *ßftz1* (Fortier et al., 2003). In adult females the role of ecdysone seems to be mainly limited to the ovaries and the control of oogenesis (Garen et al., 1977; Carney and Bender, 2000; Gaziova et al., 2004).

Phenotype of mutants in the ecdysone pathway

The phenotypes of mutants in the ecdysone pathway are variable depending on the tissues and developmental stages at which the individual genes are expressed, and the penetrance of any given mutations. Mutations in the *EcR* for instance vary from $EcR^{10\text{-}2}$, which is embryonic lethal (Bender et al., 1997), to $EcR\text{-}B1^{dsRNA.B1}$ which is viable but developmentally delayed

(Biyasheva et al., 2001). Developmental delay is a consistent hallmark of ecdysone pathway mutants. This makes sense since ecdysone and a response to ecdysone are required for the progression from each stage to the next. Also, a majority of the lethal mutants die during the third instar larval stage. Lethality at this time is consistent both with the large titer of ecdysone needed to progress to pupation and with depletion of the supply of maternally provided gene products by this point in development.

In *Manduca sexta* it has been shown that ecdysteroid control is essential for the proliferation of the optic lobes in the brain (Champlin and Truman, 1998). When ecdysteroid levels drop below a critical threshold, the optic lobe neuroblasts arrest in G2 of the cell cycle. In *Drosophila* cell culture, the addition of ecdysone increases the rate of cell proliferation (Kirschenbaum et al., 1995). This increase in proliferation has also been observed in transplanted *ecdysoneless* imaginal disc cells (Gaziova et al., 2004).

III. Hybrid incompatibility in *Drosophila*

Successful matings between closely related species are prevented by either prezygotic or postzygotic mechanisms. Prezygotic mechanisms include mate discrimination, gametic incompatibility, and temporal isolation. While inter-mating in the *Drosophila melanogaster* clade does exhibit some prezygotic mate discrimination, the work described in this thesis focuses on postzygotic reproductive isolation. In particular, I have investigated the inviability of hybrids, since the causes of this type of incompatibility are poorly understood. Dobzhansky pioneered the study of *Drosophila* hybrid sterility by looking specifically at male sterility in hybrids from what he described as races A and B of *Drosophila pseudoobscura* but which were later determined to be

D. pseudoobscura and *D. persimilis* [see (Coyne and Orr, 1998; Ortiz-Barrientos et al., 2007) for more comprehensive review]. Work by additional researchers has shown that many pair-wise matings between *Drosophila* species result in postzygotic hybrid inviability, with the phenotype generally increasing in severity with the evolutionary divergence between the parental species.

Hybrids in the *Drosophila melanogaster* clade

The *Drosophila melanogaster* clade is comprised of *D. melanogaster, D. sechelia, D. simulans, and D. mauritiana* (Figure 1.2A). Hybrids between *D. melanogaster* and *D. simulans* were first described by Sturtevant (1920; 1929) and have been extensively studied since then. Matings between *D. melanogaster* females and males from any of its sibling species occur at a low frequency; female progeny are viable but sterile while male progeny die at the third instar stage of development or as pseudopupae [Figure 1.2 B, (Sturtevant, 1920; Sturtevant, 1929; Hadorn, 1961; Sánchez, 1983)]. Inverse crosses (with *D. melanogaster* males and sibling species females) are also possible but result in significantly fewer progeny with males being viable but sterile, and females which are embryo lethal. This latter result shows that hybrid incompatibility, as a phenomenon, is not sex specific.

Figure 1.2 Evolution in the *Drosophila melanogaster* clade

(A) The *D. melanogaster* and *D. obscura* branches of the *Drosophila* phylogenic tree, modified from http://rana.lbl.gov/drosophila/ (07 March 2007). *Drosophila* species have diverged over millions of years: even *D. melanogaster* and its closely related sibling species are separated by over 4 million years. (B) The Dobzhansky-Muller model fitted with *Hmr* diverging in *D. melanogaster* from the common ancestor of the two species and *Lhr* diverging in *D. simulans* to explain the observed hybrid lethality. This scheme is modified from Brideau et al., 2006. (C) A cross scheme showing the phenotypes of the various classes of F1 progeny obtained from matings between *D. melanogaster* females with a single copy of *Hmr* deleted, and male *D. simulans* with vermilion eyes.

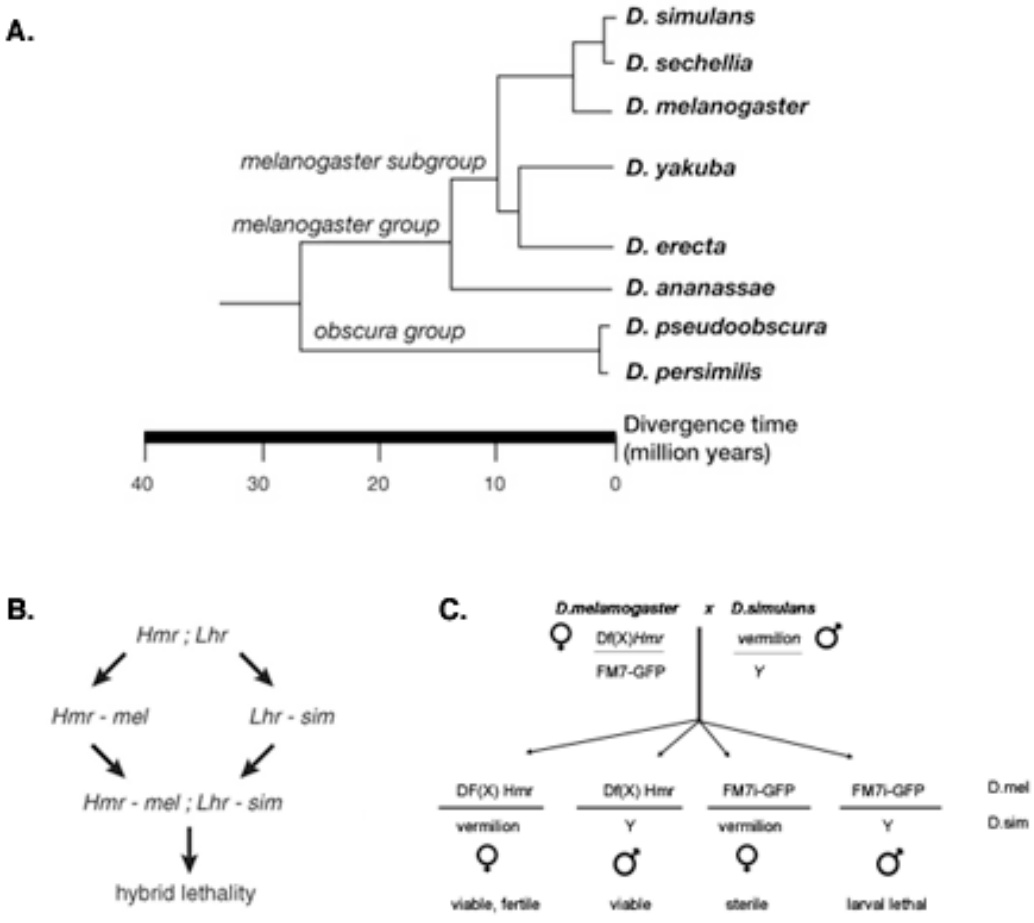
A.
D. simulans
D. sechellia
D. melanogaster
melanogaster subgroup
D. yakuba
melanogaster group
D. erecta
D. ananassae
obscura group
D. pseudoobscura
D. persimilis
Divergence time
(million years)
40
30
20
10
0
B.
Hmr ; Lhr
Hmr - mel
Lhr - sim
Hmr - mel ; Lhr - sim
hybrid lethality
C.
D.melamogaster
x
D.simulans
Df(X)Hmr
FM7-GFP
vermilion
Y
DF(X) Hmr
vermilion
Df(X) Hmr
Y
FM7i-GFP
vermilion
FM7i-GFP
Y
D.mel
D.sim
viable, fertile
viable
sterile
larval lethal

Genetic basis of *Drosophila* hybrid incompatibility

The incompatibility between *D. melanogaster* and its siblings seems to be due to at least one *D. melanogaster* gene on the X chromosome and a minimum of one autosomal gene in the genome of the sibling species (Sturtevant, 1929; Pontecorvo, 1943; Hadorn, 1961; Hutter and Ashburner, 1987; Orr, 1991; Yamamoto, 1992). The Dobzhansky-Muller model proposes that the loss of fitness between two recently diverged species is due to an independently derived mutation in each of the species in genes that have a required interaction (Dobzhansky, 1936; Muller, 1942; Orr, 1995) [See (Johnson, 2002; Welch, 2004) for an in-depth review]. Since both mutations are in different lineages and thus have not existed in the same background, the genes are no longer compatible and cause inviability in the resulting hybrid (Figure 1.2C).

In *D. melanogaster* the X-linked *Hybrid male rescue* (*Hmr*) gene encodes a rapidly evolving protein (Barbash et al., 2003); the null mutation of this gene is able to rescue the lethality of the resulting males (Figure 1.2B), (Watanabe, 1979; Hutter and Ashburner, 1987; Barbash and Ashburner, 2003). *Lethal hybrid rescue* (*Lhr*) is also a rapidly evolving gene, but it is autosomally located on the second chromosome in both species. Consistent with the Dobzhansky-Muller model, mutations in the *D. simulans* copy but not the *D. melanogaster* contributed copy of *Lhr* are also able to rescue the lethality of the hybrid males. The functions of the proteins coded by *Hmr* and *Lhr* have been to date only minimally addressed.

Hmr shares homology with the MYB-related family of DNA binding transcriptional regulators, and contains two MADF domains (Barbash et al., 2003) and a putative BESS Domain (Brideau et al., 2006). BESS domains

frequently interact with MADF domains to facilitate protein-protein interactions. Lhr also contains a Bess domain. While there is no data supporting a direct physical interaction between Hmr and Lhr, it still remains possible that they interact directly or though other proteins; the Bess domains in both proteins suggests a possible method of interaction.

Lhr has been shown to interact physically with Heterochromatic Protein 1 (HP1) (Giot et al., 2003; Brideau et al., 2006; Greil et al., 2007) in yeast two hybrid studies. In addition Lhr and HP1 co-localize on polytene chromosomes, specifically at centromeres, telomeres and on the fourth chromosome. All of these regions are marked by high levels of heterochromatin, a state that HP1 has been proposed to help maintain (Eissenberg and Elgin, 2000). These data taken together suggest that the lethality seen in hybrids may be due to an improper maintenance of heterochromatic DNA.

Mitotic defect proposed as a cause of hybrid lethality

In 1997 Orr and colleagues (Orr et al., 1997) proposed that a mitotic defect is the proximate cause of the lethality of hybrid males. These authors reported that the brains of hybrid third instar male larvae contain many unusual cells, which they classified as under-condensed mitotic cells (Figure 1.3). The frequency of these cells dramatically increases with time in culture: in uncultured brains fixed immediately after dissection from the larvae, such cells constitute only 0.25% of the identifiable cells; however, with culturing for 90 minutes in 0.7% NaCl, this frequency increases one hundred fold to 25%. The same increase occurs in the presence or absence of the spindle poison colchicine while culturing.

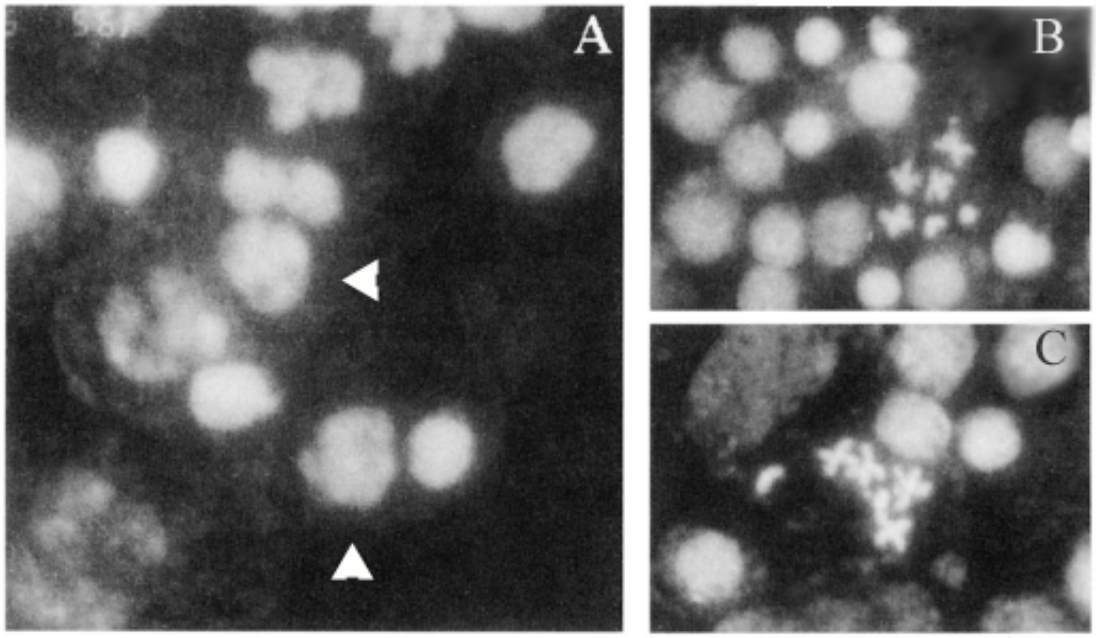

Figure 1.3 Hybrid male mitotic phenotype as previously described

Modified from Orr *et al* 1997. (A) Colchicine arrested hybrid male brain showing mitotic figures. Arrowheads point to what were described as nuclei containing uncondensed mitotic chromosomes. (B,C) Wild-type *D. mauritiana* mitotic brains showing normal chromosome morphology including mitotic figures.

In males of either single species an increase in mitotic index is seen only when the brains are cultured in colchicine and even this increase is only a modest four-fold after 90 minutes. When we examined the cells in question using the mitotic marker Phosphohistone H3, we discovered that these aberrant cells are not mitotic. In addition we showed that this aberrant phenotype does not occur to the same degree when the brains are cultured in the more physiological buffer of Grace's media. We therefore propose that what Orr *et al*. (1997) described as mitotic arrest is in fact an artifact of culturing in NaCl.

IV. Organization of thesis

This thesis describes projects that were all initiated because they were originally believed to reflect difficulties in mitosis. However, my work subsequently demonstrated that for the phenomena described in Chapters 2 and 3 of this thesis, the presumptive mitotic phenotype was either an artifact or secondary to a different defect.

Chapter 2 focuses on characterization of the Trus protein and the *trus*[1] mutant. The visible phenotypes associated with homozygosity for this mutation are a low amount of cellular proliferation, developmental delays, and eventual lethality as third instar larvae. I will show that all of these phenotypes are related to a deficiency in ecdysone signaling. I will also show that Trus most likely acts downstream of PTTH but upstream of EcR and so is somehow involved in Ecdysone synthesis. I have cloned the *trus* gene and have shown that it is expressed at particularly high levels in the ring gland, one of the major locations of ecdysone production in the animal. In collaboration with Dr. Byron Williams, I have identified proteins that interact with Trus; the nature of these

interactors suggests that Trus acts to control the translation of mRNAs for proteins involved in ecdysone synthesis.

Chapter 3 is a modified version of a paper on hybrid incompatibility that has recently been accepted by the journal *Genetics*. In this chapter, I will show that mitotic arrest is not the cause of the hybrid lethality. To study further the supposed mitotic defect causing this phenotype in hybrid male larvae, I initially attempted to replicate the results of Orr *et al*. (1997). But although I obtained mitotic indices similar to those reported by the previous investigators and also observed an increase of cells with abnormally condensed chromatin, when I probed these same brains with an antibody to Phosphohistone H3 (which stains chromatin starting in early prophase), I found that the frequency of mitotic brain cells in hybrid males remained low, even after culturing. Thus, the large numbers of cells with abnormal chromatin appear not to be in mitosis, in conflict with the interpretation proposed by Orr *et al*. (1997).

I hypothesized instead that these "mitotic" cells are actually undergoing apoptosis, since the initial stages of programmed cell death involve chromosome condensation (Thummel, 2001); and could thus be mistaken for uncondensed mitotic cells. I will show that although the levels of apoptosis are not high there is a massive amount of cell death occurring in the brains of hybrid males upon culturing in 0.7% NaCl.

Chapter 4 discusses possible future avenues of research on both of these aforementioned projects.

Appendix 1 contains a modified form of a paper published in the journal *Development* on dLKB1, which is the Drosophila homologue of the human LKB1 (STK11) that is mutated in patients with Peutz-Jeghers

syndrome. In collaboration with the laboratory of Professor Maurizio Gatti (University of Rome, Italy) we show that dLKB1 is essential for proper formation and stability of mitotic spindles and for asymmetrical neuroblast divisions. The mitotic phenotype seen in *dlkb1* mutants is also exaggerated when combined with mutations in *pins,* whose protein product has been also shown to form a sub-complex with Gαi that is essential for asymmetrically dividing cells.

Appendix 2 presents an overview of my work mapping and identifying genes responsible for mitotic mutants identified in the lab. Specifically these mutants were identified as having defects in chromosome condensation. I was able to determine the identity of the genes responsible for four of the mutants. The genes responsible were *cdc6, DNApol-delta,* and 2 alleles of polo kinase. Two of the mutants were not mapped to a small enough region to determine their identity. However, the phenotypes associated with these genes are still quite interesting and so I have included them in this section to guide future efforts in their study.

LITERATURE CITED

Ashburner, M. (1974). Sequential gene activation by ecdysone in polytene chromosomes of Drosophila melanogaster. II. The effects of inhibitors of protein synthesis. *Dev Biol* **39**, 141-57.

Baker, B. S., Smith, D. A. and Gatti, M. (1982). Region-specific effects on chromosome integrity of mutations at essential loci in Drosophila melanogaster. *Proc Natl Acad Sci U S A* **79**, 1205-9.

Barbash, D. A. and Ashburner, M. (2003). A novel system of fertility rescue in Drosophila hybrids reveals a link between hybrid lethality and female sterility. *Genetics* **163**, 217-26.

Barbash, D. A., Siino, D. F., Tarone, A. M. and Roote, J. (2003). A rapidly evolving MYB-related protein causes species isolation in Drosophila. *Proc Natl Acad Sci U S A* **100**, 5302-7.

Bayer, C. A., Holley, B. and Fristrom, J. W. (1996). A switch in broad-complex zinc-finger isoform expression is regulated posttranscriptionally during the metamorphosis of Drosophila imaginal discs. *Dev Biol* **177**, 1-14.

Bayer, C. A., von Kalm, L. and Fristrom, J. W. (1997). Relationships between protein isoforms and genetic functions demonstrate functional redundancy at the Broad-Complex during Drosophila metamorphosis. *Dev Biol* **187**, 267-82.

Becker, H. J. (1959). [The puffs of salivary gland chromosomes of Drosophilia melanogaster. Part 1. Observations on the behavior of a typical puff in the normal strain and in two mutants, giant and lethal giant larvae.]. *Chromosoma* **10**, 654-78.

Bender, M., Imam, F. B., Talbot, W. S., Ganetzky, B. and Hogness, D. S. (1997). Drosophila ecdysone receptor mutations reveal functional differences among receptor isoforms. *Cell* **91**, 777-88.

Bialecki, M., Shilton, A., Fichtenberg, C., Segraves, W. A. and Thummel, C. S. (2002). Loss of the ecdysteroid-inducible E75A orphan nuclear receptor uncouples molting from metamorphosis in Drosophila. *Dev Cell* **3**, 209-20.

Birkenbeil, H. (1998). Intracellular calcium in prothoracic glands of Manduca sexta. *J Insect Physiol* **44**, 279-286.

Birkenbeil, H. (2000). Pharmacological study of signal transduction during stimulation of prothoracic glands from Manduca sexta. *J Insect Physiol* **46**, 1409-1414.

Birkenbeil, H. and Dedos, S. G. (2002). Ca(2+) as second messenger in PTTH-stimulated prothoracic glands of the silkworm, Bombyx mori. *Insect Biochem Mol Biol* **32**, 1625-34.

Biyasheva, A., Do, T. V., Lu, Y., Vaskova, M. and Andres, A. J. (2001). Glue secretion in the Drosophila salivary gland: a model for steroid-regulated exocytosis. *Dev Biol* **231**, 234-51.

Bodenstein, D. (1943). Factors Influencing growth and metamorphasis of the salivary gland in *Drosophila*. *Biological Bulletin Marine Biology Laboratories Woods Hole* **84**, 13-33.

Brideau, N. J., Flores, H. A., Wang, J., Maheshwari, S., Wang, X. and Barbash, D. A. (2006). Two Dobzhansky-Muller genes interact to cause hybrid lethality in Drosophila. *Science* **314**, 1292-5.

Buszczak, M., Freeman, M. R., Carlson, J. R., Bender, M., Cooley, L. and Segraves, W. A. (1999). Ecdysone response genes govern egg chamber development during mid-oogenesis in Drosophila. *Development* **126**, 4581-9.

Carney, G. E. and Bender, M. (2000). The Drosophila ecdysone receptor (EcR) gene is required maternally for normal oogenesis. *Genetics* **154**, 1203-11.

Champlin, D. T. and Truman, J. W. (1998). Ecdysteroid control of cell proliferation during optic lobe neurogenesis in the moth Manduca sexta. *Development* **125**, 269-77.

Chavez, V. M., Marques, G., Delbecque, J. P., Kobayashi, K., Hollingsworth, M., Burr, J., Natzle, J. E. and O'Connor, M. B. (2000). The Drosophila disembodied gene controls late embryonic morphogenesis and codes for a cytochrome P450 enzyme that regulates embryonic ecdysone levels. *Development* **127**, 4115-26.

Cherbas, L., Hu, X., Zhimulev, I., Belyaeva, E. and Cherbas, P. (2003). EcR isoforms in Drosophila: testing tissue-specific requirements by targeted blockade and rescue. *Development* **130**, 271-84.

Coyne, J. A. and Orr, H. A. (1998). The evolutionary genetics of speciation. *Philos Trans R Soc Lond B Biol Sci* **353**, 287-305.

Demerec, M. (1950). Biology of Drosophila. New York,: Wiley.

Dobzhansky, T. (1936). Studies on Hybrid Sterility. II. Localization of Sterility Factors in Drosophila Pseudoobscura Hybrids. *Genetics* **21**, 113-35.

Eissenberg, J. C. and Elgin, S. C. (2000). The HP1 protein family: getting a grip on chromatin. *Curr Opin Genet Dev* **10**, 204-10.

Foe, V. E. (1989). Mitotic domains reveal early commitment of cells in Drosophila embryos. *Development* **107**, 1-22.

Foe, V. E. and Alberts, B. M. (1983). Studies of nuclear and cytoplasmic behaviour during the five mitotic cycles that precede gastrulation in Drosophila embryogenesis. *J Cell Sci* **61**, 31-70.

Fortier, T. M., Vasa, P. P. and Woodard, C. T. (2003). Orphan nuclear receptor betaFTZ-F1 is required for muscle-driven morphogenetic events at the prepupal-pupal transition in Drosophila melanogaster. *Dev Biol* **257**, 153-65.

Fristrom, D., Wilcox, M. and Fristrom, J. (1993). The distribution of PS integrins, laminin A and F-actin during key stages in Drosophila wing development. *Development* **117**, 509-23.

Garen, A., Kauvar, L. and Lepesant, J. A. (1977). Roles of ecdysone in Drosophila development. *Proc Natl Acad Sci U S A* **74**, 5099-5103.

Gatti, M. and Goldberg, M. L. (1991). Mutations affecting cell division in Drosophila. *Methods Cell Biol* **35**, 543-86.

Gaziova, I., Bonnette, P. C., Henrich, V. C. and Jindra, M. (2004). Cell-autonomous roles of the ecdysoneless gene in Drosophila development and oogenesis. *Development* **131**, 2715-25.

Gilbert, L. I., Rybczynski, R., Song, Q., Mizoguchi, A., Morreale, R., Smith, W. A., Matubayashi, H., Shionoya, M., Nagata, S. and Kataoka, H. (2000). Dynamic regulation of prothoracic gland ecdysteroidogenesis: Manduca sexta recombinant prothoracicotropic hormone and brain extracts have identical effects. *Insect Biochem Mol Biol* **30**, 1079-89.

Giot, L., Bader, J. S., Brouwer, C., Chaudhuri, A., Kuang, B., Li, Y., Hao, Y. L., Ooi, C. E., Godwin, B., Vitols, E. et al. (2003). A protein interaction map of *Drosophila melanogaster*. *Science* **302**, 1727-36.

Greil, F., de Wit, E., Bussemaker, H. J. and van Steensel, B. (2007). HP1 controls genomic targeting of four novel heterochromatin proteins in Drosophila. *Embo J* **26**, 741-51.

Hadorn, E. (1961). Zur Autonomie und Phasenspezifiat der Letalitat von Bastarden zwischen *Drosophila melanogaster* und *Drosophila simulans*. *Revue Suisse De Zoologie* **68**, 197-207.

Hutter, P. and Ashburner, M. (1987). Genetic rescue of inviable hybrids between *Drosophila melanogaster* and its sibling species. *Nature* **327**, 331-3.

Johnson, N. A. (2002). Sixty years after "Isolating Mechanisms, Evolution and Temperature": Muller's legacy. *Genetics* **161**, 939-44.

King-Jones, K. and Thummel, C. S. (2005). Nuclear receptors--a perspective from Drosophila. *Nat Rev Genet* **6**, 311-23.

Kirschenbaum, S. R., Higgins, M. R., Tveten, M. and Tolbert, L. P. (1995). 20-Hydroxyecdysone stimulates proliferation of glial cells in the developing brain of the moth Manduca sexta. *J Neurobiol* **28**, 234-47.

Mizoguchi, A., Ohashi, Y., Hosoda, K., Ishibashi, J. and Kataoka, H. (2001). Developmental profile of the changes in the prothoracicotropic hormone titer in hemolymph of the silkworm Bombyx mori: correlation with ecdysteroid secretion. *Insect Biochem Mol Biol* **31**, 349-58.

Muller, H. (1942). Isolating mechanisms, evolution and temperature. *Biological Symposia* **6**, 71-125.

Nijhout, H. F. (1994). Insect Hormones. Princeton: Princetone University press.

Orr, H. A. (1991). Genetic basis of postzygotic isolation between D. melanogaster and D. simulans. *Dros. Inf. Serv.* **70**, 161-162.

Orr, H. A. (1995). The population genetics of speciation: the evolution of hybrid incompatibilities. *Genetics* **139**, 1805-13.

Orr, H. A., Madden, L. D., Coyne, J. A., Goodwin, R. and Hawley, R. S. (1997). The developmental genetics of hybrid inviability: a mitotic defect in Drosophila hybrids. *Genetics* **145**, 1031-40.

Ortiz-Barrientos, D., Counterman, B. A. and Noor, M. A. (2007). Gene expression divergence and the origin of hybrid dysfunctions. *Genetica* **129**, 71-81.

Pontecorvo, G. (1943). Viability interactions between chromosomes of Drosophila melanogaster and Drosophila simulans. *J. Genet.* **45**, 51-66.

Prigent, C. and Dimitrov, S. (2003). Phosphorylation of serine 10 in histone H3, what for? *J Cell Sci* **116**, 3677-85.

Prigent, C. and Giet, R. (2003). Aurora A and mitotic commitment. *Cell* **114**, 531-2.

Rewitz, K. F., Rybczynski, R., Warren, J. T. and Gilbert, L. I. (2006). The Halloween genes code for cytochrome P450 enzymes mediating synthesis of the insect moulting hormone. *Biochem Soc Trans* **34**, 1256-60.

Richards, G. (1981). The radioimmune assay of ecdysteroid titres in Drosophila melanogaster. *Mol Cell Endocrinol* **21**, 181-97.

Riddiford, L. M. (1993). Hormone receptors and the regulation of insect metamorphosis. *Receptor* **3**, 203-9.

Riddiford, L. M., Hiruma, K., Zhou, X. and Nelson, C. A. (2003). Insights into the molecular basis of the hormonal control of molting and metamorphosis from Manduca sexta and Drosophila melanogaster. *Insect Biochem Mol Biol* **33**, 1327-38.

Sánchez, L. D., A. (1983). Development of imaginal discs from lethal hybrids between *Drosophila melanogaster* and *Drosophila mauritiana*. *Development Genes and Evolution* **192**, 48-50.

Smith, W., Priester, J. and Morais, J. (2003). PTTH-stimulated ecdysone secretion is dependent upon tyrosine phosphorylation in the prothoracic glands of Manduca sexta. *Insect Biochem Mol Biol* **33**, 1317-25.

Smith, W. A., Gilbert, L. I. and Bollenbacher, W. E. (1984). The role of cyclic AMP in the regulation of ecdysone synthesis. *Mol Cell Endocrinol* **37**, 285-94.

Sturtevant, A. (1920). Genetic studies on Drosophila simulans. I. Introduction. Hybrids with *Drosophila melanogaster. Genetics* **5**, 488-500.

Sturtevant, A. (1929). The genetics of *Drosophila simulans*. In *Contributions to the genetics of Drosophila simulans and Drosophila melanogaster*, (ed. S. B. M. M. Li), pp. 5-9. Washington: Carnegie Institution of Washington.

Thummel, C. S. (1995). From embryogenesis to metamorphosis: the regulation and function of Drosophila nuclear receptor superfamily members. *Cell* **83**, 871-7.

Thummel, C. S. (2001). Molecular mechanisms of developmental timing in C. elegans and Drosophila. *Dev Cell* **1**, 453-65.

Titschack, E. (1926). Untersuchungen uber dasWachstum der Kleidermotte *Tineola biselliella* Hum. Gleichzeitig ein Beitrage zur Klarung der Inskektenhuatung. *Z. Zool* **128**, 509-569.

Warren, J. T., Yerushalmi, Y., Shimell, M. J., O'Connor, M. B., Restifo, L. L. and Gilbert, L. I. (2006). Discrete pulses of molting hormone, 20-hydroxyecdysone, during late larval development of Drosophila melanogaster: correlations with changes in gene activity. *Dev Dyn* **235**, 315-26.

Watanabe, T. K. (1979). A gene that rescues the lethal hybrids between *Drosophila melanogaster* and *D. simulans*. *Jpn J. Genet* **54**, 325-331.

Welch, J. J. (2004). Accumulating Dobzhansky-Muller incompatibilities: reconciling theory and data. *Evolution Int J Org Evolution* **58**, 1145-56.

Yamamoto, M. T. (1992). Inviability of hybrids between *D. melanogaster* and *D. simulans* results from the absence of simulans X not the presence of simulans Y chromosome. *Genetica* **87**, 151-8.

Zelhof, A. C., Yao, T. P., Chen, J. D., Evans, R. M. and McKeown, M. (1995). Seven-up inhibits ultraspiracle-based signaling pathways in vitro and in vivo. *Mol Cell Biol* **15**, 6736-45.

CHAPTER 2

TOYS ARE US: A NOVEL PROTEIN INVOLVED IN ECDYSONE SIGNALING

INTRODUCTION

Development is a highly regulated process. In holometabolous insects, metamorphosis and molting are controlled by hormone-dependent pathways. In *Drosophila melanogaster*, this control is regulated by ecdysone and juvenile hormone titers (Riddiford, 1993). The synthesis of ecdysone in the ring gland is triggered by prothoracicotrophic hormone (PTTH) (Gilbert et al., 2002). Part of the pathway downstream of PTTH has already been characterized, but there are still a number of unknown components and regulatory controls.

Although peaks in ecdysone concentration are observed at every developmental transition, the most studied are the transitions beginning in third instar larvae and continuing through metamorphosis. Commitment to enter metamorphosis occurs in response to a small ecdysone peak during the mid-third instar stage (Korge, 1977; Andres and Thummel, 1992). We have identified a mutation in a gene we call *toys are us* (*trus*) that causes a developmental delay throughout development and causes the animals to arrest after this critical stage, so mutants remain as "wandering" third instar larvae for up to 10 days before their death. We believe that the Trus protein is required for the ecdysone pulses that regulate metamorphosis from the mid-third larval instar onward.

In this chapter, I describe the initial identification of the *trus*^{1} mutant, molecular characterizations of the *trus* gene and its protein product, and data indicating that *trus* is involved in the ecdysone pathway. I found that *trus*

corresponds to the transcriptional unit CG5333, and that it encodes a novel but highly conserved cytoplasmic protein with a putative cell death domain (PDCD2L). CG5333 is highly expressed in cells that produce ecdysone, particularly the prothoracic cells of the ring gland. The phenotypic effects of *trus*^{1} mutations are partially rescued by ecdysone feeding. I also report the results of an experiment performed in collaboration with Dr. Byron Williams indicating that the Trus protein is complexed with at least one ribosomal protein, and perhaps also with a translation factor. These results considered together suggest a model in which the Trus gene product is involved in regulating the translation of mRNAs for genes that participate in the ecdysone pathway.

MATERIALS AND METHODS

Flies

Flies were reared on standard yeast glucose media unless otherwise noted and raised at room temperature of approximately 23°C. Fly stocks were received from the following sources. The *trus*^{1} mutant was isolated from the Zucker EMS mutant collection (Koundakjian et al., 2004) as described in the text. Enhancer trap lines P0206 and P0163 expressing GAL4 in the prothoracic cells of the ring gland were a gift from Dr W. Janning (http://FlyView.uni-muenster.de). All other stocks were received from the *Drosophila* stock center (Bloomington, IN).

When testing double heterozygotes for abnormal phenotypes, crosses were set up by crossing *trus*^{1} / TM6B*Tb,Hu* males with virgin females carrying the mutant of interest over a balancer chromosome.

Mapping of the *trus*^{1} mutation

Our collaborator Fiammetta Verní at the University of Rome first roughly localized the *trus*^{1} mutation to region 87B by recombination mapping against a multiply marked third chromosome. I then determined this location more precisely by complementation tests for lethality with deletions containing known breakpoints (Figure 2.1A). This analysis delimited *trus* to a genomic region of 21 Kb, containing 10 transcriptional units. The coding regions of these ten genes on the mutant chromosome were then amplified by PCR from wild type and homozygous mutants, and the PCR products were sequenced by the Biotechnology Resource Center (BRC, Cornell University, Ithaca, NY).

Transgenic rescue of the *trus*^{1} mutation

To confirm the identity of the gene responsible for the *trus* phenotype, an ~5 kb fragment of genomic DNA was PCR amplified using the following primers (forward: CGGGGTACCCCGAATTCCGTTGTGGGACTCAGAGGA, reverse: CGCGGATCCGCGAGAATTAGAATGGATTTCTGCAAGTTGG) from wild type larval DNA; this fragment contained the entire coding region of CG5333 as well as 2 kb of DNA upstream of the start of the cDNA and 1 kb of DNA beyond the 3' end of the transcriptional unit (Figure 2.1A). This fragment was cloned into the PW8 vector (Klemenz et al., 1987) using the KpnI and BamHI restriction sites. The construct was injected into embryos by Genetic Services Inc (Sudbury, MA). Resulting transgenic lines were screened for integration into the genome by presence or absence of w^{+} eye color. The transgene was mapped to a given chromosome by looking at segregation with known markers on each chromosome. The transgene was then crossed into a *trus*^{1} homozygote background to check for complementation.

Figure 2.1 Identification of CG5333 as the gene responsible for the trus phenotype

(A) Modified from Flybase 2007. A gene map of the cytological region 87B9 to 87C3 of chromosome 3 containing the *trus* gene. Lines in green represent deletions that complemented the *trus* mutant, while lines in red represent deletions that failed to complement. The blue vertical lines delineate the region containing the *trus* gene. The purple fragment represents the area cloned for a genomic rescue of the *trus* mutation. CG5333, which has since been renamed *trus* in Flybase, is highlighted in pink. Genes in black represent known lethals in the region that complemented the *trus* mutant. (B) Western blot of whole larvae against the Trus protein with α-Tubulin as a loading control. There is no detectable Trus protein in *trus*^{1} mutants. (C) Sequence homology between Trus and its homologues in other organisms (Numbers represent % similarity to Trus). Also shown is most closely related protein in *Drosophila*, Zfrp8. Trus and Zfrp8 proteins are the only two to contain the putative domain cell death 2 (PDCD2) shown in green. The N-terminal regions, in blue, share a high level of unidentified sequence similarity. Zfrp8 also contains a zinc finger (pink).

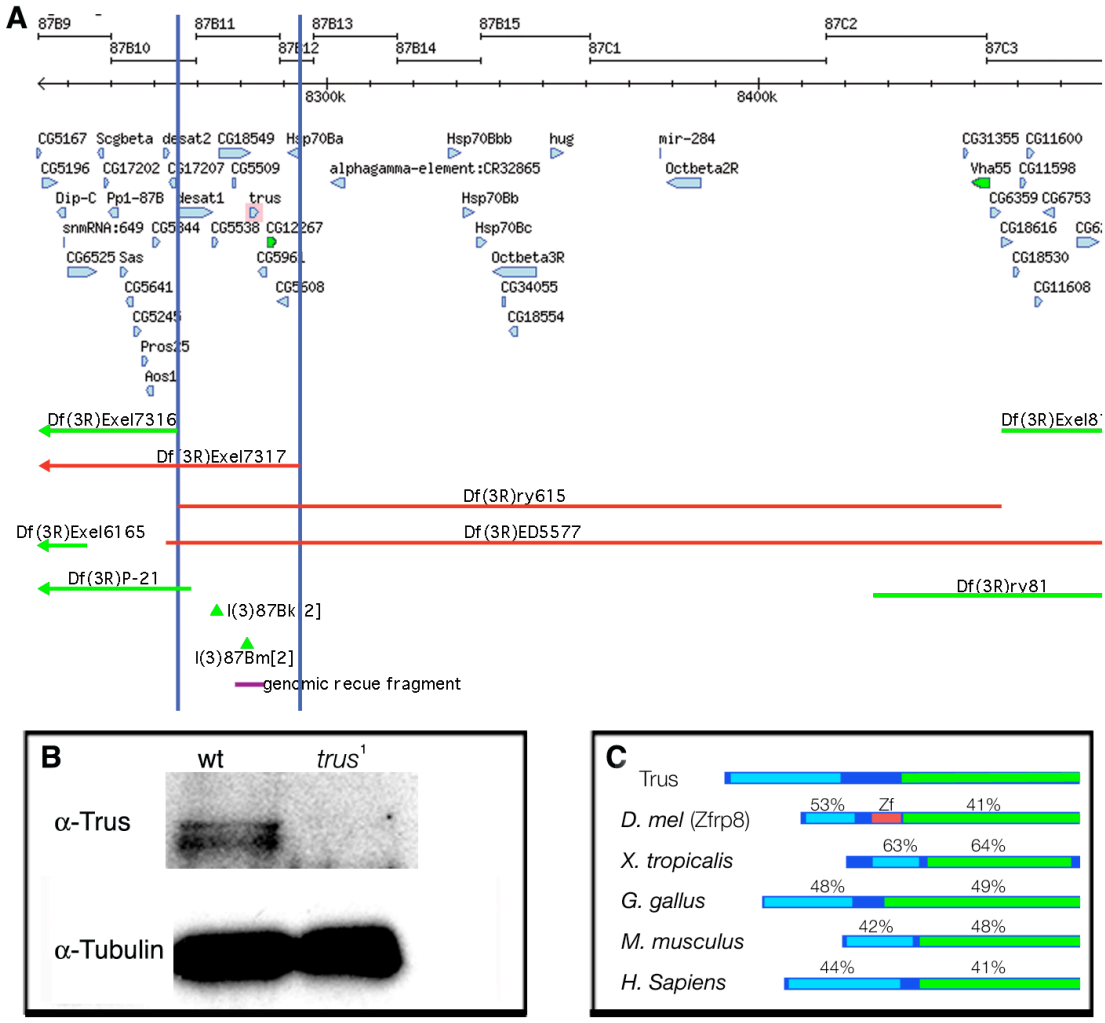
A
87B9
87B10
87B11
87B12
87B13
87B14
87B15
87C1
87C2
87C3
8300k
8400k
CG5167 Scgbeta desat2 CG18549 Hsp70Ba
CG5196 CG17202 CG17207 CG5509
Dip-C Pp1-87B desat1 trus
snmRNA:649 CG5844 CG5538 CG12267
CG6525 Sas
CG5641
CG5245
Pros25
Aos1
CG5961
CG5508
Hsp70Bbb hug
alphagamma-element:CR32865
Hsp70Bb
Hsp70Bc
Octbeta3R
CG34055
CG18554
mir-284
Octbeta2R
CG31355 CG11600
Vha55 CG11598
CG6359 CG6753
CG18616
CG18530
CG11608
Df(3R)Exel7316
Df(3R)Exel7317
Df(3R)ry615
Df(3R)Exel6165
Df(3R)ED5577
Df(3R)P-21
Df(3R)ry81
l(3)87Bk[2]
l(3)87Bm[2]
genomic recue fragment
B
wt
trus1
α-Trus
α-Tubulin
C
Trus
D. mel (Zfrp8)
53%
Zf
41%
X. tropicalis
63%
64%
G. gallus
48%
49%
M. musculus
42%
48%
H. Sapiens
44%
41%

Antibody production and purification

A 1.5 kb fragment of the full-length *trus* cDNA clone RE69372 containing the coding region for amino acids 1 to 485 was cloned into the pDONR201 vector using the BP clonase system (Invitrogen) as described in the instruction manual. The reaction mix was transformed into DH5α cells; individual colonies were grown up and purified using the QIAprep Spin Miniprep Kit (Qiagen, Germantown, MD). Clones were test-digested with BsrGI, and candidate clones with the predicted restriction pattern were sequenced (BRC). The *trus* cDNA insert from a verified clone was cloned into the pMAL-GW vector using the LR clonase system (Invitrogen). A single clone with the correct sequence was grown in LB broth (1% w/v BactoTryptone, 0.5% w/v yeast extract, 0.17 M NaCl), and expression of Trus was induced with 2 mM IPTG. Maltose purification was done as described in the manual (New England Biolabs) and described briefly here. Cells were spun down and resuspended in Column Buffer (20mM Tris-HCl, 200 mM NaCl, 1 mM EDTA, 1 mM DTT). Samples were then frozen o/n at -20˚C and thawed in an ice water bath the following day, followed by 2 min of sonication to break cells open. Samples were then centrifuged for 30 min to removed cell debris and the supernatant was diluted 1:5 in Column Buffer. The crude protein solution was then loaded over an amylose resin column (New England Biolabs) and washed 12 times with Column Buffer. Finally the protein was eluted in Column Buffer + 10 mM maltose. Protein concentration was measured using the Bradford Assay and high concentration fractions were pooled and loaded on an SDS-PAGE gel. A gel band of the expected size for the Trus-MBP (maltose binding protein) fusion protein was isolated and sent to Cocalico

Biologicals Inc (Reamstown, PA) for injection into rabbits for antibody production.

Antibodies were purified from serum using the Econo-Pac Serum IgG Purification Kit (BioRad, Hercules, CA) as described in the instruction manual. For some experiments, antibodies were further affinity purified against the Trus-fusion protein as described by Starr et al (2000), with the exception that the column was made using cyanogen bromide-activated Sepharose 4B beads (Sigma, St. Louis, MO).

Cytology

Mitotic indices (MIs) were determined as described in Williams *et al*. (1992); briefly, the MI is presented as the number of mitotic figures per microscope field, and is a measure of the amount of mitosis in a tissue sample.

Whole tissue immunofluorescence was done by dissecting the tissue from third instar larvae in Phosphate Buffered Saline (PBS), permeabilizing the brains for 10 min in PBX (PBS + 0.3% Triton X100), fixing the samples in 4% paraformaldehyde (Electron Microscopy Sciences, Hatfield, PA), and then briefly rinsing the samples 3X in PBS before antibody staining. Antibodies were diluted in PBS as described below, and tissues were incubated in primary antibodies overnight at 4˚C. Tissues were rinsed 3X in PBX before being incubated in secondary antibody for 2-3 hours at room temperature. Tissues were again rinsed with PBS before being counterstained with ToproIII (Invitrogen, Carlsbad, CA) at a concentration of 1:10,000 in PBS. Tissues were imaged on a Leica TCS SP2 system. Primary antibodies were used at the following concentrations: rabbit anti-Phosphohistone H3 (Upstate,

Charlottesville, VA) a 1:500 dilution, rabbit anti-Trus at 1:1000, and anti-Daschund (Developmental Studies Hybridoma Bank, University of Iowa, Iowa City, IA) at 1:20. Secondary antibodies were all used at a concentration of 1:1000 and included: TRITC (tetrarhodamineisothiocyanate)-conjugated donkey anti-rabbit IgG (Jackson Immunoresearch, West Grove, PA), TRITC-conjugated anti-mouse (Jackson Laboratories) and Cy2-conjugated anti-mouse (Jackson Laboratories); the latter anti-mouse reagent was used in conjunction with the TRITC anti-rabbit for double staining.

Western Blots

Whole larvae or specific tissues dissected in ice-cold PBS were homogenized in Laemmli Sample Buffer (BioRad, Hercules, CA) containing 5% 2-mercaptoethanol. Samples on the same gel were equalized to correspond to the same number of animals or to yield the same sample mass as indicated on each figure. After homogenization, samples were boiled for 10 min, cooled on ice for 1 min, and centrifuged briefly to remove non-soluble debris. Proteins were separated on a standard 10% SDS-polyacrylamide gel, and then transferred from the gel to Immobilon-P Transfer Membranes (Millipore, Beford, MA). Blots were blocked in 5% milk in Tween Tris Buffered Saline (TBST; 20mM Tris-HCl, 137mM NaCl, 0.02% Tween-20, pH=7.6) for 1 hour before incubation in primary antibody overnight at 4˚C and secondary antibody for 2 hrs at room temperature. Purified Anti-Trus was used at a dilution of 1:5000, while mouse anti-EcR and anti-BrC were both from the Developmental Studies Hybridoma Bank and used at dilutions of 1:100. Secondary antibodies were HRP-coupled anti-rabbit IgG (Sigma) and HRP-coupled anti-mouse IgG (Sigma). Both secondary antibodies were used at a

1:10000 dilution. After three 10 min washes in TBST, blots were processed with ECL as described in the instruction manual (Amersham Corp, Arlington Height, IL).

Purification of protein complexes containing Trus[1]

The entire coding sequence of *trus* from cDNA clone RE69372 was cloned into pMK33-NTAP (Veraksa et al., 2005), and the resulting constructs were stably transfected into *Drosophila* Kc tissue cells using Cellfectin (Invitrogen). The TAP-Trus fusion protein was assayed on Western blots using HRP-conjugated anti-Protein A antibody (Rockland, Gilbertsville PA) and by immunofluorescence of fixed cells using goat anti-Protein A antibody at 1:1000 followed by TRITC-conjugated anti-goat antibody (Jackson Laboratories) at a dilution of 1:500. Protein complexes from one liter of TAP-Trus-expressing cells were isolated following (Puig et al., 2001), using a lysis buffer for making *Drosophila* extracts (Veraksa et al., 2005). After purification using IgG-Sepharose and Calmodulin-Sepharose beads (Invitrogen), the final eluate was precipitated with trichloroacetic acid (TCA), resolubilized in Laemmli sample buffer (Bio-Rad, Hercules CA) and subjected to SDS-PAGE. Bands were excised, trypsinized and analyzed by MALDI (Cornell Bioresource Center.) Further details on these procedures can be found in (Williams et al., 2007).

Ecdysone feeding

Ecdysone was fed to larvae as described in (Riddiford, 1993). Briefly, 20-Hydroxyecdysone (20HE, Sigma) was diluted to 1 mM in 5% ethanol and

[1] All post-cloning work on Tap-tagging was done by Dr. Byron Williams

mixed with 0.5 g dry yeast to make a yeast paste. Second- and third-instar larvae were transferred to plates containing the yeast paste and observed over time. Rescue of the developmental block was defined as a significant increase in the percentage of animals undergoing pupation. The following precursors were also fed to larvae in exactly the same way: cholesterol (Alfa Aesar, Ward Hill, MA), 7,7-dehydrocholesterol (7dC, MP Biomedicals, Solon, OH), and alpha-ecdysone (E, Axxora, San Diego, CA).

Sucrose gradient fractionation of S2 cell extracts[2]

S2 cells were treated with 100 μg/ml cycloheximide (Sigma) for 10 min and lysed in 0.6 ml of 50 mM Hepes-KOH, pH=7.2, 100 mM KCl, 10 mM $MgCl_2$, 0.1% Triton X-100, 1 mg/ml heparin, 2 mM dithiothreitol, 100 μg/ml cycloheximide, and 0.1% RNAguardTM (Amersham Biosciences). Cell debris was removed via centrifugation for 10 min at 13,000 rpm, and extracts were resolved on 7.5–60% sucrose density gradients by centrifugation for 4.5 hours at 39,000 rpm at 4 °C using an SW41Ti rotor (Beckman). 600 μl fractions were collected while recording the A254 profile using a single path UV monitor (Amersham Biosciences).

RESULTS

Identification of the *trus* gene as CG5333

The *trus*[1] mutation was originally identified by Dr. Fiammetta Verní of the University of Rome in a screen of the Zuker collection of *Drosophila*

[2] This protocol was received as personal communication from Ditte Andersen (Cancer Research UK London Research Institute) who performed the work, and is modified from Andersen et al. (2007).

mutations induced by high concentrations of the mutagen EMS (Koundakjian et al., 2004). The screen selected for mutant stocks in which homozygotes died as third instar larvae or pupae, since many mitotic mutants die at that stage due to the depletion of the maternally supplied gene product (Gatti and Goldberg, 1991). Initial observations classified *trus*^{1} as a mitotic mutant since homozygotes exhibited only a low number of proliferating cells in the larval brain and modest abnormalities in chromosome morphology. However, as will be explained below, these effects are subsidiary to primary defects in the ecdysone pathway. For the genetic mapping of *trus,* we scored the phenotypes of developmental delays and third instar larval/pupal lethality that will be discussed in more detail below.

Dr. Verní roughly mapped the original *trus*^{1} mutation (stock MA27) to the right arm of chromosome 3 by recombination relative to visible markers. By testing the *trus*^{1} chromosome for complementation with a variety of third chromosome deletions, I was able to narrow down the *trus*-containing region to polytene chromosome bands 87B10-12. This region contains 16 known genes (Figure 2.1A); by complementation testing of *trus*^{1} with known lethal mutations in the region, I was able to eliminate 6 genes from consideration, leaving 10 transcriptional units as *trus*^{1} candidates (Figure 2.1A). Sequencing of the coding regions of these 10 genes identified only one non-synonymous mutation, which was located in the ATG start codon of gene CG5333. The ATG -> ACG mutation should disrupt the initiation of the translation of this gene, leading us to believe that CG5333 could be the gene responsible for the *trus* phenotype. To verify this conclusion, I cloned a wild type copy of CG5333 including its endogenous promoter (Figure 2.1A; see also Materials and Methods) and introduced this construct into the *Drosophila* germline. This

transgene was sufficient to rescue the lethality and developmental defects observed, supporting the correspondence of CG5333 with *trus.*

Additional support for this conclusion was gained using an antibody generated against a fusion protein expressed in bacteria that contained CG5333 epitopes (Materials and Methods). On Western blots, a prominent band of approximately 70 kD is observed in larval brains and attached tissues of wild type third instar larvae that is missing in *trus*^{1} mutant extracts (Figure 2.1B). Although the presumptive Trus protein runs slower on this gel than its predicted size of 53165 Daltons, this was also a characteristic of the bacterial fusion protein used to make the anti-Trus antibody. Other experiments described below provide additional assurance that this retardation of electrophoretic mobility is indeed a property of Trus proteins.

The *toys are us* (CG5333) gene encodes a novel protein with a putative cell death domain (PDCD2). In addition to *trus,* one other *Drosophila melanogaster* gene called *Zfrp8* contains this domain. The Zfrp8 protein also includes a single Zinc Finger domain that Trus lacks (Figure 2.1C). The genomes of all eukaryotic organisms from plants to humans contain genes homologous to both *trus* and *zfrp8*; the homologs of Zfrp8 in several other organisms are called PDCD2. The function of Trus has not to our knowledge been investigated in any organism, but PDCD2 has been proposed to have a function in negative regulation of cell proliferation in human cell culture and lymphomas (Scarr and Sharp, 2002; Chen et al., 2005) and a recent article suggests that *Drosophila* Zfrp8 plays a role in control of cell proliferation and lymph gland development (Minakhina et al., 2007). It seems likely that Trus and Zfrp8 are functionally unrelated since mutations in the two genes complement each other (data not shown). Moreover, *zfrp8* mutations are

associated with an increase in cell proliferation, while (as shown below) *trus*^{1} mutants have decreased proliferation. Interestingly, no published study has found a role of the PDCD2-containing proteins in cell death (Scarr and Sharp, 2002; Chen et al., 2005; Minakhina et al., 2007), so the original name for this domain may be a misnomer.

Trus is expressed cytoplasmically in relevant ecdysis tissues

The amino acid sequence of Trus lacks a nuclear localization signal and so it is predicted that its expression would be cytoplamic. We used immunofluoresence with the antibody we generated to visualize Trus' localization in various tissues at different developmental stages and found in all cases that Trus was indeed cytoplasmically localized (Figure 2.2). In third instar larvae, the highest apparent expression of this protein was observed in the ring gland, particularly in the prothoracic cells in which ecdysone is synthesized (Gilbert et al., 2000). Other significant sites of Trus protein accumulation include the salivary glands and the midgut, which while they do not make ecdysone, are tissues undergoing ecdysone regulated reorganization during this stage. In adults expression was seen in the ovaries, which also make and require ecdysone.

Defective proliferation of *trus*^{1} neuroblasts

trus^{1} was initially identified by Dr. Verní as a mitotic mutant, mostly because she detected a mild chromosome condensation defect in the brains of third instar larvae homozygous for the third chromosome bearing the *trus*^{1} mutation.

Figure 2.2 Expression of the Trus protein

(A) Trus is expressed in all stages of development; however, the strongest expression is in the third larval instar. This is also the stage when ecdysone peaks are the strongest. Adult female expression is also higher than in adult males, which may correspond to the higher levels of ecdysone needed in the ovaries. (B-E) Immunofluorescence analysis of Trus localization and expression; Trus is in red, DNA is in blue. (B) Trus in oocytes remains cytoplasmic and seems to be highly concentrated around the developing nucleus and around the outside of the oocytes. (C) In whole embryos, Trus remains highly localized on the cortex of the embryo. (D) In third instar larvae the expression is highly concentrated in the prothoracic cells of the ring gland. (E) The Trus is also detectable in the salivary glands of the third instar larvae. (F,G) Higher magnification of ring gland and salivary glands, Trus is in red overlaid on the corresponding DIC image. (F) In the ring gland Trus is strictly cytoplasmic, where it stains in a punctate pattern. (G) In salivary glands, the Trus pattern is also punctate. The protein appears to accumulate as well at the border between cells.

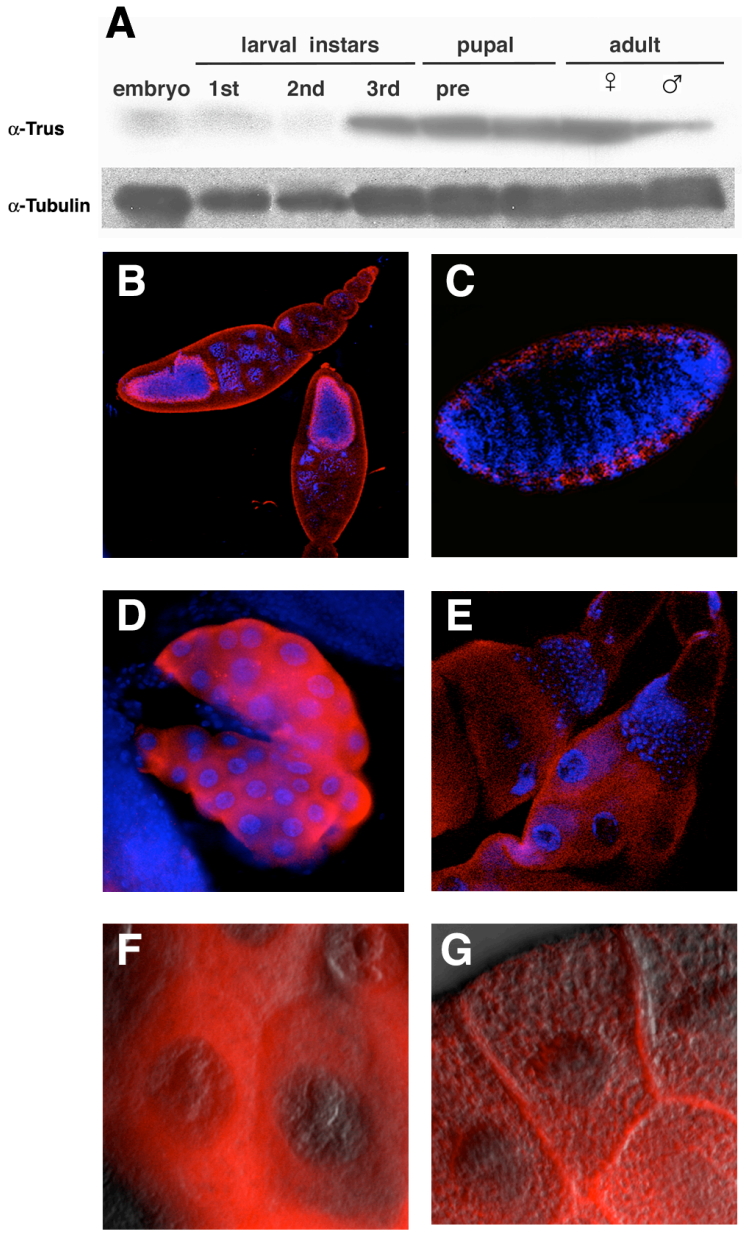
A
larval instars
pupal
adult
embryo
1st
2nd
3rd
pre
♀
♂
α-Trus
α-Tubulin
B
C
D
E
F
G

When I examined the mitotic index (the number of mitotic figures per field of view) of *trus*^{1} mutant brains, I measured a value of 0.63, which is roughly half of the value of 1.29 seen in wild type brains. These observations point to problems in cell proliferation; however, I was unable to detect any obvious cytological defects in the mitotic cells themselves such as those reported by Dr. Verní.

Other experiments verify the lack of cell proliferation in *trus*^{1} mutants. When whole brains were examined with 5-Bromodeoxyuridine, used to mark replicating cells, a complete lack of staining in the optic lobes was observed (Figure 2.3 A-D). Staining against Dachshund, which is expressed in undifferentiated neuroblasts, showed a similar staining pattern to PH3 with near-normal populations of non-differentiated scattered neuroblasts (Figure 2.3 E-H) but a lack of non-differentiated optic lobe neuroblasts. At least some neuroblasts were, however, able to differentiate as shown by staining for Elav, which is only expressed in differentiated neuroblasts (Yao and White, 1994; Robinow et al., 1988) (Figure 2.3 A-D). Thus the low mitotic index observed is due mostly to a lack of proliferating optic lobe neuroblasts and not a general problem in entering mitosis or in cell differentiation after division.

Defects in some *trus*^{1} mutant salivary glands

In normal development, cells in the salivary gland are all the same size when the animal hatches to become a first instar larva. In wild type and in 75% of *trus*^{1} mutant individuals, these salivary gland cells are then able to differentiate and propagate different cell types, including the imaginal ring, which will develop into the adult salivary tissue (Figure 2.4A).

Figure 2.3 *trus*^{1} larvae fail to develop optic lobe neuroblasts

(A, C, E,G) BrDU (red) is only incorporated into actively dividing cells, while Elav (green) stains neuroblasts that have differentiated into neurons. (A,C) Wild type (WT) brains show rings of dividing cells marking the optic lobes as well as scattered neuroblasts. (E,G) The *trus*^{1} animals have scattered neuroblasts that are dividing but lack dividing optic lobe cells. Neuroblasts differentiation appears to be unaffected in *trus*^{1} mutant brains. (B, D, F, H) Dachshund (Dasc, red; DNA counter-stain, blue)is expressed in non-differentiated neuroblasts. (B,D) WTt brains show Dachshund expression in both the rings of optic lobe cells similar to that seen with BrDU and also scattered neuroblasts. (F,H) Optic lobe staining is considerably reduced in *trus*^{1} mutant brains.

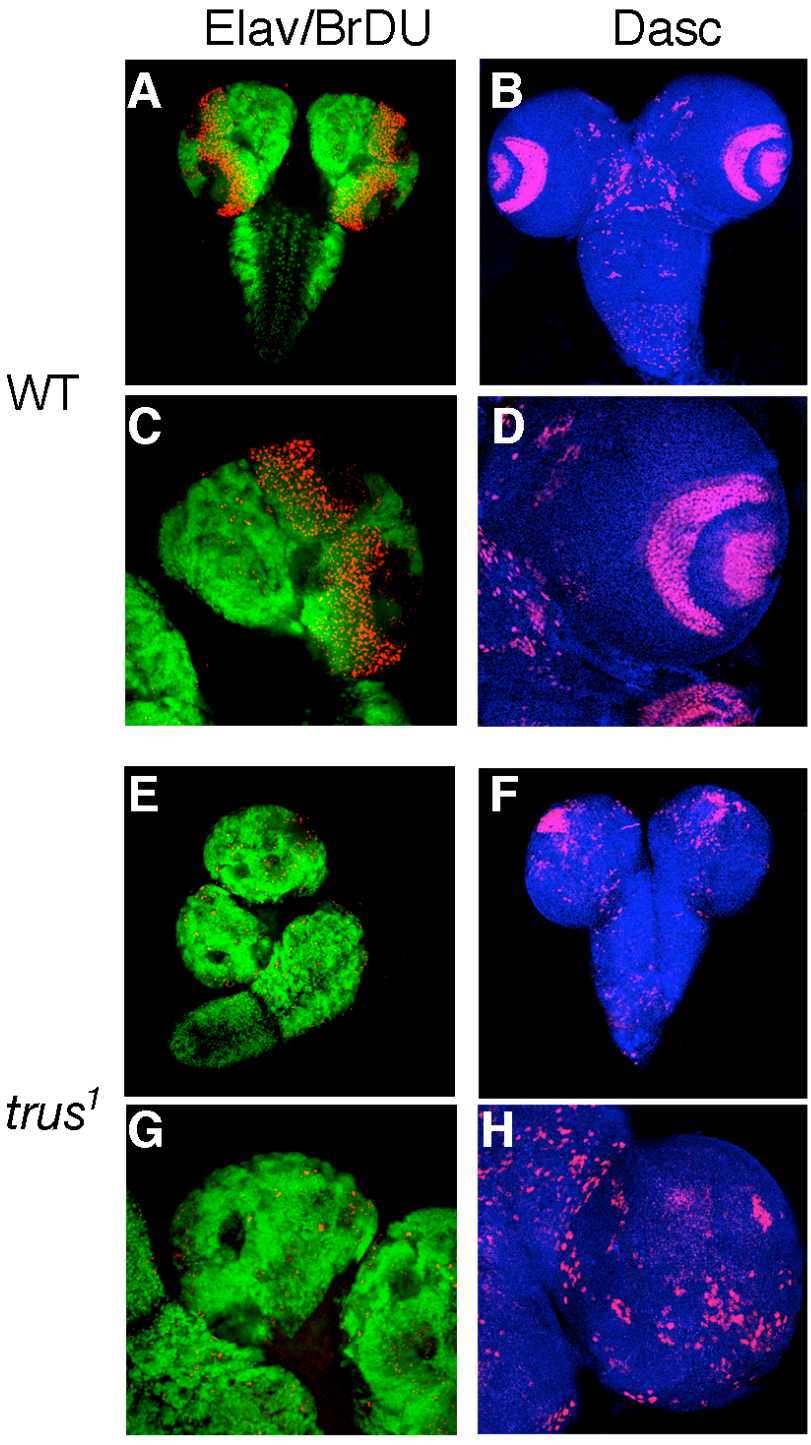
Elav/BrDU
Dasc
A
B
WT
C
D
E
F
trus1
G
H

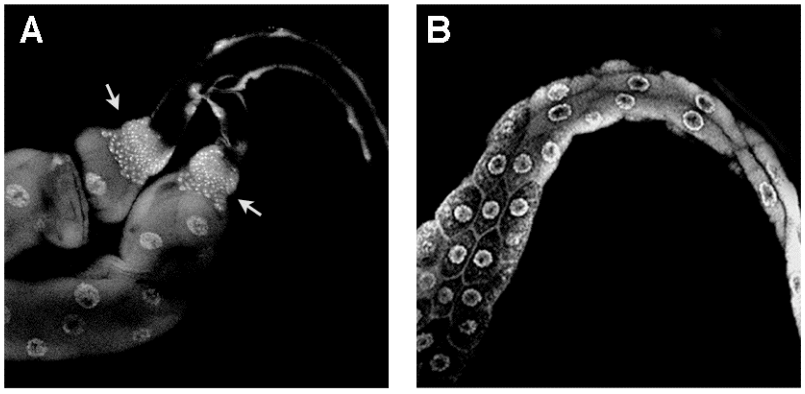

Figure 2.4 Development of imaginal ring cells of the salivary glands.

Immunofluorescence staining of DNA by ToproIII of third instar larval salivary glands. (A) In wild type animals the salivary glands are composed of large polyploidy cells involved in making larval secretions and a small ring of imaginal cells (arrow) that will comprise the adult salivary tissues after metamorphosis. (B) In 25% of *trus* mutants the salivary glands are missing this imaginal tissue. However, 75% of *trus*^{1} animals have apparently normal rings of imaginal cells, suggesting that differentiation of this cell type is not absolutely dependant on ecdysone or Trus.

However, in 25% of the *trus*^{1} larvae, all of the cells remain the same size and the imaginal ring cells are missing (Figure 2.4B). It is unclear if this latter cell type is missing because of a defect in proliferation or differentiation.

Trus mutants exhibit developmental delay and arrest

A wild type *Drosophila* raised at 25˚C will take nine days to progress from being laid to eclosing from its pupal case as an adult (Demerec, 1950). However, in a bottle containing a balanced stock for the *trus*^{1} mutation, the developmental delay of homozygous *trus*^{1}/ *trus*^{1} individuals is obvious relative to the progress of their heterozygous siblings (*trus*^{1} / Balancer). By the time half of the homozygotes reach the third instar stage at day 12, 95% of their siblings have already formed pupae (Figure 2.5 A-C). Not only do the homozygous *trus* mutants take 8.5 days longer to reach the third instar than wild type flies, but they also remain at this stage of development for an extended period (Figure 2.6). Homozygotes for *trus*^{1} spend an average of 12.5 days as third instar larvae, with 88% of these larvae dying before pupariating. The remaining 12% of larvae that do manage to pupariate subsequently die within 24 hours, without reaching the point of pupal cutical tanning, which occurs normally at 12 hours post-pupariation (Demerec, 1950).

Heterozygotes for *trus*^{1} are partially temperature-sensitive for eclosion

When pupae that are heterozygous for the *trus*^{1} mutation are shifted from 25˚C to 30˚C, they exhibit a defect in eclosion as well as a significant increase in pupal lethality (Table 2.1).

Figure 2.5 Development in *trus* mutants is delayed.

(A) It takes an average of 12.5 days for *trus* homozygous mutant larvae to reach the third instar stage of development, whereas wild type larvae only take an average of 3.5 days post egg deposition to reach this same stage. Feeding of 20-hydroxyecdysone (20HE) to homozygotes is able to partially rescue this delay. (B) Feeding of 20HE is able to lower the third instar lethality in mutant animals from 89.1% to nearly 7.5%. (C) After 20HE feeding, 91.5% of homozygote larvae are able to pupariate, compared with only 13% raised in food without 20HE.

A.

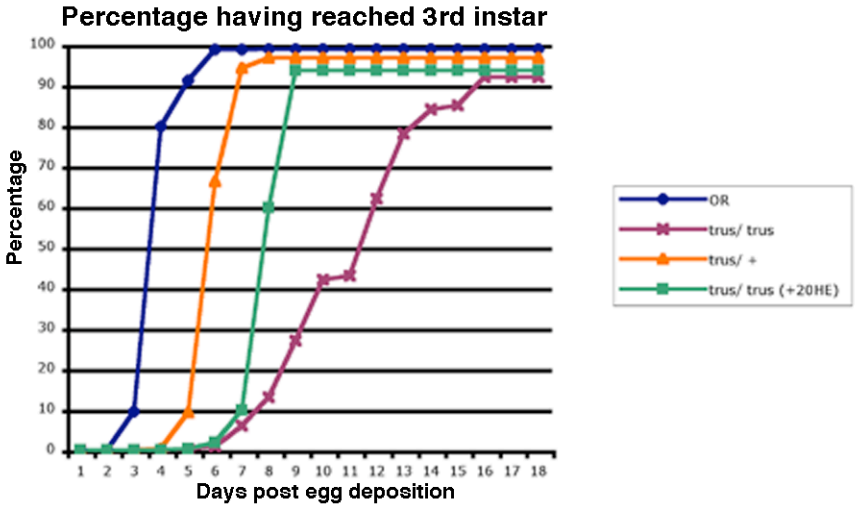
Percentage having reached 3rd instar
Percentage
Days post egg deposition
OR
trus/ trus
trus/ +
trus/ trus (+20HE)

B.

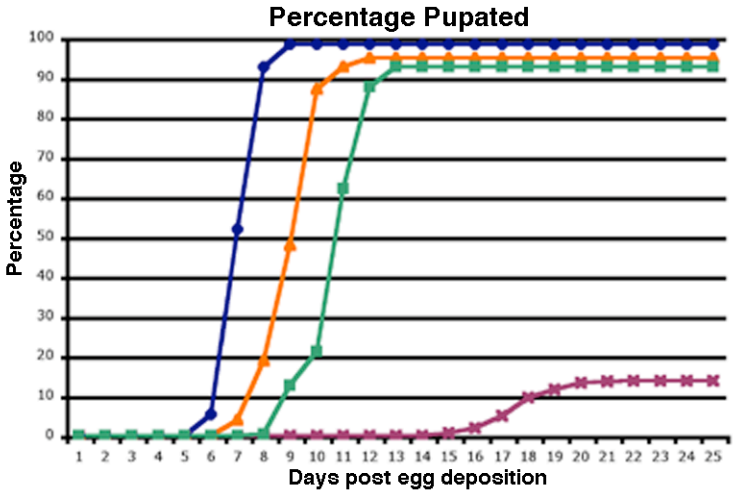
Percentage Pupated
Percentage
Days post egg deposition

C.

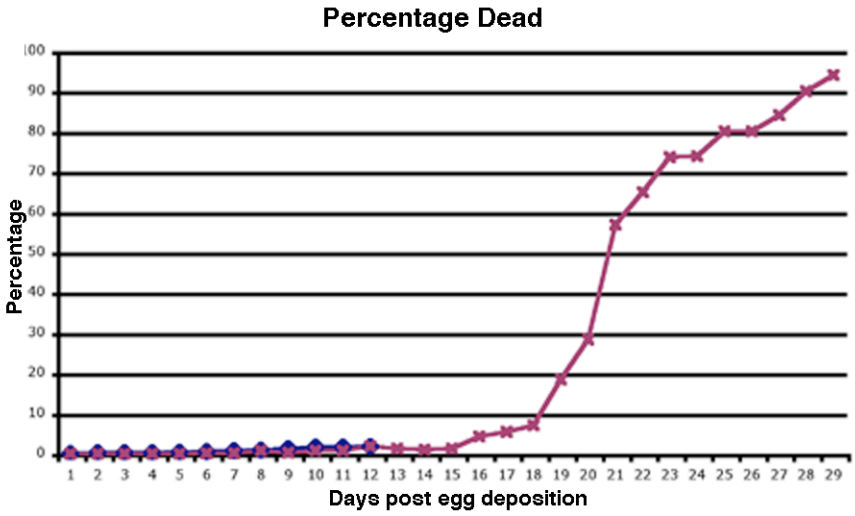
Percentage Dead
Percentage
Days post egg deposition

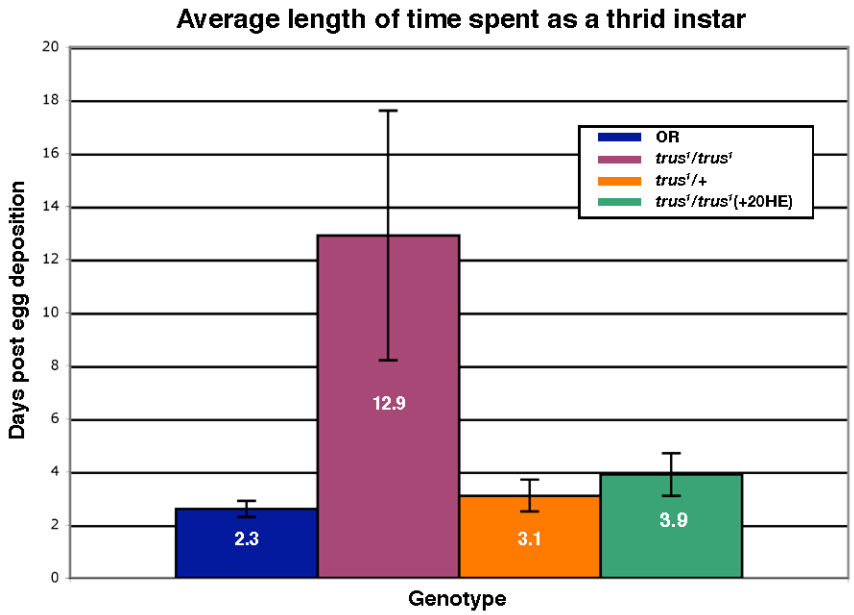

Figure 2.6 *trus*^{1} mutants spend an extended period as third instar larvae

Homozygous mutant larvae that are unable to pupariate do not die immediately, but instead spend a considerable amount of time (up to 16 days) as third instar larvae. The feeding of 20HE is also able to rescue this phenotype, as was seen with the developmental delays (see Figure 2.5)

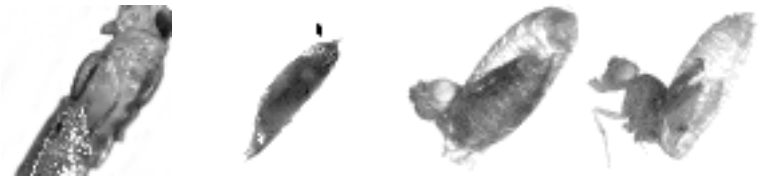

	Normal eclosion	Pupal lethal	Head eclosion	Half body eclosion	n
OR 25˚C	100	<1	0	0	500
OR 30˚C	97.2	2.6	<1	0	1289
***trus*[1] 25˚C**	100	<1	0	0	750
***trus*[1] 30˚C**	64.8	25.1	3.1	7.1	512
ecd*[1] *25˚C	95.2	4.1	<1	0	420
ecd*[1] *30˚C	76	19.2	2.9	1.7	140
trus/+; ecd/+ 25˚C	97.1	2.9	0	0	107
trus/+; ecd/+ 30˚C	44.0	40.3	5.4	10.3	853

Table 2.1 Eclosion phenotypes at 25˚C and 30˚C Normal eclosion is occurs quickly with the fly emerging from the top of the pupal case in approximately 30 seconds. Pupal lethals often have a characteristic air bubble showing their inability to invert their head (which is an early step of metamorphasis), as well as mass cell death visible with the naked eye. Some pharate adults are able to begin the eclosion process but unable to complete eclosion and die stuck in their pupal case. *ecdysoneless*[1] is known to be a temperature sensitive allele, however, I was surprised to discover that at 30˚C *trus*[1] heterozygotes also exhibit a temperature sensitive pupal and eclosion phenotype. When animals carrying the temperature-sensitive mutation *ecd*[1] are raised at restrictive

temperature, they exhibit similar phenotypes, suggesting that the developmental issues associated with *trus*^{1} mutations might be related to decreases in the ecdysone titer.

The larval lethality of *trus*^{1} mutants can be rescued by an ecdysone-enriched diet

Several of our observations suggested the possibility that the phenotypes associated with *trus*^{1} mutations might be due to defects in ecdysone-related pathways. First, several mutants in the genes involved in these pathways exhibit developmental defects similar to those we describe above for *trus*^{1} mutants. Second, we saw low proliferation of optic lobe neuroblasts; in *Manduca sexta*, this specific phenotype is seen in animals with low ecdysteroid levels (Champlin and Truman, 1998). Finally, the Trus protein accumulates to its highest levels in tissues that are involved in ecdysone synthesis.

I used a feeding strategy to determine whether the *trus*^{1} phenotypes described above are caused by a lack of ecdysone. Larvae that are competent to undergo molts to the next stage but are unable to do so because of a deficiency in ecdysone can be rescued to the next stage by the addition of ecdysone to their food (Garen et al., 1977; Riddiford, 1993). When 0.5 mg/ml of 20-Hydroxyecdysone (20HE) was fed to second instar *trus*^{1} larvae, it increased the rate at which they reached the third instar stage. 20HE-fed animals reached the third instar an average of 7.8 days post hatching (Figure 2.5 A), significantly later than the 3.9 days required for wild type animals, but significantly earlier than the 12.5 days needed by mutant siblings that are not fed ecdysone. Even more dramatic is the increase in pupariation, from 12.5%

in unfed populations to 92% with an ecdysone-enriched diet (Figure 2.5 B). This ability to pupariate represents rescue of the phenotype even though the animals die at this stage (Ono et al., 2006), since they have stopped feeding at the wandering third instar stage of development and so are no longer aided by the ecdysone enriched food.

If Trus was acting in the pathway that converts cholesterol to 20HE, we could in theory narrow down the step of its action by testing the ability of intermediates in the pathway to rescue the developmental delay and ability to pupariate. Trus does not have any sequence similarity with cytochrome p450 or other known enzyme in this pathway, however, it remains possible that Trus plays an unknown direct or indirect role in a specific part of the pathway. I found that Cholesterol, 7dC, Ecdysone, and 20HE were all able to rescue the pupariation defect of *trus*^{1} mutants (Table 2.2). The rescue effected by earlier precursors such as Cholesterol was weaker than that produced by 20HE feeding, but this same effect has previously been noted in the rescue of genes known to function early in the pathway (Ono et al., 2006). This decrease in efficiency possibly is due to the need to coordinate the timing of multiple pathways involved in ecdysone synthesis and signaling that is not fulfilled when animals are presented with any form of exogenous ecdysone or its precursors.

Table 2.2 Percentage eclosion based on sterol additions to media

	Cholesterol	7dC	Ecdysone	20 HE	EtOH only	dH20 only
OR	93	93	100	100	95	95
trus / trus	14	31	75	95	5	6
trus / +	100	94	92	100	97	95
*dis /dis**	0	0	20	27	0	0

disembodied (*dis*) is the gene that codes for CYP302A1, which converts Ketotriol to 2-deoxyecdysone in the ecdysone synthesis pathway
(see Figure 1.1)

* sterols provided on plates from time of egg laying

Second-site noncomplementation of *trus*^{1} with mutations in known ecdysone pathway genes

Many animals that are simultaneously heterozygous for mutations in two different genes functioning in the edysone pathway (double heterozygotes) die as larvae or pupae, or display other developmental phenotypes including sterility (Bialecki et al., 2002). Many heterozygous ecdysone mutants appeared to have a normal phenotype in a *trus*^{1}/+ background (Table 2.3). However, animals simultaneously heterozygous for *trus* and mutations in any of several genes operating earlier in the pathway, including *ecd* and the ecdysone immediate genes *BrC, E74,* and *E75,* showed substantial decreases in fitness measured by their eclosion as adults (Table 2.3). In these latter cases, survivors that were able to eclose were then sterile. Sterility resulting from double heterozygosity was also seen in cases involving other mutations that at least partially complemented *trus*^{1} for viability, including *broad*^{1}*, ecd*^{1}*, and EcR*^{Q50st}.These genetic interactions with ecdysone-related genes provides yet more assurance that Trus also acts somewhere in the ecdysone pathway.

Expression levels of proteins up-regulated by ecdysone are low in *trus*^{1} mutants

Since ecdysone directly up-regulates EcR, the expression level of EcR in the larvae can be used as a crude measurement of ecdysone titer (Bender et al., 1997). I determined EcR protein levels by Western blot analysis, and found that in *trus*^{1} third instar larvae, the concentration of EcR is 19 times lower than in their wild type counterparts (Figure 2.7 A).

Table 2.3 double heterozygote phenotype with *trus*[1]

	Lethal	Sterile
br[1]	No[a]	Female
br[npr-3]	Male	Female
dib[2]	No	n/a
ecd[1]	Partial[b]	Female
EcR[6410]	Yes	n/a
EcR[Q50st]	Partial	Yes
EF1a48D	Partial	Yes
Eip74EF[Dl-1]	Partial	No
Eip75[A81]	Partial	No
ftz-f1[BG01734]	No	No
InR[05545]	Partial	Female
l(2)gl[01433]	No	n/a
Mef2[X1]	No	No
Pep[KG00294]	No	n/a
Pfk[06339]	No	n/a
rig[05056]	No	n/a
sop[c01273]	No	Female
spo[1]	No	No
trol[13]	Partial	n/a
Usp[4]	No	Male[d]
Zfrp8	No[c]	No

a: not lethal but has dorsal appendage phenotype and slow development
b: partial lethality is defined as less than 50% of expected double heterozygotes
c: double homozygotes are embryonic lethal
d: *Usp* males are hemizygous sterile without *trus*
n/a : not assayed

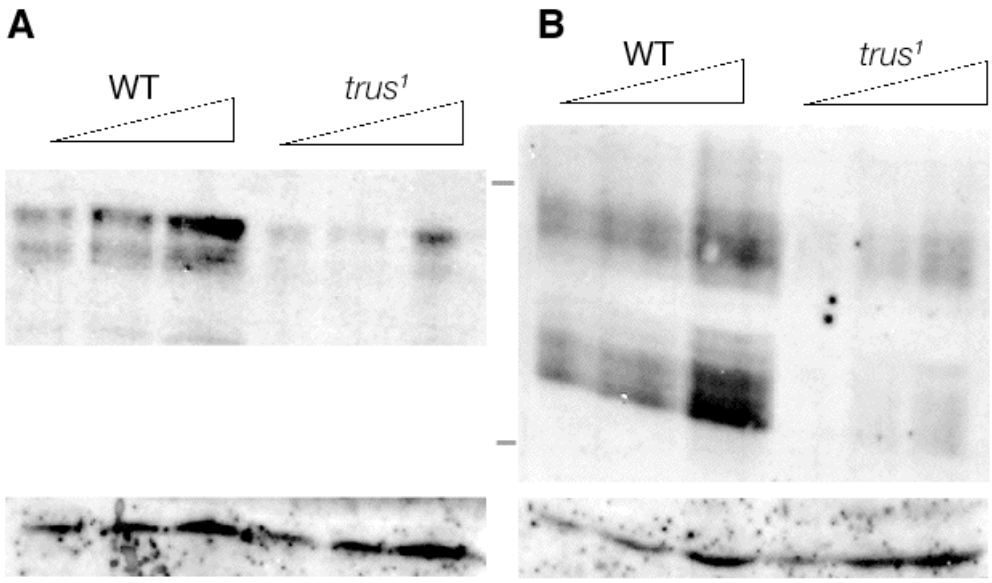

Figure 2.7 Expression of EcR and BrC is significantly decreased in *trus*[1] mutants

Wild type and mutant larvae were normalized by weight (rather than by number, since *trus*[1] mutants are smaller than wild type. Wild type extracts were loaded in amounts corresponding to approximately 1/4, 1/2, and 1 larvae. (A) The *trus*[1] mutants appear to have significant decreased expression of EcR. (B) Not surprisingly (since Broad is up-regulated by EcR), the concentration of BrC is also significantly reduced in *trus* mutant animals; the effect seems to be consistent for all of the isoforms of Broad. The antibody used is against the Broad core that is expressed in all of the isoforms. Size markers delineated by grey lines between the panels are 100 and 70 kD, respectively. The loading control is α-Tubulin.

Expression of the Broad Complex is also significantly decreased in *trus*^{1} mutant larvae (Figure 2.7 B), which is expected since the BrC is up-regulated by the ecdysone, USP, EcR heterotrimer (Bayer et al., 1997).

The expression of all isoforms of EcR and BrC appears to be equally affected. Since some of these isoforms are tissue specific (Bayer et al., 1997; Bender et al., 1997), this finding suggests that the effect of the *trus*^{1} mutant is not tissue specific but is instead more general. This further suggests that Trus acts to regulate ecdysone synthesis and thus systemic levels of this hormone, rather than participating in an early response to ecdysone or the ability of the organism to respond to ecdysone.

Trus forms one or more complexes with String of Pearls and perhaps with Elongation Factor 1 alpha

To search for possible Trus interactors, we used the Tap-tagging system described by (Veraksa et al., 2005), which identifies interactions that form at least transiently stable complexes. Drosophila S2 tissue culture cells expressing a Tap-Trus fusion were lysed, and interacting proteins were isolated by affinity chromatography against the tag. The final eluate from the affinity column had two major bands and one band of somewhat lower intensity that were not found in controls (Figure 2.8). One of these bands was (as expected) Trus itself; this band assignment was verified both by Western blotting with anti-Trus and by mass spectrometry. It should be noted that the Trus band migrated on gels at ~70 kD, and thus had the same mobility as the Western blot band assigned to Trus in larval extracts (see Figure 2.2 above). The other major band (band 3 on Figure 2.8) is String of Pearls (Sop), which is the S2 subunit of the 40S ribosomal subunit (Cramton and Laski, 1994).

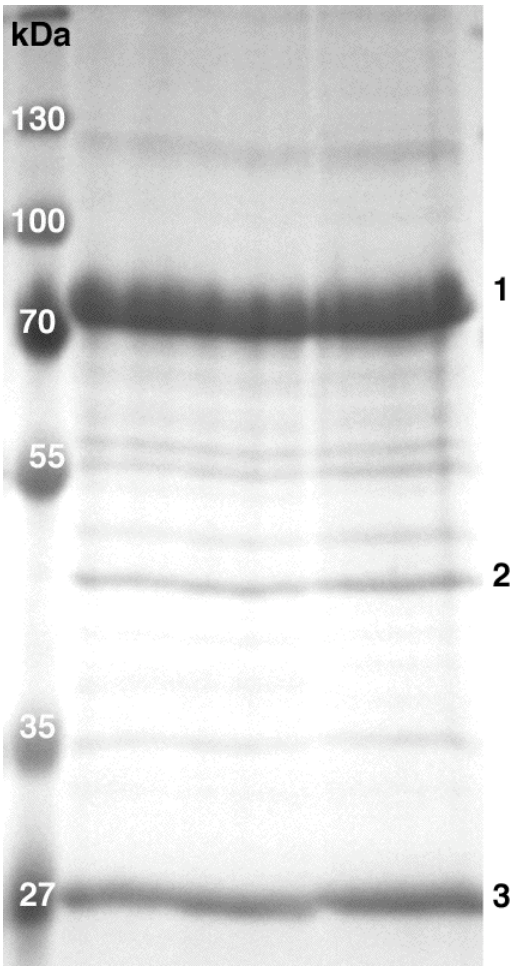

Figure 2.8 Tap-tagging reveals stable binding of Trus with Sop and Ef1-α

The three strongest bands visualized with Coomassie Blue staining on a SDS-Page gel after Tap-tagging with Trus are (1) Trus (2) Ef1-α and (3) Sop. Identifications were made using MALDI-Mass spectrometry. To limit false positives, bands selected for mass spectrometry were unique when compared against proteins pulled down with a tag only construct and also other Tap-tagged proteins in the lab.

Mass spectrometry determined that the minor band (band 2 on Figure 2.8) is Elongation Factor 1-alpha (EF1-α-48D), a factor that plays a role in shuttling tRNAs to the ribosome during translation (Negrutskii and El'skaya, 1998).

From a global yeast two hybrid interaction screen with *Drosophila* proteins, Giot and colleagues (2003) obtained additional data indicating that Trus can associate with Sop. We are less confident that Trus truly forms a complex with EF-1α, since this latter protein is very highly abundant. However, we have never detected EF-1α as in the final eluate of Tap-tagging experiments with several other baits, and the fact that both Sop and EF-1α are involved in translation further suggests that this interaction may be real.

Trus fails to co-sediment with ribosomes or polysomes

Based on the results in the previous section, we hypothesized that Trus would interact with Sop and/or EF1-α within the context of a ribosomal subunit or intact ribosome. To test this possibility, we fractionated cytoplasmic extracts of tissue culture cells on sucrose gradients and examined the sedimentation of Trus relative to that of the ribosomal subunits and ribosomes (which were detected with antibodies against components of the two ribosomal subunits). Surprisingly, Trus did not co-sediment with ribosomal units, ribosomes, or polysomes. Instead, Trus migrated at a position corresponding with lower molecular weight components (Figure 2.9).

Figure 2.9 Sucrose gradients show Trus does not associate with ribosomal subunits or intact ribosomes.

(A) Fractions of a 7.5-60% sucrose gradient were run on an SDS-page gel and then subjected to Western blot analysis with antibodies against translation factors and ribosomal proteins (HRPA is a component of the 60S subunit; while RpS25 is a component of the 40S subunit). Trus does not fractionate with ribosomal subunits, intact ribosomes, or polysomes. However, Trus is present in the same fractions as Ef1-α, consistent with their possible interaction. It also remains possible that Trus interacts with Sop in the early (lower molecular weight) fractions, but this hypothesis cannot currently be tested due to the lack of an antibody against *Drosophila* Sop. All work in panel A was completed by Ditte Andersen (see materials and methods for details). (B) Further sucrose gradients and western blots verify that Trus migrates in a low molecular weight fraction much smaller than ribosomes. RNA concentration in each fraction was determined by UV spectroscopy.

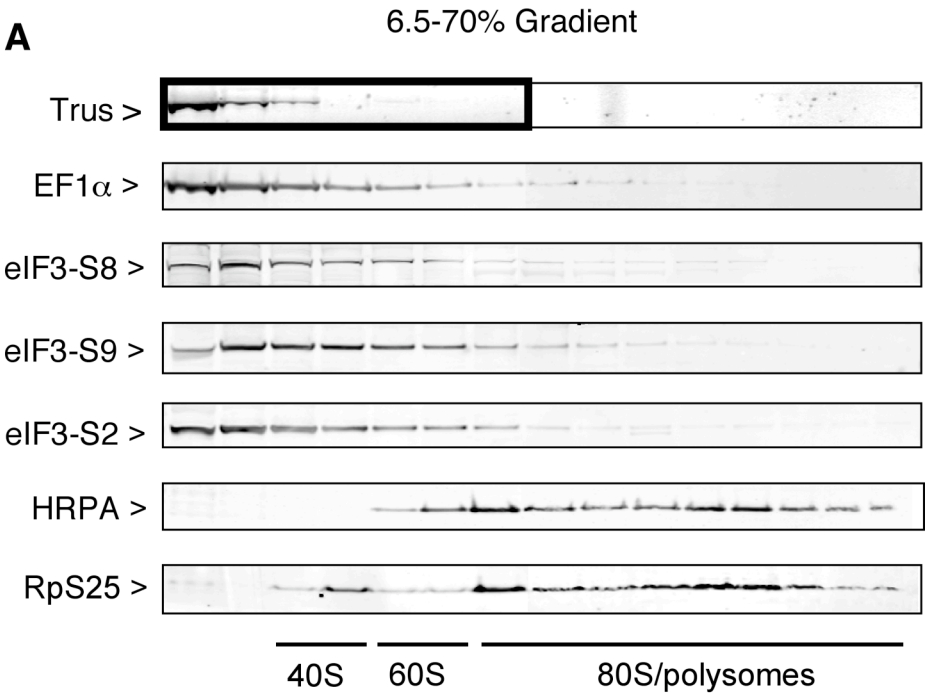
A
6.5-70% Gradient
Trus >
EF1α >
eIF3-S8 >
eIF3-S9 >
eIF3-S2 >
HRPA >
RpS25 >
40S
60S
80S/polysomes

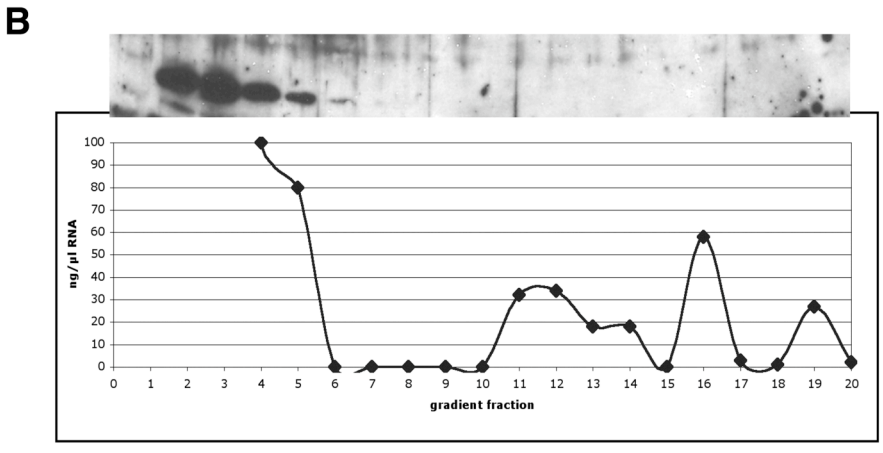
B
ng/µl RNA
gradient fraction

The mouse homologue of *trus,* (*pdcd2l*) is expressed in discrete areas of the brain in developing embryos[3]

Trus is conserved in all eukaryotic organisms from plants to humans. While ecdysone does not exist outside of holometabolous insects and molting arthropods, many of the proteins involved in ecdysone signaling are used for signaling by other hormones in higher organisms (Gilbert et al., 2002). We therefore were interested in examining the expression pattern of *pdcd2l* (*trus*) in the mouse; in particular to determine whether it is specifically expressed in tissues involved in hormone manufacture that might be analogous to the fly's ring gland.

Two stages of early mouse development were examined by in situ hybridization for *pdcd2l* mRNAs. At embryo stage e8.5 (e8.5 is 8.5 days post-partum), staining was restricted to neural tissue and epithelial layers (Figure 2.10A). The neural tissue staining was the strongest in the cephalic neural fold (developing forebrain) and in the neural epithelium. The anterior-most section of the developing head showed the highest level of staining (Figure 2.10E,G,I). The staining seen in the epithelial layers was non-mesenchymal in nature. It is also possible that the inside of the yolk sac and the amnion stain weakly for Trus, but further *in situs* would be needed to confirm this result. Of interest to hormone signaling at this age of development, there was no staining in the outer yolk sac, the trophoblast (developing placenta), or even any other neural tissues including the neural tube.

[3] This section was done in collaboration with the Garcia Lab, MBG, Cornell University. Mouse cDNA was isolated and prepared by Dr. Garcia, and all *in situ* work was done by Dr. Maegan Harden. For protocols on the techniques used see Nagy, A. (2003).

Figure 2.10 Mouse Trus (*pdcd2l*) is expressed in specific regions of the brain in 8.5e and 10.5e embryos.

(A,B) Whole mount *in situ* hybridizations. (A) Embryos 8.5 days post partum (e8.5) are devoid of staining in the trophoblast. Scale bar = 0.5 mm. (B) By e10.5, staining of *trus* is isolated to the head region of the animal. Scale bar = 1 mm. (C,D) Diagrams depicting essential regions of the e8.5 and e10.5 embryos. Red lines show the region and the angle of dissected sections for panels E-J. (E,G) Sections through the brain region of e8.5 embryos show Trus expression within neural and epithelial layers including the yolk sac. Scale bar = 7 mm. (F) Section of the developing head of an e10.5 embryo. Staining is epithelial, on the interior of the telencephalic vesicles "T", developing mid brain "M" and hindbrain "H". Scale bar = 1.5 mm. (H) Higher magnification of F showing a strongly stained region of cells of unidentified lineage (arrowhead) as well as the epithelial staining. Scale bar = 7 mm. (I,J) Higher magnifications showing the cells staining within the epithelial layers of the developing brain. Scale bar = 5 mm.

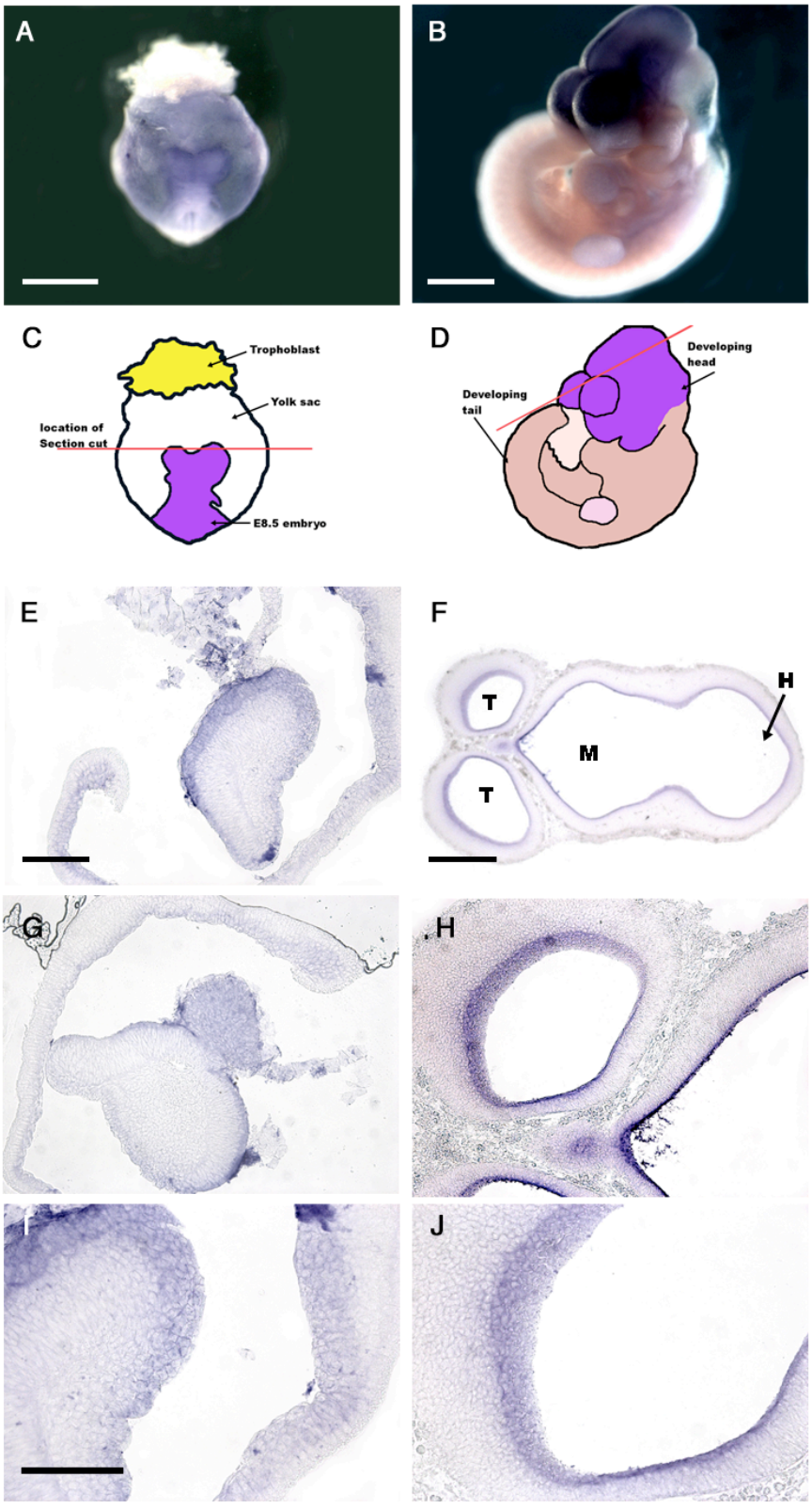
A
B
C
Trophoblast
Yolk sac
location of
Section cut
E8.5 embryo
D
Developing
head
Developing
tail
E
F
T
M
T
H
G
H
I
J

The yolk sac controls signaling from the outside environment, the trophoblast controls the passage of signals, nutrients, and hormones between the mother and the embryo, and the neural tube is a site of signaling within the developing embryo.

At e10.5, the staining pattern was similar to that at e8.5 in that signal was only seen in the developing head (Figure 2.10B,F,H,J). However, at this later time, *trus* expression was observed in the midbrain and hindbrain as well as the forebrain. This staining was not diffuse, and seemed to be restricted to certain areas of these broader regions.

DISCUSSION

We have identified a novel protein with a critical function in ecdysone synthesis in *D. melanogaster*. This protein, Trus, is the *Drosophila* homolog of mammalian PDCD2L, contains a conserved putative Programmed Cell Death Domain. Trus and its mouse homolog are expressed in the cytoplasm of specific cells and tissues.

We have shown that Trus interacts genetically with multiple members of the ecdysone pathway. Trus also decreases expression of EcR and BrC, which are ecdysone immediate genes that are up-regulated by ecdysone. Further, the larval lethality exhibited by *trus*^{1} mutants is rescued by augmenting their food with 20HE. All of these results indicate that Trus plays a role in the synthesis of ecdysone. This idea is also consistent with the high level of Trus expression in the prothoracic cells of the ring gland, since these are the cells most involved in ecdysone synthesis in developing larvae.

Tap-tagging experiments have identified the small ribosomal protein Sop and the translation factor Ef1-α as potential Trus interactors, suggesting

that Trus is involved in a mechanism that activates the translation of mRNAs encoding proteins involved in ecdysone synthesis. There are several precedents for translational controls in hormone biogenesis. In mice, Ef1-α and RpS6 (a component of the small ribosomal subunit) are both targets of S6 kinase during insulin signaling (Chang and Traugh, 1997). In the moth *Manduca,* RpS6 has been proposed to be essential for PTTH-sensitive gated translation in the ring gland. Although Sop is also a part of the 40S ribosome in *Drosophila*, we have found no evidence that Trus associates with the intact 40S subunit. It is possible that Trus became dissociated from ribosomes during the sucrose gradient fractionation shown in Figure 2.9; for example, since Ef1-α is a GTP-binding protein, Trus binding to ribosomes might be conditional upon the addition of a non-hydrolyzable GTP analog to the buffers in which the cell extract was made and in which the gradient was run. If this is not the case, it remains possible that Trus might nonetheless associate with Sop and/or Ef1-α in small complexes that regulate the ability of these proteins to interact with the intact ribosome, thus allowing Trus to regulate the translation of proteins needed for ecdysone synthesis.

The mouse homolog of Trus is expressed early in development and is restricted to certain neural tissues and certain undefined cell populations within these tissues. However, our limited data provide no support for the hypothesis that PDCD2L plays a function in mice analogous to its role in *Drosophila* ecdysteroid synthesis, since we failed to detect PDC2L expression in tissues involved in hormone synthesis. It remains possible that we simply looked at mouse embryos that were too young to have initiated certain kinds of hormonal signaling, but it is also possible that PDC2L plays other roles in

mouse development. These questions can only be answered by examining mice “knocked-out” for this gene.

LITERATURE CITED

Andersen, D. S. and Leevers, S. J. (2007). The essential Drosophila ATP-binding cassette domain protein, pixie, binds the 40 S ribosome in an ATP-dependent manner and is required for translation initiation. *J Biol Chem* **282**, 14752-60.

Andres, A. J. and Thummel, C. S. (1992). Hormones, puffs and flies: the molecular control of metamorphosis by ecdysone. *Trends Genet* **8**, 132-8.

Bayer, C. A., von Kalm, L. and Fristrom, J. W. (1997). Relationships between protein isoforms and genetic functions demonstrate functional redundancy at the Broad-Complex during Drosophila metamorphosis. *Dev Biol* **187**, 267-82.

Bender, M., Imam, F. B., Talbot, W. S., Ganetzky, B. and Hogness, D. S. (1997). Drosophila ecdysone receptor mutations reveal functional differences among receptor isoforms. *Cell* **91**, 777-88.

Bialecki, M., Shilton, A., Fichtenberg, C., Segraves, W. A. and Thummel, C. S. (2002). Loss of the ecdysteroid-inducible E75A orphan nuclear receptor uncouples molting from metamorphosis in Drosophila. *Dev Cell* **3**, 209-20.

Champlin, D. T. and Truman, J. W. (1998). Ecdysteroid control of cell proliferation during optic lobe neurogenesis in the moth Manduca sexta. *Development* **125**, 269-77.

Chang, Y. W. and Traugh, J. A. (1997). Phosphorylation of elongation factor 1 and ribosomal protein S6 by multipotential S6 kinase and insulin stimulation of translational elongation. *J Biol Chem* **272**, 28252-7.

Chen, Q., Qian, K. and Yan, C. (2005). Cloning of cDNAs with PDCD2(C) domain and their expressions during apoptosis of HEK293T cells. *Mol Cell Biochem* **280**, 185-91.

Cramton, S. E. and Laski, F. A. (1994). string of pearls encodes Drosophila ribosomal protein S2, has Minute-like characteristics, and is required during oogenesis. *Genetics* **137**, 1039-48.

Demerec, M. (1950). Biology of Drosophila. New York,: Wiley.

Garen, A., Kauvar, L. and Lepesant, J. A. (1977). Roles of ecdysone in Drosophila development. *Proc Natl Acad Sci U S A* **74**, 5099-5103.

Gatti, M. and Goldberg, M. L. (1991). Mutations affecting cell division in Drosophila. *Methods Cell Biol* **35**, 543-86.

Gilbert, L. I., Rybczynski, R., Song, Q., Mizoguchi, A., Morreale, R., Smith, W. A., Matubayashi, H., Shionoya, M., Nagata, S. and Kataoka, H. (2000). Dynamic regulation of prothoracic gland ecdysteroidogenesis: Manduca sexta recombinant prothoracicotropic hormone and brain extracts have identical effects. *Insect Biochem Mol Biol* **30**, 1079-89.

Gilbert, L. I., Rybczynski, R. and Warren, J. T. (2002). Control and biochemical nature of the ecdysteroidogenic pathway. *Annu Rev Entomol* **47**, 883-916.

Klemenz, R., Weber, U. and Gehring, W. J. (1987). The white gene as a marker in a new P-element vector for gene transfer in Drosophila. *Nucleic Acids Res* **15**, 3947-59.

Korge, G. (1977). Direct correlation between a chromosome puff and the synthesis of a larval saliva protein in Drosophila melanogaster. *Chromosoma* **62**, 155-74.

Koundakjian, E. J., Cowan, D. M., Hardy, R. W. and Becker, A. H. (2004). The Zuker collection: a resource for the analysis of autosomal gene function in Drosophila melanogaster. *Genetics* **167**, 203-6.

Minakhina, S., Druzhinina, M. and Steward, R. (2007). Zfrp8, the Drosophila ortholog of PDCD2, functions in lymph gland development and controls cell proliferation. *Development* **134**, 2387-96.

Nagy, A. (2003). Manipulating the mouse embryo : a laboratory manual. Cold Spring Harbor, N.Y.: Cold Spring Harbor Laboratory Press.

Negrutskii, B. S. and El'skaya, A. V. (1998). Eukaryotic translation elongation factor 1 alpha: structure, expression, functions, and possible role in aminoacyl-tRNA channeling. *Prog Nucleic Acid Res Mol Biol* **60**, 47-78.

Ono, H., Rewitz, K. F., Shinoda, T., Itoyama, K., Petryk, A., Rybczynski, R., Jarcho, M., Warren, J. T., Marques, G., Shimell, M. J. et al. (2006). Spook and Spookier code for stage-specific components of the ecdysone biosynthetic pathway in Diptera. *Dev Biol* **298**, 555-70.

Riddiford, L. M. (1993). Hormone receptors and the regulation of insect metamorphosis. *Receptor* **3**, 203-9.

Robinow, S., Campos, A. R., Yao, K. M. and White, K. (1988). The elav gene product of Drosophila, required in neurons, has three RNP consensus motifs. *Science* **242**, 1570-2.

Scarr, R. B. and Sharp, P. A. (2002). PDCD2 is a negative regulator of HCF-1 (C1). *Oncogene* **21**, 5245-54.

Veraksa, A., Bauer, A. and Artavanis-Tsakonas, S. (2005). Analyzing protein complexes in Drosophila with tandem affinity purification-mass spectrometry. *Dev Dyn* **232**, 827-34.

Williams, B. C., Karr, T. L., Montgomery, J. M. and Goldberg, M. L. (1992). The *Drosophila zw10* gene product, required for accurate mitotic chromosome segregation, is redistributed at anaphase onset. *J Cell Biol* **118**, 759-73.

Yao, K. M. and White, K. (1994). Neural specificity of elav expression: defining a Drosophila promoter for directing expression to the nervous system. *J Neurochem* **63**, 41-51.

CHAPTER 3

DEVELOPMENTAL AND CELL CYCLE PROGRESSION DEFFECTS IN *DROSOPHILA* HYBRID MALES[4]

ABSTRACT

Matings between *D. melanogaster* females and males of sibling species in the *D. melanogaster* complex yield males that die prior to pupal differentiation. We have re-examined a previous report suggesting that the developmental defects in hybrid males may be the consequence of problems in mitotic chromosome condensation. We find in contrast that the frequencies of mitotic figures and of nuclei staining for the mitotic marker Phosphohistone H3 in the brains of hybrid male larvae are extremely low. We also find that very few of these brain cells in hybrids are in S phase, as determined by BrDU incorporation. The cells in hybrid male brains appear to be particularly sensitive to environmental stress; our results indicate that certain in vitro incubation conditions induce widespread cellular necrosis in these brains, causing an abnormal nuclear morphology noticed by previous investigators. We also document that hybrid larvae develop very slowly, particularly during the second larval instar.

INTRODUCTION

Speciation requires reproductive isolation between diverging populations (Mayr, 1942). One type of barrier that can isolate emerging species is the inviability or infertility of hybrids. For example, although the

[4] This chapter is modified from a paper submitted to Genetics. 2007. Bonnie J. Bolkan, Ronald Booker, Michael L. Goldberg and Daniel A. Barbash. Daniel Barbash is corresponding author.

species in the *Drosophila melanogaster* complex (*D. melanogaster* and its sibling species *D. simulans, D. mauritiana,* and *D. sechellia*) are very closely related and morphologically almost indistinguishable, matings between *D. melanogaster* females and males of any of the sibling species yield F1 females that are semi-viable but sterile, as well as males that die as developmentally delayed larvae or pseudopupae with small or nonexistent imaginal disks (Sturtevant, 1920; Sturtevant, 1929; Hadorn, 1961; Sánchez, 1983).

The lethality of hybrid males appears to be due to an incompatibility between one or more genes on the *D. melanogaster* X chromosome and one or more autosomal genes in the other species (Sturtevant, 1920; Sturtevant , 1929; Pontecorvo, 1943; Hadorn, 1961; Hutter et al., 1990; Yamamoto, 1992; Brideau et al., 2006). Hybrid lethality is not sex-specific, since hybrid females homozygous for the *D. melanogaster* X chromosome also die at the same stage of development (Hutter et al., 1990; Orr, 1993). The X-linked *Hybrid male rescue* (*Hmr*) gene in *D. melanogaster* and the *Lethal hybrid rescue* (*Lhr*) gene in *D. simulans* are major players in causing this hybrid lethality because loss-of-function alleles in these genes suppress the lethality (Watanabe, 1979; Hutter and Ashburner, 1987; Barbash et al., 2000; Barbash et al., 2003; Brideau et al., 2006). Despite this progress in studying the genetic basis of hybrid male inviability, the developmental causes of the phenomenon remain poorly understood. One study proposed that hybrid males suffer from limited cell proliferation due to a failure in mitotic chromosome condensation (Orr et al., 1997). The investigators observed that the brains of hybrid male larvae incubated in 0.7% NaCl and in both the presence and absence of colchicine (a drug used to arrest cells in metaphase) contained very few normal mitotic

figures, but many cells displayed masses of diffuse chromatin. These latter cells were interpreted to have entered a defective mitosis in which the chromatin remains under-condensed relative to that normally seen in the prometaphase/metaphase mitotic figures in neuroblasts from each pure species.

To better understand the nature of the apparent chromosome condensation defects in hybrid male larval brains, we wished to characterize this phenotype with techniques developed since the publication of the earlier report. To our surprise, we found that the frequency of mitosis in these brains is extremely low. Although we observed in 0.7% NaCl-incubated brains the same high frequency of cells with masses of diffuse chromatin seen by the previous investigators, we established that these cells were not in mitosis but were instead dying. The very low mitotic index in the brains of male hybrid larvae is reflected in the extremely slow progression of these animals through the second larval instar stage of development. Our results suggest that the cells of hybrid male larvae display physiological defects that prevent mitotic entry and that render them particularly susceptible to cell death when environmentally stressed.

MATERIALS AND METHODS

Fly strains and cultures

Flies were reared on standard yeast glucose media and raised at 23°C on a 12 hr light / 12 hr dark cycle. All hybrid crosses were initiated with one-day-old *D. melanogaster* virgin females and 5-day-old *D. simulans* males. *D. melanogaster* females were either y^1 w^1 received from the Drosophila stock

center (Bloomington, IN) or *Df(1)Hmr⁻, y w v / FM7i, P{w^{+mC}=ActGFP}JMR3* (Barbash and Lorigan, 2007). All *D. simulans* males were *vermilion / Y*.

Cytology for Analysis of Mitosis

Larval brains were dissected, fixed, and squashed as described in Williams *et al*. (1992) except that incubation in 3.7% formaldehyde was decreased to 20 min. Incubations with antibodies were done overnight at 4°C in phosphate buffered saline (PBS) containing 0.1% Triton X (PBT). Rabbit anti-Phosphohistone H3 (Upstate, Charlottesville, VA) was used at a 1:500 dilution followed by incubation with TRITC (tetrarhodamineisothiocyanate)-conjugated anti-rabbit IgG (Jackson Immunoresearch, West Grove, PA), and DNA was detected by staining with 0.05 μg/ml Hoechst 33742 (Sigma, St. Louis, MO) in PBS for 5 min. Imaging was done on an Olympus BX-50 microscope with a Qimaging Retiga Exi CCD camera (Burnaby, BC, Canada) and MetaMorph 6.1 software (Universal Imaging, Downington, PA).

For aceto-orcein staining, larval brains were dissected in 0.7% NaCl and transferred immediately to a drop of aceto-orcein stain (2% orcein in 45% acetic acid) on a cover slip and squashed onto a glass slide (Gatti and Goldberg, 1991). In some experiments, brains were incubated in 0.5×10^{-5} M colchicine in 0.7% NaCl for 0.5, 1, or 2 hrs after dissection prior to transfer to aceto-orcein. Mitotic indices were determined as previously described (Williams et al., 1992); briefly, the mitotic index of a sample was defined as the number of PH3-staining mitotic cells per standard field of view at 1000X magnification. Individual stages of mitosis were scored in PH3-positive cells. Cells in prophase and prometaphase were characterized by their relatively low levels of chromosome condensation. Metaphase figures were scored on the

basis of their more highly condensed chromosomes. Anaphase and telophase were identified by the separation of chromatids into distinct populations, but these two stages could not be separately distinguished.

Determination of S Phase using Bromodeoxyuridine

Whole dissected brains were incubated in Grace's Media plus 1mg/ml 5-Bromo 2-Deoxyuridine (BrDU; Sigma) for 1 hr, and then fixed, permeabilized, and antibody stained as described in (Truman and Bate, 1988). Mouse anti-BrDU and rat anti-Elav were used at a dilution of 1:150 in PBT overnight at 4˚C. These antibodies were received from the Developmental Studies Hybridoma Bank developed under the auspices of the NICHD and maintained by the University of Iowa, Department of Biological Sciences, Iowa City, IA 52242. After five 10-min washes in PBT, brains were incubated overnight at 4˚C with the following secondary antibodies: AlexaFluor 488-conjugated donkey anti-mouse (Molecular Probes, Eugene, OR) and Cy3-conjugated donkey anti-rat (Jackson Immunoresearch) diluted to 1:1000 in PBT + 1% donkey serum. Brains were imaged on a Leica TCS SP2 confocal microscope system.

Cell Death Assays

Cell death was assayed using Trypan Blue 0.4% (Gibco, Carlsbad, CA) at a 1:100 dilution in PBS. Brains were stained for 10 min and then rinsed for 10 min in PBS. As a positive control, cell death was induced in *D. melanogaster* y^1 w^1 brains by treatment for 1 hr in 100 mM cycloheximide immediately before Trypan Blue staining.

Apoptosis was detected using the Vybrant Apoptosis Assay Kit #2 (Molecular Probes) following the manufacturer's instructions. Whole brains were incubated for 20 min in a 1:4 dilution of Alexa Fluor 488-conjugated Annexin V stock solution in Annexin Binding Buffer (ABB). After a brief rinse in ABB, DNA was additionally counterstained for 5 min using To-Pro-3 (Molecular Probes) at $1x10^{-3}$ dilution in the same buffer. The brains were then mounted in 80% glycerol and imaged immediately on a Leica TCS SP2 confocal microscope. As a positive control, apoptosis was induced in *D. melanogaster* y^1 w^1 larvae by incubating dissected brains in 10 mM cycloheximide in 0.7% NaCl for 1 hr followed by recovery in Grace's media (Invitrogen, Carlsbad, CA) at 25°C for 30 min before treating as above to detect apoptosis.

Autophagic cell death was detected using LysoTracker Green DND-26 (Molecular Probes) as described in the product manual. Briefly, LysoTracker Green was diluted to 75 nM in Grace's media and warmed to 37°C. Dissected brains were incubated in the diluted LysoTracker at 37° for 1 hr before washing with PBS, counterstaining DNA with To-Pro-3, and imaging as above.

Ecdysone Feeding

20-Hydroxyecdysone (20HE; Sigma) was diluted to 1 mg/ml in 5% ethanol and mixed with 0.5 g dry yeast to make a yeast paste. Second- and third-instar larvae were transferred to plates containing the yeast paste and observed over time. Rescue of the developmental block was defined as a significant increase in the percentage of animals undergoing pupariation.

Larval staging and brain-size estimation

Females were allowed to lay eggs for a 24 hr period, and progeny were assayed for stage of development every 24 hrs after removal of adults. Larvae were staged by characterizing either mouth hook morphology or tracheal development. Mouth hooks were dissected from larvae and imaged at 400X magnification. Second-instar larvae have only 5-15 teeth per mouth hook, while third-instar larvae have 20-30 teeth per mouth hook (Demerec, 1950). For staging of live animals, larvae with unextended, balled trachea were classified as second instars, while larvae with extended trachea and inflated spiracles were classified as third instars (Park et al., 2002).

Brain sizes were measured as length of the ventral ganglion and width of the distance between the center of the larval brain hemispheres. Size was also estimated in squashes by the number of fields of view each brain occupied at 100X magnification.

RESULTS

Developmental Delays in Hybrid Males

It has long been known that the F_1 males resulting from crosses between *D. melanogaster* mothers and *D. simulans* fathers develop more slowly than their sister F_1 females or animals from either pure species (Sánchez, 1983). Since these developmental delays have never been described in detail, we took a closer look at the progression of hybrid males through the three larval instars and the pupal stage. Using the morphologies of both the mouth hooks and tracheal spiracles as markers to stage larvae (see Materials and Methods), we found that in comparison with controls, the hybrid males progress more slowly through each post-embryonic stage (Table 3.1), and died with high

frequencies at each step (Table 3.2). Controls included males and females of each pure species, hybrid females, and hybrid males rescued by a deletion of the *Hmr* gene, *Df(1)Hmr*$^{-}$. Developmental delay was particularly noticeable in the period preceding the molt into the third instar. While wild-type animals of either species spend approximately only 1 day as second-instar larvae, F_1 hybrid males remained in the second instar for more than 7 days on average. There was considerable variation in the length of the second-instar period. The slowest-developing hybrid-male second instars remained in that stage for 11-12 days (that is, until roughly 15 days after egg deposition). These animals became very large and could thus be mistaken for small third instars (Figure 3.1A), but the mouth hook and tracheal markers confirmed they were indeed in the second instar. All of these large second instars failed to molt and were thus responsible for the elevated lethality observed during the second-instar phase (Table 3.2). The majority (75.3%) of hybrid males eventually became third instars (Figure 3.1B). This third instar stage is also where the size difference in the brain became most distinct (Figure 3.1C-D, Table 3.3)Most of these third instars failed to pupariate, and died within 2-3 days of the second-to-third instar molt. A small number of hybrid males (6.7% of the total) pupariated; these tended to be the individuals that progressed most quickly through the second-instar phase. In all cases, pupariating animals died within 24 hours. Less than 1% of hybrid males were still alive at 16 days post egg deposition.

TABLE 3.1. Days post egg deposition taken to reach indicated stage of development

Genotype [a]	1st instar	2nd instar	3rd instar	Pupa	*n*
Hmr⁻/FM7 D. mel. f	1.3 ± .045	2.6 ± 0.62	3.7 ± 0.42	6.8 ± 0.35	903
Hmr⁻/Y D. mel. m	1.2 ± 0.24	2.4 ± 0.48	3.6 ± 0.36	6.7 ± 0.41	576
$y^1 w^1$ *D. mel*. [b]	1.2 ± 0.29	2.2 ± 0.62	3.5 ±0.53	6.8 ± 0.48	862
v_{sim} *D. sim*. [b]	1.3 ± 0.26	2.1 ± 0.47	3.4 ± 0.40	6.9 ± 0.43	625
FM7/X$_{sim}$ hybrid f	1.2 ± 0.21	2.0 ± 0.53	3.0 ± 0.38	6.3 ± 0.30	398
FM7/Y$_{sim}$ hybrid m	2.1 ± 0.56	4.1 ± 2.61	11.5 ± 4.8	12.1 ± 1.17	472
Hmr⁻/X$_{sim}$ hybrid f	1.3 ± 0.26	2.4 ± 0.46	3.6 ± 0.55	6.9 ± 0.69	637
Hmr⁻/Y$_{sim}$ hybrid m	1.5 ± 0.54	3.0 ± 0.81	4.4 ± 0.91	7.9 ± 1.90	452

[a] *D. simulans* chromosomes are indicated with the subscript "*sim*".

[b] Males and females were counted together.

TABLE 3.2. Lethality during indicated developmental stage

	% Lethality			
Genotype [a]	1st instar	2nd instar	3rd instar	pupal
Hmr^{-}/*FM7 D. mel.* females	2.1	1.1	<1%	1.0
Hmr^{-}/Y *D. mel*. males	2.0	0.9	<1%	1.1
$y^{1}w^{1}$ *D. mel*. [b]	1.0	<1%	<1%	1.2
v_{sim} *D. sim.* [b]	1.1	1.2	1.2	2.1
FM7/X_{sim} hybrid females	2.3	1.5	2.3	1.4
FM7/Y_{sim} hybrid males	5.3	19.4	68.6	6.8
Hmr^{-}/X_{sim} hybrid females	n/a[c]	1.2	1.8	1.2
Hmr^{-}/Y_{sim} hybrid males	n/a[c]	2.8	3.8	2.4

Larvae were raised at 23˚C and all *n*'s are > 100.

[a] *D. simulans* chromosomes are indicated with the subscript "*sim*".

[b] Males and females were counted together.

[c] Rescued hybrids were not scored at 1st instar.

Figure 3.1. **Developmental progress of hybrid males.** (A) Second instar hybrid males are smaller than pure species of the same age, but they can continue to grow and become much larger than wild type second instars. The smaller and larger hybrid male second instar larvae at the bottom are 6 days and 12 days post egg deposition, respectively. (B) Third instar male larvae are smaller than those of either pure species, but considerably larger than second instar hybrids. The hybrid third instar is 12 days post egg deposition. Scale bar = 1 mm for A and B. (C) Brains from hybrid second instar larvae are slightly smaller than those of the corresponding pure species stage (2.4 versus 2.6 mm in length on average, $n>20$). (D) By the third instar, the discrepancy in brain size becomes more obvious (3.2 versus 5.3 mm in length on average, $n>20$). Hybrid male third instar larvae also lack the imaginal discs seen in the pure species (arrows). Scale bar = 0.5 mm for C and D.

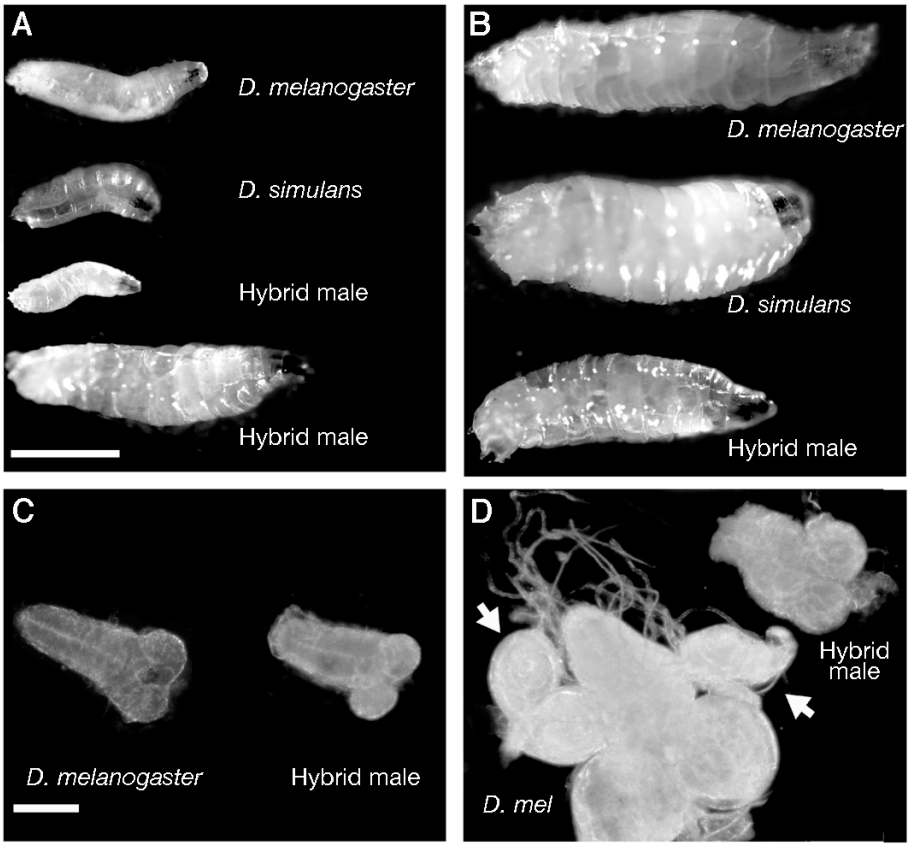
A
D. melanogaster
D. simulans
Hybrid male
Hybrid male
B
D. melanogaster
D. simulans
Hybrid male
C
D. melanogaster
Hybrid male
D
Hybrid male
D. mel

TABLE 3.3 Brain sizes

			Brain size (cm)			
	Instar	Days Old	Brain length (A)	Lobe width (B)	Ganglion width (C)	# of Brains scored
D.melanogaster	2nd	4	0.26	0.23	0.07	10
	3rd	6	0.53	0.39	0.1	10
Hybrid males	2nd	4	0.24	0.21	0.07	11
	2nd	11	0.31	0.24	0.14	11
	3rd	14	0.32	0.28	0.15	11

Defects in Ecdysone-Induced Behavior

Normal-sized hybrid second-instar larvae initiated the normal pre-molting behaviors of moving their bodies in an anterior-posterior fashion and biting with their mouth hooks to free the cuticle (Park et al., 2002). However, these animals often failed to molt, even after 30 minutes of trying, and returned to a wandering pattern of behavior.

As molting behaviors are induced by ecdysone (Park et al., 2002), we attempted to rescue these phenotypes by feeding the larvae 20-hydroxyecdysone at different stages of larval development (see Materials and Methods). This feeding, regardless of the protocol used, failed to rescue either the slow rate of development or the extended attempts at molting exhibited by hybrid males (data not shown). 20-hydroxyecdysone was however able to rescue the molting ability of control second- or third-instar larvae homozygous for mutations in the *Eip75B* gene, a gene that responds early within the ecdysone-induction pathway [(Segraves and Hogness, 1990); data not shown]. These results suggest that the developmental and behavioral abnormalities encountered by hybrid male larvae are unlikely to reflect defects in pathways mediated by ecdysone.

Low Mitotic Frequencies in Hybrid Male Larvae

It was previously proposed (Orr et al., 1997) that many cells in the brains of hybrid male larvae enter mitosis, but fail to condense their chromosomes properly and thus arrest in an aberrant prophase-like stage. To characterize these apparent mitotic defects in more detail, we examined preparations of larval brains stained either with orcein or with a combination of Hoechst 33742 (for DNA) and an antibody to phosphohistone H3 (anti-PH3) to

track mitotic chromatin (Hendzel et al., 1997). We were surprised to find a nearly complete absence of mitotic figures in second-instar hybrid male brains: usually only 0-1 cells per brain stained positive with anti-PH3. Third-instar hybrid male larval brains displayed more, but still very few mitotic figures (<10), as compared with several hundred PH3-staining cells in control single species brains from the same developmental stage (data not shown).

Of the few mitotic figures that were seen in the brains of hybrid male larvae, almost all were in prophase/prometaphase (79%) or metaphase (20%)(Figure 3.2), with less than 1% being in anaphase/telophase (Table 3.4). In contrast, about 20% of mitotic figures from pure species males are in anaphase/telophase. These data suggest that the spindle checkpoint may be activated in the very small number of hybrid male cells that do in fact enter mitosis. The deletion of *Hmr* in male hybrids returned the proportion of mitotic figures in anaphase/telophase to near single-species ratios, but the mitotic index remained somewhat lower than the controls (Table 3.4). Chromosome morphology in the rescued hybrid male larvae was often unusually elongated and spindly (Figure 3.3A,B). Thus, although the deletion of *Hmr* rescues the lethality of hybrid males, cell cycle progression in these animals is not completely normal.

TABLE 3.4. Percentage of mitotic figures in pure species and hybrid 3rd instar larvae

Genotype [a]	Percentage of mitoses in indicated stage			Mitotic index	Avg. no. fields / brain	Number of fields examined
	Prophase / prometaphase	Metaphase	Anaphase / telophase			
D. melanogaster males	70	10	20	0.56	103	947
D. melanogaster *Hmr*$^{-}$ males	71	10	19	0.60	109	526
D. melanogaster females	69	11	20	0.57	111	511
D. simulans males	70	11	19	0.59	106	932
D. simulans females	68	10	22	0.58	114	496
FM7/Y_{sim} hybrid males	79	20	<1	0.13	20	532
Hmr-/Y_{sim} hybrid males	70	13	17	0.33	81	776
FM7/X_{sim} hybrid females	52	3	45	1.04	92	404
Hmr-/X_{sim} hybrid females	69	12	18	0.80	104	628

[a] *D. simulans* chromosomes are indicated with the subscript "*sim*".

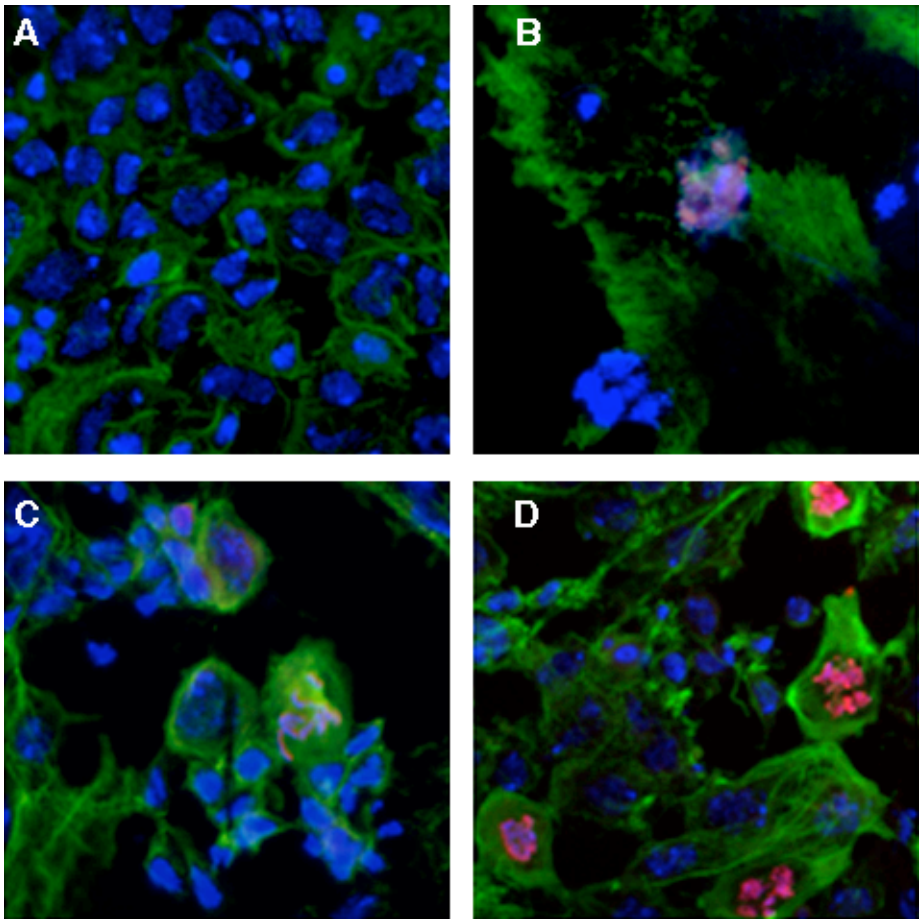

Figure 3.2 Progress of mitosis based on the age of larvae. All mitotic figures shown are at the same magnification and are the only mitotic figures observed in the entire brain. (A) Second instar larvae rarely show any mitotic figures. (B) In brains where there are cells dividing the chromosomes usually appear highly under-condensed. (C) Young third instars show mitotic figures that have chromosomes that are individually distinguishable. (D) Larvae that reach the third instar stage and continue to develop during this stage can be seen with four, eight, or even rarely sixteen mitotic figures. These larvae are also the “escapers” that are capable of pupating.

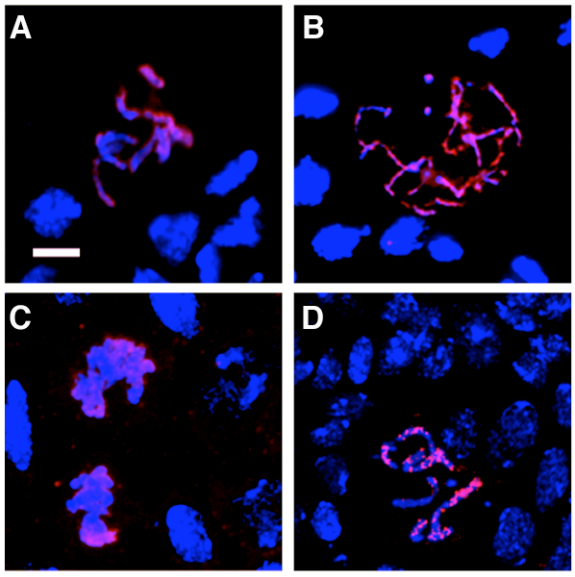

Figure 3.3 Chromosome morphology in hybrid brains.

In all panels, DNA is shown in blue and PH3 in red. (A) *D. simulans* mitotic figure with condensed and clearly defined chromosomes. (B) Many (>50%) mitotic figures in *Df(1)Hmr*$^{-}$ hybrid male larval brains show a diffuse thread-like chromosome morphology. (C) In *FM7/X*$_{sim}$ hybrid females, mitotic chromosomes are generally under-condensed, despite their positive PH3 signal. (D) *Df(1)Hmr*$^{-}$*/X*$_{sim}$ hybrid female with normal appearing mitotic chromosomes. Scale bar = 5 μm.

TABLE 3.5 Mitotic indices of larval brain cells before and after colchicine treatment

		0 min[a]	60 min	120 min
D. melanogaster				
2nd instar	0.7% NaCl	0.45	0.43	0.42
	+Colchicine	n.d.	0.91	1.96
3rd instar	0.7% NaCl	0.68	0.72	0.63
	+Colchicine	n.d	1.59	3.45
X_{mel}/Y_{sim} **hybrid**				
2nd instar	0.7% NaCl	0.078	0.057	0.061
	+Colchicine	n.d.	0.063	0.074
3rd instar	0.7% NaCl	0.15	0.16	0.15
	+Colchicine	n.d.	0.14	0.13

Mitotic indices were calculated as the number of PH3-positive cells per microscope field.

[a]Amount of time cultured after dissection but pre-fixation.

n's are ≥ 15 brains.

n.d. = not determined.

Consistent with the low levels of mitosis seen in the larval brains of the male hybrids, these brains were smaller in size than those of control second or third instar larvae (Figure 3.1C,D; see also the "Number of fields per brain" column in Table 3.4), as noted previously by Orr *et al.* (1997). This difference was particularly stark for third instars, where the total volume of hybrid male brains was only about 1/5 that of control brains (Figure 3.1D, Table 3.4). We measured the mitotic index (defined as the number of mitotic figures per field of view) to normalize the amount of mitosis relative to the brain volume, and found that the mitotic index of third-instar hybrid brains was decreased by roughly four-fold relative to the single species at the same developmental stage (Tables 3.4 and 3.5).

A similar reduction in the mitotic index was also observed in second instar larvae. The absence of cell division in hybrid larvae was not restricted to the brains; these larvae also showed a near complete absence of imaginal disc tissue (Figure 3.1D), as previously reported (Seiler and Nothiger, 1974; Sánchez, 1983). In a further attempt to gauge the frequency of mitosis in hybrid males, we cultured larval brains in colchicine, a drug that inhibits microtubule polymerization and thus arrests cells in mitosis. When the brains of control pure species larvae were treated with colchicine in 0.7% NaCl [the solution normally employed for cytological analysis in *Drosophila* (Gatti and Goldberg 1991), mitotic indices increased roughly 2-fold after one hour and 4-fold after two hours incubation (Table 3.5). In contrast, the frequency of mitosis in hybrid brains did not increase even after two hours of colchicine treatment.

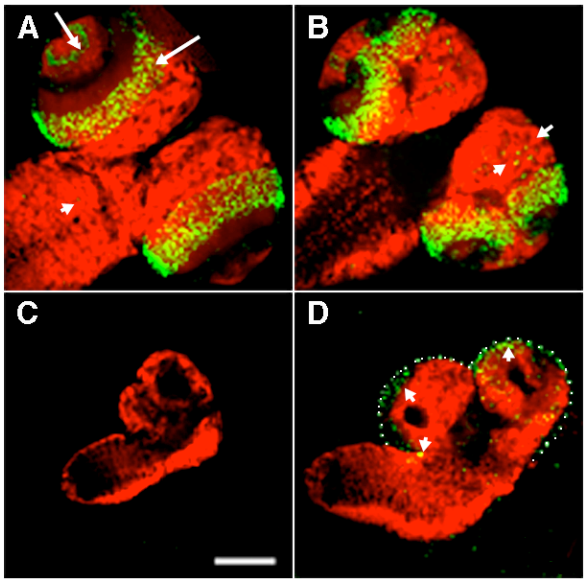

Figure 3.4 Hybrid male larval brains lack cells in S phase.

(A,B) Wild type *D. melanogaster* brains incorporate substantial BrDU in the developing optic lobe (arrows; antibody against BrDU is in green). Some scattered neuroblasts are also observed to undergo DNA replication (arrowheads). As a counterstain, differentiated neurons are marked by anti-Elav (red). (C,D) Brains from third instar hybrid larvae have no (C) or few (arrowheads in D) BrDU-incorporating cells. Because hybrid male brains have poorly-developed optic lobes, the outline of the brain tissue in (D) is shown with white dots. Scale bar = 0.5 mm.

This latter result is consistent with the idea that the brains of hybrid larvae have very few cells competent to enter mitosis. Interestingly, cells in hybrid females also appear to encounter difficulties in cell cycle progression, though these problems may be of a different nature. First, few of the PH3-positive mitotic figures in hybrid female larval brains display the degree of chromosome condensation characteristic of metaphase (Table 3.4; Figure 3.3C). Second, the mitotic index of female hybrid brains is ~1.8X higher than that of males or females in the single species, while at the same time an unexpectedly high proportion of cells in female hybrid brains are in anaphase/telophase (Table 3.4). Such problems in cell cycle progression may explain the sterility of adult hybrid females, since extensive cell division is required for amplification of the female germline and for oogenesis. This hypothesis is supported by findings that deletion of *D. melanogaster Hmr* in hybrid females normalizes both mitotic progression (Table 3.4) and chromosome condensation (Figure 3.3D), while at the same time *Hmr* deletion partially suppresses the sterility of these animals (Barbash and Ashburner, 2003).

Low Frequency of S Phase in the Brains of Hybrid Male Larvae

Since few cells in hybrid male larval brains are competent to enter mitosis, we also wanted to determine by BrDU incorporation whether any of these cells were in S phase. In the brains of third instar larvae from the pure species, the majority of DNA replication occurs in two bands in each optic lobe, but several neuroblasts scattered throughout the remainder of the brain also replicate their DNA (Figure 3.4A,B). In contrast, smaller third instar hybrid male brains displayed no BrDU incorporation (Figure 3.4C), while only a small number of cells were replicating their DNA in larger hybrid brains (Figure

3.4D). The low levels of DNA replication and mitosis seen in hybrid larval brains suggest that the large majority of cells in this tissue are unable to enter either S or M phases, but these data do not discriminate between arrest in G1 or G2 phases.

Orr *et al.* (1997) reported that when the brains of hybrid (*D. melanogaster / D. mauritiana*) male larvae were cultured in the presence or absence of colchicine in 0.7% NaCl, there was a dramatic increase in the number of cells displaying dense but diffuse chromatin. These authors interpreted such cells as being arrested in an early stage of mitosis, with chromatin more condensed than interphase chromatin but less condensed than the chromatin seen in metaphase mitotic figures. Even though we examined hybrids between *D. melanogaster* and a different sibling species (*D. simulans*), we were able to reproduce these results: cultured brains from hybrids but not from *D. melanogaster* rapidly fill with cells showing this aberrant chromosome morphology (Figure 3.5A-D; Table 3.6). However, the fact that the PH3-positive mitotic index does not increase when the brains of hybrid males are exposed to 0.7% NaCl in the presence or absence of colchicine indicates that these cells are not actually in mitosis (Table 3.4; Figure 3.5E-H).

When male hybrid brains were incubated in Grace's Media instead of 0.7% NaCl, the frequency of cells showing aberrant nuclear morphology decreased by 85% (Table 3.6). This result suggests that the changes in the appearance of chromatin are mostly an artifact of incubation in 0.7% NaCl.

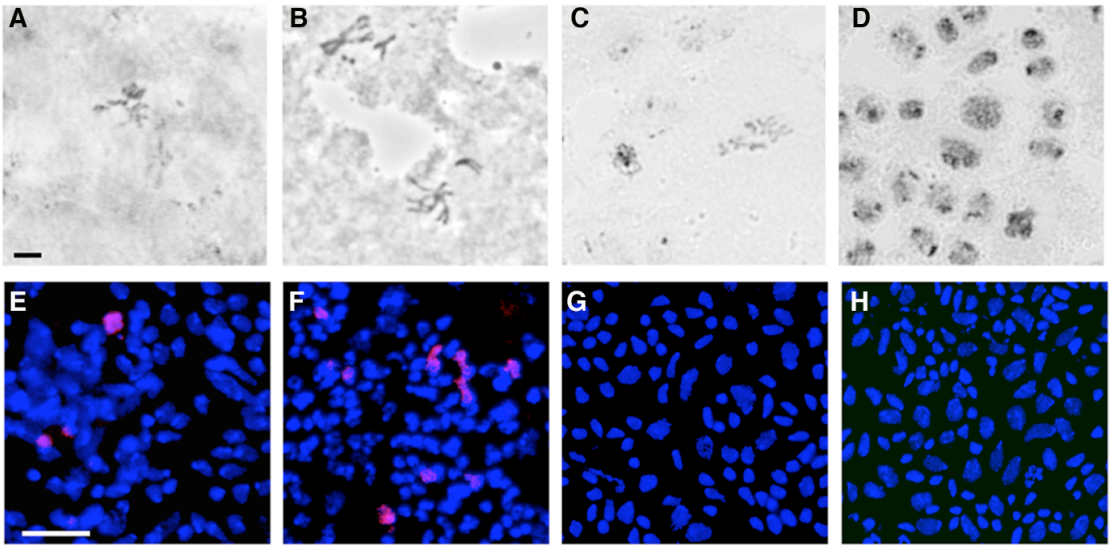

Figure 3.5 Cells with aberrant nuclear morphology seen in the cultured brains of hybrid males are not in mitosis. (A, B, E, F) Control *D. melanogaster* third instar larval brains. (C, D, G, H) Hybrid male third instar larval brains. The brains in panel A, C, E and G were squashed immediately after dissection, while those in B, D, F and H were examined after a 1 hr incubation in colchine. (A-D) Orcein stained brain squashes. The mitotic index in pure species brains increases after colchicine treatment (A, B). ~25% of the cells in hybrid male larval brains develop an abnormally dense chromatin morphology after the same treatment (C, D). Scale bar = 5 μm for A-D. (E-G) Brain squashes stained for DNA (blue) and phosphohistone H3 (PH3; red) to visualize mitotic chromosomes. The mitotic index as measured by PH3 staining increases in pure species with colchicine incubation (E, F), but few cells in hybrids stain with PH3 in the presence or absence of colchcine (G, H). Scale bar = 15 μm for E-H.

TABLE 3.6 Percentage of aberrant cells in larval brains

		0 min[a]	60 min	120 min
D. melanogaster				
2nd instar	0.7% NaCl	0	0	2.8
	Grace's Media	0	0	0
3rd instar	0.7% NaCl	0	0	3.1
	Grace's Media	0	0	0
Hybrid male				
2nd instar	0.7% NaCl	3	23.8	48.6
	Grace's Media	2.8	3.7	4.8
3rd instar	0.7% NaCl	3.5	27.9	47.2
	Grace's Media	3.6	4.2	5.1

Percentage of total cells showing aberrant chromatin morphology.

[a]Amount of time cultured after dissection pre-fixation.

n's ≥10 brains

However, freshly dissected hybrid male larval brains that were either placed into Grace's Media or immediately prepared for cytological analysis without any incubation showed a low frequency (2-4%) of aberrant cells (Table 3.6). It thus appears that 0.7% NaCl hastens a process that had already begun in hybrid larval brains prior to exposure to the salt solution.

We suspected that the cells with aberrant nuclear morphology were either dead or dying, so we stained larval brains with the vital dye Trypan Blue which labels degenerating cells (Krebs and Feder, 1997). Though control brains incubated in 0.7% NaCl for 1 hour had few if any cells that stained with this dye, a very high percentage of cells in identically-treated hybrid male larval brains were positive for Trypan Blue (Figure 3.6A,B). The levels of cell death were roughly equivalent to those achieved by exposing larval brains from either pure species to cycloheximide for 1 hour to induce apoptosis (Figure 3.6C). Cell death was much reduced (though still visible in a few cells) in hybrid male brains incubated in Grace's Media (Figure 3.6D).

Further characterization of the dead or dying cells in the brains of hybrid male larvae after salt treatment suggests that this phenotype is the result of necrosis rather than apoptosis or autophagy. Although there was a reproducible, slight elevation of apoptosis in these brains as determined by detection of the apoptotic marker Annexin V (van den Eijnde et al., 1998), the frequency of apoptotic cells was far too low to explain the high prevalence of cell death (Figure 3.6E-H). When hybrid larval brains in 0.7% NaCl were stained with Lysotracker, which measures pH changes in lysosomes indicative of autophagic cell death (Anderson and Orci, 1988), little if no staining was observed (data not shown).

Figure 3.6 Cell death is increased in 0.7% NaCl cultured third instar hybrid male brains. (A-D) Trypan Blue staining of dead cells. (A) *D. melanogaster* brain showing no cell death after incubation in 0.7% NaCl for 1 hour. (B) Hybrid male brains incubated under the same conditions show massive cell death. (C) As a positive control, *D. melanogaster* brains cultured in 10 mM cycloheximide for 1 hour and allowed to recover for 30 minutes to induce cell death similarly show intensive staining with Trypan Blue. (D) Hybrid male brains incubated in Grace's media for one hour instead of 0.7% NaCl. The number of dead cells is greatly diminished. Single species brains incubated in Grace's media had virtually no Trypan Blue staining (data not shown). Scale bar =50 μm for A-D (E-H) Annexin V staining to visualize apoptosis. Neither *D. melanogaster* (E) nor hybrid brains incubated in 0.7% NaCl (F) or Grace's media (G) display many apoptotic cells. (H) A positive control in which apoptosis was induced in *D. melanogaster* brains by cycloheximide. Scale bar = 1 mm for E-H.

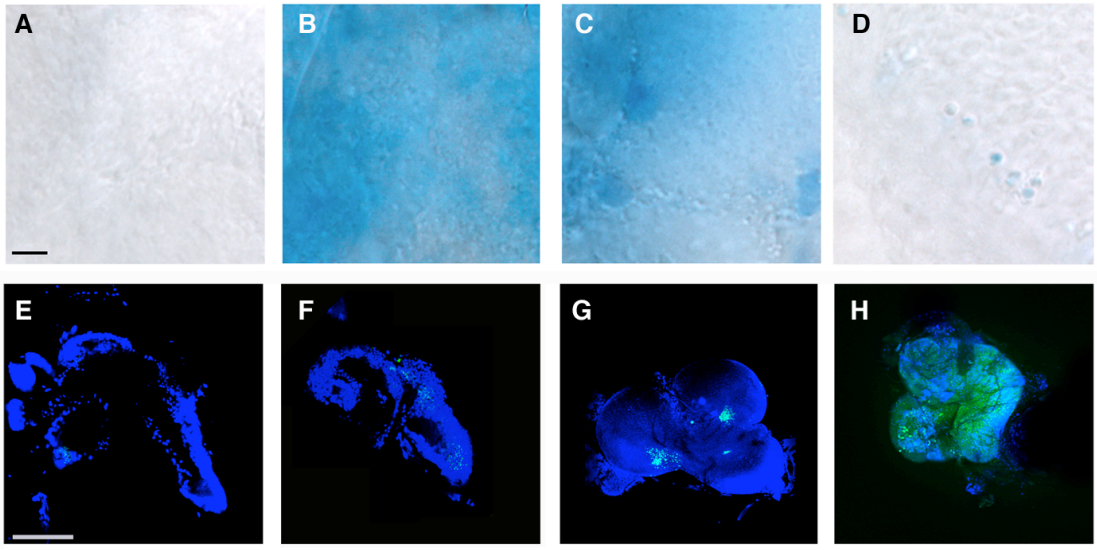
A
B
C
D
E
F
G
H

Hybrid male larvae also contained obvious melanotic masses, primarily in gut tissues but also occasionally in salivary glands (Figure 3.7). These melanotic masses might be caused by cell death, but they could in theory also result from an aberrant immune response generated in these unhealthy larvae (Minakhina and Steward, 2006).

DISCUSSION

Although hybrid incompatibility between *D. melanogaster* and its sibling species was first studied in the 1920s (Sturtevant, 1920; Sturtevant, 1929), the cellular and developmental basis of hybrid male lethality remains unknown. To our knowledge, the first direct examination of this issue was performed by Orr *et al*. (1997), who proposed that hybrid lethality was caused by mitotic defects associated with failure of proper chromosome condensation. The results reported here verify that hybrid male larvae do in fact suffer from problems in cell proliferation. However, we find that these defects largely reflect the inability of cells to enter mitosis; cells in hybrid male larval brains are not, as described in the previous study, subject to cell-cycle arrest that occurs after M phase has initiated. The failure of most cells to enter mitosis would explain not only the almost total absence of brain cells that stain positive for phosphohistone H3 (Figure 3.5E-H), but also the small brain size and the absence of imaginal disks in hybrid male larvae [Figure 3.1; see also (Sánchez, 1983; Seiler and Nothiger, 1974)]. Since there is virtually no incorporation of BrdU in hybrid male brains (Figure 3.4), it is clear that very few cells are in S phase at any particular time, so the majority of cells must instead be arrested either in G1 or G2 phases.

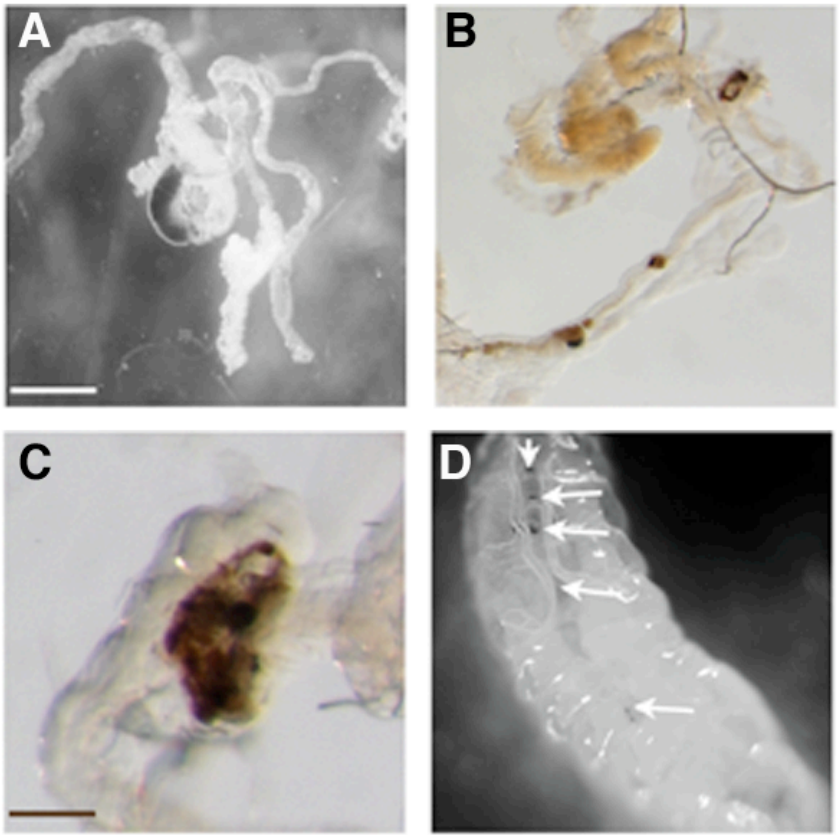

Figure 3.7 Naturally forming melanotic tumors from third instar hybrid males. These tumors form primarily in gut tissue (A-D), although they also develop in salivary glands (not shown). Scale bar =100 μm for E,F and 250 μm for G. (D) Lower magnification of several gut tumors in a single larvae.

Our results further suggest that cells in the brains of hybrid males are particularly sensitive to environmental stress. Incubation of brain tissue from hybrid male larvae in 0.7% NaCl, a solution thought to be of physiological osmolarity and widely used for *Drosophila* cytology (Gatti and Goldberg, 1991), induces considerable cell death (Figure 3.5). We believe that the aberrant nuclear morphology reported by Orr *et al.* (1997) and interpreted as incomplete mitotic chromosome condensation is mostly the result of artifactual cell death resulting from exposure to 0.7% NaCl (Table 3.6). With the benefit of hindsight, the results of these previous investigators do not comfortably fit their hypothesis of a mitotic arrest. The proportion of cells with aberrant nuclear morphology after 90 min of incubation was reported to be more than 25%, a frequency more than 5 times higher than the mitotic index of the strongest known metaphase arrest mutants in *Drosophila* (Gatti and Goldberg, 1991). Past experience thus suggests that such a high percentage of cells are highly unlikely to enter mitosis within a few hours of incubation. Moreover, the interpretation of Orr *et al.* (1997) fails to explain the much lower frequency of such cells (0.25%) they observed in freshly dissected hybrid brains. If 0.7% NaCl is truly physiological and the cells with aberrant nuclear morphology represent mitotic arrest, one would expect their frequency to be high prior to incubation as well.

The most straightforward interpretation of our results is that cellular physiology in hybrid male larvae is substantially altered, leading in vivo to a dramatic decline in the rate of cell proliferation and a modest increase in the level of cell death. Many of the surviving cells are sensitized to environmental conditions, and die readily by necrosis after exposure to 0.7% NaCl. We found

that the induction of cell death by 0.7% NaCl occurs in dissected tissue, and that the slow development of hybrid male larvae is not rescued by treatment with 20-hydroxyecdysone. More direct evidence that the cellular defects are cell-autonomous comes from Orr *et al.* (1997), who showed that X/O somatic clones induced in hybrid females are extremely small and thus proliferation-deficient; the growth defects of the clones are not rescued by adjacent X/X tissue.

While our results provide little direct guidance about the molecular basis of hybrid lethality, they do affirm that hybrids are defective in cellular physiology and proliferation. Since we have shown that the lethality of hybrid larvae does not reflect arrest in M phase, what alternative mechanisms are plausible? A recent microarray-based transcriptional profiling comparison of lethal and viable [*Df(1)Hmr*$^{-}$-rescued] hybrids found a surprisingly small magnitude of transcriptional differences between these genotypes, suggesting that hybrid lethality is also not caused by large-scale transcriptional misregulation (Barbash and Lorigan, 2007). Recent studies instead hint that hybrids may have defects in chromatin structure. Pal-Bhadra *et al*. (2006) found that dosage compensation proteins fail to localize to the hybrid male X chromosome. Dosage compensation defects are unlikely to be the sole explanation of hybrid lethality because this lethality is fully penetrant in both male and females that are hemizygous or homozygous for the *D. melanogaster* X chromosome. These results do however suggest that the hybrid male X chromosome has an aberrant chromatin structure, since proper localization of dosage compensation proteins requires a unique X chromosome chromatin state (reviewed in Akhtar, 2003). Brideau *et al.* (2006) recently found that the hybrid lethal gene *Lhr* encodes a protein that interacts

and colocalizes with Heterochromatin Protein 1 (HP1). Greil *et al.* (2007) also independently found that LHR (alternatively referred to as HP3) colocalizes with HP1 and depends on HP1 for its correct localization in cultured cells. The requirement of HP1 for the maintenance of heterochromatin states (Eissenberg and Elgin, 2000) suggests the possibility that hybrid lethality may result from an altered structure of heterochromatin. Mechanistic studies of *Lhr* and *Hmr* will be required to test these speculations and to understand why cells do not proliferate properly in hybrids.

ACKNOWLEDGEMENTS

This work was supported by NIH grants to D.A.B. (5R01GM074737-02) and to M.L.G. (5R01GM048430-14). Antibodies were received from the Developmental Studies Hybridoma Bank at the University of Iowa, Iowa City, IA. I would also like to thank W Dr. H. Allen Orr and Dr. Patrick Ferree for helpful comments on the manuscript.

LITERATURE CITED

Akhtar, A. (2003). Dosage compensation: an intertwined world of RNA and chromatin remodelling. *Curr Opin Genet Dev* **13**, 161-9.

Anderson, R. G. and Orci, L. (1988). A view of acidic intracellular compartments. *J Cell Biol* **106**, 539-43.

Barbash, D. A. and Ashburner, M. (2003). A novel system of fertility rescue in Drosophila hybrids reveals a link between hybrid lethality and female sterility. *Genetics* **163**, 217-26.

Barbash, D. A. and Lorigan, J. G. (2007). Lethality in Drosophila melanogaster/Drosophila simulans species hybrids is not associated with substantial transcriptional misregulation. *J Exp Zoolog B Mol Dev Evol* **308**, 74-84.

Barbash, D. A., Roote, J. and Ashburner, M. (2000). The Drosophila melanogaster hybrid male rescue gene causes inviability in male and female species hybrids. *Genetics* **154**, 1747-71.

Barbash, D. A., Siino, D. F., Tarone, A. M. and Roote, J. (2003). A rapidly evolving MYB-related protein causes species isolation in Drosophila. *Proc Natl Acad Sci U S A* **100**, 5302-7.

Brideau, N. J., Flores, H. A., Wang, J., Maheshwari, S., Wang, X. and Barbash, D. A. (2006). Two Dobzhansky-Muller genes interact to cause hybrid lethality in Drosophila. *Science* **314**, 1292-5.

Demerec, M. (1950). Biology of Drosophila. New York,: Wiley.

Eissenberg, J. C. and Elgin, S. C. (2000). The HP1 protein family: getting a grip on chromatin. *Curr Opin Genet Dev* **10**, 204-10.

Gatti, M. and Goldberg, M. L. (1991). Mutations affecting cell division in Drosophila. *Methods Cell Biol* **35**, 543-86.

Greil, F., de Wit, E., Bussemaker, H. J. and van Steensel, B. (2007). HP1 controls genomic targeting of four novel heterochromatin proteins in Drosophila. *Embo J* **26**, 741-51.

Hadorn, E. (1961). Zur Autonomie und Phasenspezifiat der Letalitat von Bastarden zwischen *Drosophila melanogaster* und *Drosophila simulans*. *Revue Suisse De Zoologie* **68**, 197-207.

Hendzel, M. J., Wei, Y., Mancini, M. A., Van Hooser, A., Ranalli, T., Brinkley, B. R., Bazett-Jones, D. P. and Allis, C. D. (1997). Mitosis-specific phosphorylation of histone H3 initiates primarily within pericentromeric heterochromatin during G2 and spreads in an ordered fashion coincident with mitotic chromosome condensation. *Chromosoma* **106**, 348-60.

Hutter, P. and Ashburner, M. (1987). Genetic rescue of inviable hybrids between Drosophila melanogaster and its sibling species. *Nature* **327**, 331-3.

Hutter, P., Roote, J. and Ashburner, M. (1990). A genetic basis for the inviability of hybrids between sibling species of Drosophila. *Genetics* **124**, 909-20.

Krebs, R. A. and Feder, M. E. (1997). Tissue-specific variation in Hsp70 expression and thermal damage in Drosophila melanogaster larvae. *J Exp Biol* **200**, 2007-15.

Mayr, E. (1942). Systematics and the origin of species. New York, New York: Columbia University Press.

Minakhina, S. and Steward, R. (2006). Melanotic mutants in Drosophila: pathways
and phenotypes. *Genetics* **174**, 253-63.

Orr, H. A. (1993). Haldane's rule has multiple genetic causes. *Nature* **361**, 532-3.

Orr, H. A., Madden, L. D., Coyne, J. A., Goodwin, R. and Hawley, R. S. (1997). The developmental genetics of hybrid inviability: a mitotic defect in Drosophila hybrids. *Genetics* **145**, 1031-40.

Park, Y., Filippov, V., Gill, S. S. and Adams, M. E. (2002). Deletion of the ecdysis-triggering hormone gene leads to lethal ecdysis deficiency. *Development* **129**, 493-503.

Pontecorvo, G. (1943). Viability interactions between chromosomes of Drosophila melanogaster and Drosophila simulans. *J. Genet.* **45**, 51-66.

Sánchez, L. D., A. (1983). Development of imaginal discs from lethal hybrids between *Drosophila melanogaster* and *Drosophila mauritiana*. *Development Genes and Evolution* **192**, 48-50.

Segraves, W. A. and Hogness, D. S. (1990). The E75 ecdysone-inducible gene responsible for the 75B early puff in Drosophila encodes two new members of the steroid receptor superfamily. *Genes Dev* **4**, 204-19.

Seiler, T. and Nothiger, R. (1974). Somatic cell genetics applied to species hybrids of Drosophila. *Experientia* **30**, 709.

Sturtevant, A. (1920). Genetic studies on Drosophila simulans. I. Introduction. Hybrids with Drosophila melanogaster. *Genetics* **5**, 488-500.

Sturtevant, A. (1929). The genetics of *Drosophila simulans*. In *Contributions to the genetics of Drosophila simulans and Drosophila melanogaster*, (ed. A. B. C. M. T. M. L. L. Sturtevant, Ju Chi), pp. 5-9. Washington: Carnegie Institution of Washington.

Truman, J. W. and Bate, M. (1988). Spatial and temporal patterns of neurogenesis in the central nervous system of Drosophila melanogaster. *Dev Biol* **125**, 145-57.

van den Eijnde, S. M., Boshart, L., Baehrecke, E. H., De Zeeuw, C. I., Reutelingsperger, C. P. and Vermeij-Keers, C. (1998). Cell surface exposure of phosphatidylserine during apoptosis is phylogenetically conserved. *Apoptosis* **3**, 9-16.

Watanabe, T. K. (1979). A gene that rescues the lethal hybrids between *Drosophila melanogaster* and *D. simulans*. *Jpn J. Genet* **54**, 325-331.

Williams, B. C., Karr, T. L., Montgomery, J. M. and Goldberg, M. L. (1992). The Drosophila l(1)zw10 gene product, required for accurate mitotic chromosome segregation, is redistributed at anaphase onset. *J Cell Biol* **118**, 759-73.

Yamamoto, M. T. (1992). Inviability of hybrids between D. melanogaster and D. simulans results from the absence of simulans X not the presence of simulans Y chromosome. *Genetica* **87**, 151-8.

CHAPTER 4
CONCLUSIONS AND FUTURE DIRECTIONS

I. TOYS ARE US (TRUS) AND ECDYSONE SYNTHESIS

The intricacies of the ecdysone-signaling pathway in Drosophila have been extensively studied (Riddiford, 1993), but many components and processes are still unknown. Based on my research, it is highly likely that Trus is involved in this pathway by regulating the production of ecdysone.

A model for ecdysis including a potential role for Trus

When a juvenile stage of development (that is, all stages before eclosion as adults) is complete, Prothoracicotrophic hormone (PTTH) is synthesized in the dorsal lateral region of the brain and then travels to the prothoracic cells of the ring gland, where it triggers a cascade that culminates in the synthesis of ecdysone (Mizoguchi et al., 2001). Based on the high levels of Trus detected in the prothoracic cells, it is unlikely that Trus acts upstream of PTTH. Instead, I suggest that Trus acts downstream of PTTH to regulate the translation of mRNAs whose products are involved in ecdysone synthesis in the ring gland. This hypothesis is based first on our finding that Trus interacts with String of Pearls (Sop), a subunit of the 40S ribosome. Our evidence that Trus does not interact with the intact ribosome would require Trus to act on/with Sop and Ef1-α prior to their association with the intact ribosome, but does not exclude Trus from having an indirect, yet essential, function in translation control. Furthermore, the literature contains precedents for the translational regulation of hormone production and action. In *Manduca*

(and likely in *Drosophila* and other insects), the S6 kinase, which phosphorylates the 40S ribosomal protein RpS6, is required for PTTH stimulated gated translation in the ring gland (Gilbert et al., 2000). RpS6 in the mouse is again the target of S6 kinase, but during insulin signaling (Mizoguchi et al., 2001). In this light, our data indicative of a possible interaction between Trus and Ef1-α acquires some plausibility since mouse Ef1-α is also part of the S6 kinase cascade.

One confusing aspect of our results is the finding that Trus does not stably bind the 40S subunit of the ribosome. Assuming that this result is not artifactual, this suggests that Trus up-regulates Sop and/or Ef1-α activity by a currently unknown mechanism that occurs outside of the context of the ribosome (Figure 4.1). These activated proteins and others are then involved in the rapid translation of certain mRNAs needed to obtain precisely timed peaks of ecdysone. Positive feedback loops provide a possible mechanism to augment this pathway, and there is considerable evidence that such a feedback loop occurs during ecdysone synthesis (Sakurai and Williams, 1989). Very little is known about the components of or direct targets of this positive feedback loop, but one study has suggested that Fucosyltransferase-A (FucTA) may be involved (Medvedova et al., 2003). Interestingly, FucTA is up-regulated by Phosphofructokinase (Pfk), which has also been proposed to be involved in ecdysone signaling (Li and White, 2003). A global yeast two-hybrid screen revealed that Trus interacts with both Pfk and FucTA (Giot et al., 2003). It is therefore possible that Trus might somehow act through these proteins to regulate the positive feedback loop.

Figure 4.1 Model of the role of Trus in control of ecdysone synthesis

When a stage of development is complete unknown clues signal the synthesis of PTTH which travels to the prothoracic cells of the ring gland and causes PTTH causes an increase in extracellular calcium and cAMP (Birkenbeil, 1998; Birkenbeil, 2000; Birkenbeil and Dedos, 2002; Gilbert et al., 2000; Smith et al., 1984). This increase in cAMP activates S6 Kinase, which phosphorylates and activates Ribosomal Protein Subunit 6 (Rps6) (Gilbert et al., 2000; Smith et al., 2003), a subunit of the 40s ribosome subunit. Our Tap-tagging results suggest that Trus is bound to Sop (another 40s subunit) and Ef1-α and cytology and western blots show Trus highly expressed in the prothoracic cells of the ring gland. I therefore, hypothesize that Trus is playing a role in regulating translation of mRNAs that a required for the synthesis of ecdysone although I do not know where in the cascade it acts.

After ecdysone is synthesized it is exported into the hemolymph where it is modified to the active for of ecdysone (20HE). 20HE then goes on to bind and activate Ecdysone Receptor (EcR) and Ultraspirical (USP). This trimer then upregulates the ecdysone immediate genes, which then upregulate the ecdysone secondary genes, which results in ecdysis.

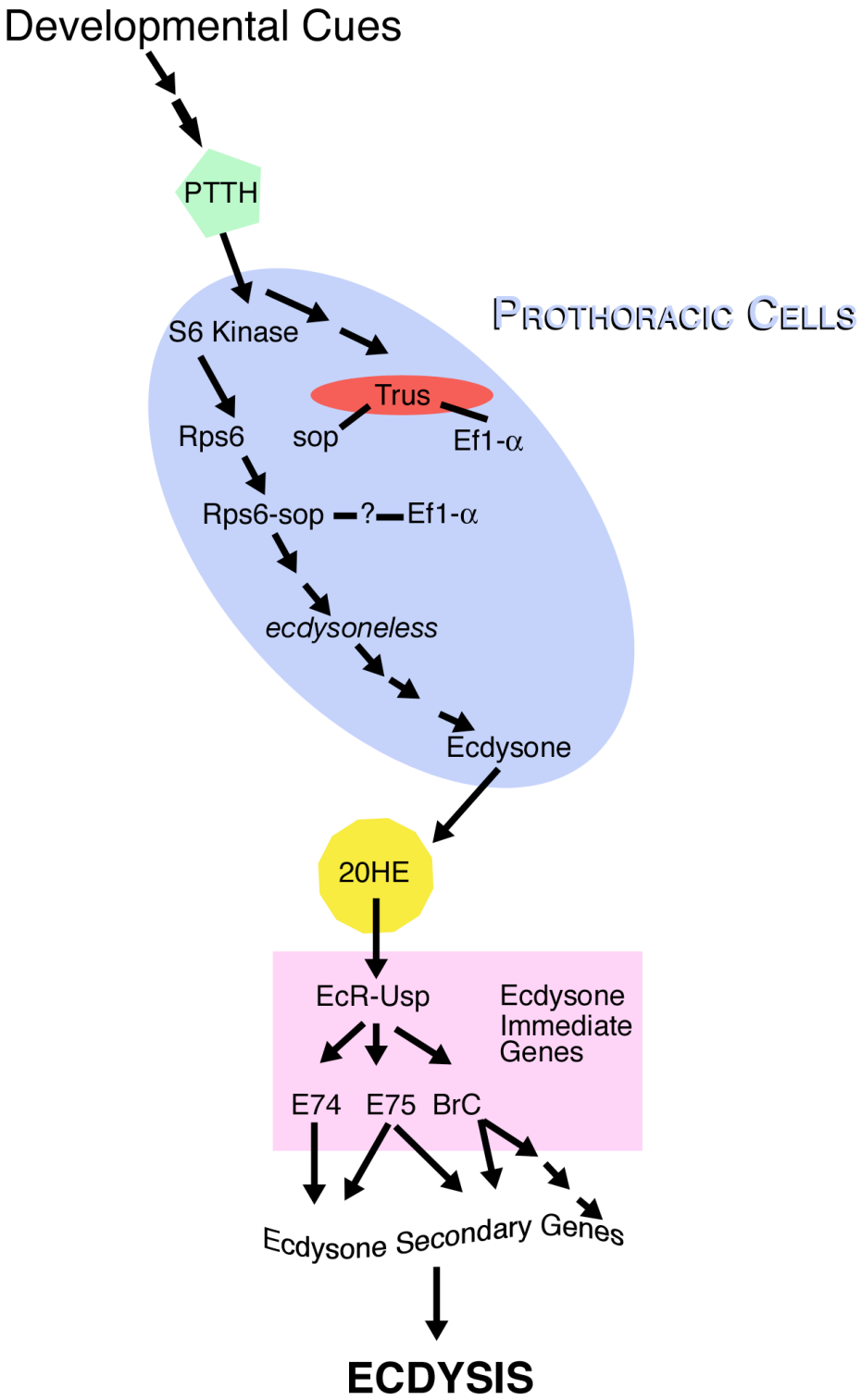
Developmental Cues
PTTH
Prothoracic Cells
S6 Kinase
Trus
Rps6
sop
Ef1-α
Rps6-sop —?— Ef1-α
ecdysoneless
Ecdysone
20HE
EcR-Usp
Ecdysone Immediate Genes
E74
E75
BrC
Ecdysone Secondary Genes
ECDYSIS

Although the *trus*^{1} mutation appears to be null or severely hypomorphic, homozygous mutant animals cannot be completely devoid of ecdysone. If this was the case, *trus*^{1} homozygotes would die during embryogenesis instead of at the third instar larval stage. The most likely explanation for this apparent paradox is that maternally supplied Trus would allow development until those stores are exhausted. It is also conceivable that Trus has a partially overlapping role with another protein, or that ecdysone synthesis is not absolutely dependent on Trus regulation because of the existence of an alternative pathway. For example, similar to some other molting insects (Gatti et al., 1974; Titschack, 1926), *trus*^{1} mutants may be able to override checkpoints and employ alternative pathways to molt to the next stage if enough time has passed between molts. *trus*^{1} mutants do not exhibit the substantially smaller size seen in all known cases of this override, but at the wandering third instar stage the mass of *trus*^{1} mutants is only 74% of normal.

Trus, Ecdysone and PTTH titers

My results provide considerable circumstantial evidence that Trus regulates ecdysone synthesis, but I believe that actual measurements of ecdysone titers in the *trus*^{1} mutants would give direct support for such a role and further insight into the type of defect. Since development occurs at a delayed and highly variable rate in the mutants, it is more difficult to determine when peaks of ecdysone would be expressed than in wild type animals. It would therefore be necessary to measure ecdysone titers at frequent intervals over the life of the larvae.

Future studies may also wish to look at PTTH titers in *trus* mutants. As PTTH is synthesized in the brain it is unlikely that Trus directly regulates PTTH

synthesis, but it is possible that larvae might increase PTTH titers in an attempt to synthesize ecdysone to compensate for deficiencies in the pathway.

trus^{1} as a possible tool in studying the ecdysone pathway

If Trus does in fact regulate the synthesis of ecdysone after PTTH signaling, this gene may become an important tool for future dissection of the ecdysone pathway. Currently, the only mutants known to cause a decrease in the ecdysone titer are in the gene *ecdysoneless*. However, the *ecd*^{1} allele is difficult to work with since it is a temperature sensitive allele and does not completely knockout ecdysone synthesis under restrictive conditions. Despite repeated attempts, no null allele of *ecd* has yet been identified (Gaziova et al., 2004).

Ring gland-specific rescue

Interesting insights into the function of ecdysone pathway proteins such as Broad (Zhou et al., 2004) have been achieved by over-expression of the protein specifically in the ring glands. I have attempted to obtain flies in which Trus is over-expressed in the ring gland by first cloning the full-length *trus* cDNA clone RE69372 into the pTWG-GW vector (Clontech, Mountain View, CA), which placed *trus* under the control of a Gal4 promoter and should produce a Trus protein containing a C-terminal GFP tag. The vector was injected into embryos by Genetic Services Inc, and screened based on eye color for integration.

Unfortunately, presumptive over-expression of Trus using the Gal4 P0163 and PO206 drivers (which both should be ring-gland specific) did not cause a visible phenotype. I nonetheless thought it might be possible to exploit

this system to see whether specific expression of the transgene in the ring gland might be sufficient to rescue the *trus*^{1} phenotype. I attempted to perform this rescue multiple times using the cross scheme shown in Figure 4.2, but I never obtained the desired PO163/+; +/Tb flies intermediate in this cross scheme, and so I was never able to test this rescue. While there is no obvious explanation of my inability to obtain these flies, it is possible that PO163 is not at its proposed location on the second chromosome or that there is some mutation in its background on the third chromosome that makes it incompatible with the TM6B balancer. However, given the high expression level of Trus in the ring gland, I still believe this would be an informative result to obtain in future research.

Insights into the function of Trus through interactors

The Tap-tagging experiments described in Chapter 2 were conducted with Kc cells that were originally isolated from embryos. This cell type may not be biologically relevant to Trus' involvement in ecdysone synthesis (although a background level of Trus expression is seen in Western blots of extracts made from these cells). Ideally, one should perform Tap-tagging or similar affinity chromatography studies in cell culture types that are more responsive to ecdysone or in ring glands or whole larvae; it is possible that additional interactors might be found in such studies that provide new clues concerning Trus' control of ecdysone synthesis.

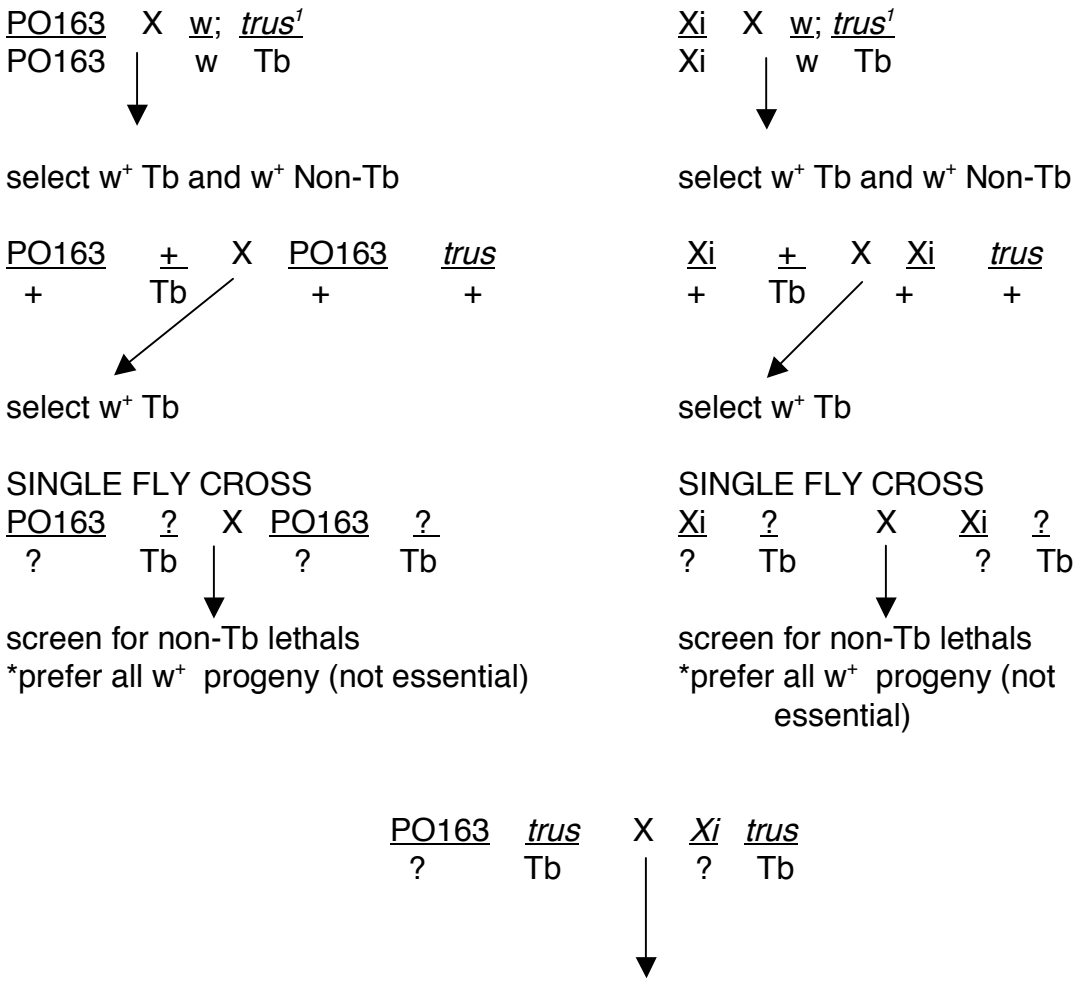

Figure 4.2 Cross scheme for ring gland specific rescue

To determine if ring gland specific expression can rescue the *trus*[1] mutation, I designed the cross scheme shown in the figure, using a Trus-GFP fusion under the control of a UAS promoter (Xi) and GAL4 driver expressed exclusively in the ring gland (PO163). After the final cross, I would in theory observe what happens to homozygous *trus*[1] larvae expressing Trus in the ring gland (GFP expressing non-Tubby animals). Unfortunately I have unexpectedly never been able to obtain the PO163/+; +/Tb flies required by the cross scheme.

Studying Trus homologs in mammals

The study of ecdysone signaling in *Drosophila* has important implications for hormone signaling in higher organisms, even though ecdysone is only found in molting insects and crustaceans. This is because several ecdysone pathway proteins are conserved and utilized in other hormone pathways in other organisms (Gilbert et al., 2000; Hsu and Schulz, 2000; Laudet et al., 1992). Often these proteins even have the same or similar interacting partners, as is the case with PTTH, S6 kinase, and Rps6 (Gilbert et al., 2000). Also, since ribosome structure is conserved in eukaryotes, it is likely that Trus-related proteins could play a fundamentally similar role in another hormone pathway.

We had hoped to elucidate some information about the function of Trus in mammals by using RNA *in situ* analysis to define the domains in which the Trus homolog is expressed in the mouse embryo. However, our data is insufficient to propose a function for PDCD2L (mouse Trus). The localized expression pattern within the developing nervous system does, however, suggest that PCDC2L is playing a cell-type specific role. Further *in situ* hybridizations conducted at later stages of development might provide a better idea of function. It would seem reasonable to continue to focus attention on the brain, as many neuroendocrine hormone signals are transmitted through brain tissues. The mouse knockout consortium has PDCD2L on its list of future knockouts to be made (Austin et al., 2004); the phenotype of such a knockout might eventually be extremely informative. However, if the gene is essential for early embryogenesis, the animals would die too early for detailed

observations. This possibility of course could be overcome by making conditional or tissue specific knockouts, but such studies would require more knowledge of the pattern of PDCD2L expression.

Research on Trus in both *Drosophila* and mammals certainly has the potential to provide a greater understanding of conserved mechanisms controlling hormone signaling.

II. HYBRID INCOMPATIBILITY

We have shown that, in contrast with previously published research, the incompatibility that causes lethality in hybrid males between *Drosophila melanogaster* and its sibling species is not due to an arrest in mitosis. We found that the brains of hybrid males are fragile and highly sensitive to environmental stress. However, the cellular or physiological basis of the lethality associated with this incompatibility remains unclear.

Mitotic defects in hybrid females and rescued hybrid males

Interestingly, hybrid males rescued from lethality by a deletion of *Drosophila Hmr* do have a mitotic defect. The brains still have a lower mitotic index than either single species and about a quarter of the cells in mitosis display spindly chromosome morphology (see Chapter 3, Figure 3.6 for images). Hybrid females that are Hmr^{+} also display a mitotic defect, but this phenotype has a higher than normal mitotic index, and many of the chromosomes appear puffy and under-condensed. The deletion of *Hmr* from these hybrid females results in a “wild type” mitotic index as well as a normal appearance of mitotic chromosomes. However, since the deletion of *Hmr* cannot rescue the males fully, *Hmr* cannot be the sole gene in *D.*

melanogaster responsible for the incompatibility and cell cycle problems, but it does play an important role in them.

Chromosome condensation defects as a potential explanation for hybrid incompatibility

As previously discussed in Chapter 3, two recent studies suggest that incompatible hybrids may have defects in chromatin structure. Pal-Bhadra *et al.* (2006)found that dosage compensation proteins fail to localize to the hybrid male X-chromosome. However, this is unlikely to be the sole explanation of hybrid lethality because this lethality is also fully penetrant in females that are homozygous for the *D. melanogaster* X chromosome. These results do, however, suggest that the hybrid male chromosome may have an aberrant chromatin structure (Akhtar, 2003). Brideau *et al* (2006) recently found that the *Lethal hybrid rescue* (*Lhr*) gene encodes a protein that interacts and co-localizes with Heterochromatin Protein 1 (HP1). Greil *et al*. (Greil et al., 2007) also independently found that *Lhr* (alternatively referred to as HP3) co-localizes with HP1 and depends on HP1 for its correct localization on heterochromatin in cell culture cells. The requirement for HP1 in the maintenance of heterochromatin states suggests the possibility that hybrid lethality may result from an altered structure of heterochromatin. It is plausible that interactions between Hmr, Lhr, and HP1 affect the ability of DNA to properly condense in male hybrids. Condensation defects that are either more limited in severity or specific to certain tissues might also explain the sterility of hybrid females (Foe, 1989; Gatti and Goldberg, 1991; Schupbach and Wieschaus, 1991). Improper chromosome condensation during interphase could alter gene expression needed for cellular physiology or for cell cycle

progression during interphase, or otherwise activate checkpoint mechanisms that could prevent cells from entering mitosis.

Exploring hybrid incompatibility through interactors of Hmr and Lhr

Some mitotic defects have been shown to cause female sterility since replication is such an essential part of oocyte development (Foe, 1989; Gatti and Goldberg, 1991; Schupbach and Wieschaus, 1991). The apparent mitotic defect in hybrid females may, therefore, partially explain the sterility seen in these animals. To further understand the mechanism of female sterility, however, I feel that an understanding of the role of Hmr, Lhr, and their interacting proteins in the single species is essential. While studies have looked at the function of HP1, little is known about Hmr or Lhr in the organism.

Determination of timing of the cell cycle arrest

I am currently using antibodies to Cyclin A and Cyclin B to stain hybrid and single species brains in hopes of determining when in the cell cycle the cells are arresting. Cyclin A is expressed from late G1 until early M, whereas Cyclin B is expressed in G2 until the metaphase/anaphase transition. Both Cyclin A and Cyclin B in association with Cdk1 are involved in triggering mitosis (Edgar and Lehner, 1996). The results of immunostaining for the two Cyclins could be particularly informative if many cells in the hybrid brains stain for Cyclin A but not Cyclin B. Such a result would suggest that the cells are arresting due to action of a DNA damage checkpoint. Staining for Grapes (a homolog of the checkpoint protein Chk1) might reveal if the G2/M checkpoint is being turned on in many cells in hybrid brains.

When do the proliferation defects begin?

It is important to remember that while my work has focused on the cells in the brain of the hybrids, the hybrid males are also missing imaginal discs and likely other cell types. Determining when these defects begin could provide additional information concerning the nature of the physiological defects in hybrids. This could be achieved by staining early embryos (and if cell types are present later animals) with antibodies to proteins expressed in the precursors of the imaginal discs and optic lobes. Such studies could determine if these cell types are created but never able to properly propagate, or instead if they are never formed.

Greater implications of hybrid incompatibility in *Drosophila*

This mechanism of *Drosophila* hybrid lethality and sterility has been of interest since Sturtevant first described these phenomena (Sturtevant, 1920; Sturtevant, 1929). It is likely that a different set of genes and/or mechanisms underlies the separation of every set of diverging species. For example, Hmr and Lhr evolve so rapidly that homologs have not been identified even in species as closely related to *Drosophila* as the mosquito. However, even if Hmr and Lhr functional orthologs do not exist outside the genus *Drosophila,* it is still possible that altered chromatin structure might be the basis of hybrid incompatibility in many evolutionary clades. These suppositions must await verification by more direct tests for aberrations in chromatin structure in a variety of hybrids.

LITERATURE CITED

Akhtar, A. (2003). Dosage compensation: an intertwined world of RNA and chromatin remodelling. *Curr Opin Genet Dev* **13**, 161-9.

Austin, C. P., Battey, J. F., Bradley, A., Bucan, M., Capecchi, M., Collins, F. S., Dove, W. F., Duyk, G., Dymecki, S., Eppig, J. T. et al. (2004). The knockout mouse project. *Nat Genet* **36**, 921-4.

Birkenbeil, H. (1998). Intracellular calcium in prothoracic glands of Manduca sexta. *J Insect Physiol* **44**, 279-286.

Birkenbeil, H. (2000). Pharmacological study of signal transduction during stimulation of prothoracic glands from Manduca sexta. *J Insect Physiol* **46**, 1409-1414.

Birkenbeil, H. and Dedos, S. G. (2002). Ca(2+) as second messenger in PTTH-stimulated prothoracic glands of the silkworm, Bombyx mori. *Insect Biochem Mol Biol* **32**, 1625-34.

Brideau, N. J., Flores, H. A., Wang, J., Maheshwari, S., Wang, X. and Barbash, D. A. (2006). Two Dobzhansky-Muller genes interact to cause hybrid lethality in Drosophila. *Science* **314**, 1292-5.

Edgar, B. A. and Lehner, C. F. (1996). Developmental control of cell cycle regulators: a fly's perspective. *Science* **274**, 1646-52.

Foe, V. E. (1989). Mitotic domains reveal early commitment of cells in Drosophila embryos. *Development* **107**, 1-22.

Gatti, M. and Goldberg, M. L. (1991). Mutations affecting cell division in Drosophila. *Methods Cell Biol* **35**, 543-86.

Gatti, M., Tanzarella, C. and Olivieri, G. (1974). Analysis of the chromosome aberrations induced by x-rays in somatic cells of Drosophila melanogaster. *Genetics* **77**, 701-19.

Gaziova, I., Bonnette, P. C., Henrich, V. C. and Jindra, M. (2004). Cell-autonomous roles of the ecdysoneless gene in Drosophila development and oogenesis. *Development* **131**, 2715-25.

Gilbert, L. I., Rybczynski, R., Song, Q., Mizoguchi, A., Morreale, R., Smith, W. A., Matubayashi, H., Shionoya, M., Nagata, S. and Kataoka, H. (2000).

Dynamic regulation of prothoracic gland ecdysteroidogenesis: Manduca sexta recombinant prothoracicotropic hormone and brain extracts have identical effects. *Insect Biochem Mol Biol* **30**, 1079-89.

Giot, L., Bader, J. S., Brouwer, C., Chaudhuri, A., Kuang, B., Li, Y., Hao, Y. L., Ooi, C. E., Godwin, B., Vitols, E. et al. (2003). A protein interaction map of *Drosophila melanogaster*. *Science* **302**, 1727-36.

Greil, F., de Wit, E., Bussemaker, H. J. and van Steensel, B. (2007). HP1 controls genomic targeting of four novel heterochromatin proteins in Drosophila. *Embo J* **26**, 741-51.

Hsu, T. and Schulz, R. A. (2000). Sequence and functional properties of Ets genes in the model organism Drosophila. *Oncogene* **19**, 6409-16.

Laudet, V., Hanni, C., Coll, J., Catzeflis, F. and Stehelin, D. (1992). Evolution of the nuclear receptor gene superfamily. *Embo J* **11**, 1003-13.

Li, T. R. and White, K. P. (2003). Tissue-specific gene expression and ecdysone-regulated genomic networks in Drosophila. *Dev Cell* **5**, 59-72.

Medvedova, L., Knopp, J. and Farkas, R. (2003). Steroid regulation of terminal protein glycosyltransferase genes: molecular and functional homologies within sialyltransferase and fucosyltransferase families. *Endocr Regul* **37**, 203-10.

Mizoguchi, A., Ohashi, Y., Hosoda, K., Ishibashi, J. and Kataoka, H. (2001). Developmental profile of the changes in the prothoracicotropic hormone titer in hemolymph of the silkworm Bombyx mori: correlation with ecdysteroid secretion. *Insect Biochem Mol Biol* **31**, 349-58.

Pal Bhadra, M., Bhadra, U. and Birchler, J. A. (2006). Misregulation of sex-lethal and disruption of male-specific lethal complex localization in Drosophila species hybrids. *Genetics* **174**, 1151-9.

Riddiford, L. M. (1993). Hormone receptors and the regulation of insect metamorphosis. *Receptor* **3**, 203-9.

Sakurai, S. and Williams, C. M. (1989). Short-loop negative and positive feedback on ecdysone secretion by prothoracic gland in the tobacco hornworm, Manduca sexta. *Gen Comp Endocrinol* **75**, 204-16.

Schupbach, T. and Wieschaus, E. (1991). Female sterile mutations on the second chromosome of Drosophila melanogaster. II. Mutations blocking oogenesis or altering egg morphology. *Genetics* **129**, 1119-36.
Smith, W., Priester, J. and Morais, J. (2003). PTTH-stimulated ecdysone secretion is dependent upon tyrosine phosphorylation in the prothoracic glands of Manduca sexta. *Insect Biochem Mol Biol* **33**, 1317-25.

Smith, W. A., Gilbert, L. I. and Bollenbacher, W. E. (1984). The role of cyclic AMP in the regulation of ecdysone synthesis. *Mol Cell Endocrinol* **37**, 285-94.

Sturtevant, A. (1920). Genetic studies on Drosophila simulans. I. Introduction. Hybrids with *Drosophila melanogaster. Genetics* **5**, 488-500.

Sturtevant, A. (1929). The genetics of *Drosophila simulans*. In *Contributions to the genetics of Drosophila simulans and Drosophila melanogaster*, (ed. S. B. M. M. Li), pp. 5-9. Washington: Carnegie Institution of Washington.

Titschack, E. (1926). Untersuchungen uber dasWachstum der Kleidermotte *Tineola biselliella* Hum. Gleichzeitig ein Beitrage zur Klarung der Inskektenhuatung. *Z. Zool* **128**, 509-569.

Zhou, X., Zhou, B., Truman, J. W. and Riddiford, L. M. (2004). Overexpression of broad: a new insight into its role in the Drosophila prothoracic gland cells. *J Exp Biol* **207**, 1151-61.

APPENDIX 1[5]

THE *DROSOPHILA* LKB1 KINASE IS REQUIRED FOR SPINDLE FORMATION AND ASSYMETRIC NEUROBLAST DIVISION

ABSTRACT

We have isolated lethal mutations in the *dlkb1* gene, the *Drosophila* homologue of *C. elegans par-4* and human *LKB1* mutated in Peutz-Jeghers syndrome. We show these mutations disrupt spindle formation, resulting in frequent polyploid cells in larval brains. In addition, *dlkb1* mutations affect asymmetric division of larval neuroblasts (NBs); they suppress unequal cytokinesis, abrogate proper localization of Bazooka, Par-6, DaPKC and Miranda, but affect neither Pins/Gαi localization nor spindle rotation. Most aspects of the *dlkb1* phenotype are exacerbated in *dlkb1 pins* double mutants, which exhibit more severe defects than those observed in either single mutant. This suggests that Dlkb1 and Pins act in partially redundant pathways to control the asymmetry of NB divisions. Our results also indicate that Dlkb1 and Pins function in parallel pathways controlling the stability of spindle microtubules. The finding that Dlkb1 mediates both the geometry of stem cell division and chromosome segregation provides novel insight into the mechanisms underlying tumor formation in Peutz-Jeghers patients.

---

[5] This appendix is modified from the following paper; Silvia Bonaccorsi[1] Violaine Mottier[1], Maria G. Giansanti[1], Bonnie J. Bolkan[2], Byron Williams[2], Michael L. Goldberg[2] and Maurizio Gatti. 2007. The *Drosophila* Lkb1 kinase is required for spindle formation and asymmetric neuroblast division**.** Development. 134(11):2183-93. Printed with permission.

Initial characterization of the *dlkb1* mutants was done by Dr. Byron Williams. I completed the mapping of the dlkb1 mutants and identified them as CG9374. After identification I cloned and purified Dlkb1 for antibody production and tested and purified the antibody. I also performed the western blot that is shown as Figure A8.1A displaying the lack of dLKB1 in the mutants. All other work in this section was completed in the laboratory of Dr. Gatti.

INTRODUCTION

Drosophila neuroblasts (NBs) are one of the best model systems for the study of the control of cell polarity and asymmetric cell division. During *Drosophila* embryogenesis NBs delaminate basally from the neuroectodermal epithelium and divide asymmetrically along the apical/basal axis to produce another NB and a smaller ganglion mother cell (GMC). The newly generated apical NB divides repeatedly in an asymmetric fashion, while the basal GMC divides symmetrically only once to generate equal-sized daughter cells that differentiate into neurons or glia (reviewed by Betschinger and Knoblich, 2004; Wodarz, 2005)

The asymmetric division of *Drosophila* NBs is regulated by several proteins that concentrate at the cell cortex. The basal cortex is enriched in the cell fate determinants Prospero (Pros) and Numb, as well as their respective adaptor proteins Miranda (Mira) and Partner of Numb (Pon). These proteins are preferentially segregated into the GMC following NB cytokinesis. Localization of Pros/Mira and Numb/Pon at the basal cortex is mediated by a large multiprotein complex that concentrates at the apical cortex. This complex includes two functionally distinct subcomplexes. One of them contains Bazooka (Baz; Par-3 in *C. elegans*), DaPKC (*Drosophila* atypical protein kinase C) and Par-6; this assembly is hereafter called the Baz/Par-6 subcomplex. The other subcomplex includes the Gαi subunit of the heterotrimeric G protein complex and Partner of inscuteable (Pins), and is hereafter named the Pins/ Gαi subcomplex. The Baz/Par-6 and Pins/Gαi subcomplexes are integrated in a larger apical complex by the Inscuteable

(Insc) protein that binds both Pins and Baz (reviewed by Betschinger and Knoblich, 2004; Wodarz, 2005).

Recent genetic analyses have shown that the Baz/Par-6 subcomplex is mainly involved in the control of proper basal localization of Pros/Mira and Numb/Pon. The Pins/Gαi subcomplex is instead required for spindle orientation during NB divisions. Both complexes, however, cooperate in controlling cleavage furrow positioning during asymmetric NB divisions. Mutations that disrupt either the Baz/Par-6 or the Pins/Gαi pathway have little or no effect on asymmetric cytokinesis. However, mutations that disrupt both pathways completely abrogate spindle displacement during telophase, leading to symmetric cytokinesis (Cai et al., 2003; Izumi et al., 2004; Shaefer et al. 2000; Yu et al. 2000; 2003).

In this study, we have addressed the role of the *Drosophila* LKB1 kinase in NB division. This kinase is mutated in the Peutz-Jeghers syndrome, an autosomal dominantly inherited disorder characterized by the formation of intestinal polyps and a high incidence of various cancer types. Somatic mutations in the *LKB1* gene have also been detected in sporadic adenocarcinomas (reviewed by Alessi et al., 2006; Baas et al., 2004b). There is evidence that LKB1 plays a conserved role in the control of cell polarity. Recent work has unambiguously shown that activation of LKB1 leads to rapid and complete polarization of human intestinal epithelial cells (Baas et al., 2004a). Similarly, Par-4, the *C. elegans* homologue of LKB1, is required for correct polarity and asymmetric division of one-cell embryos (Watts et al., 2000). Furthermore, *Drosophila* LKB1 (Dlkb1) mediates determination of anterior/posterior polarity of both egg chambers and embryos, as well as proper polarity of follicle cells (Martin and St. Johnston, 2003). Here, we

demonstrate that Dlkb1 controls many asymmetries that characterize the mitotic division of larval NBs. *dlkb1* mutations also disrupt mitotic spindle assembly, leading to the formation of frequent polyploid cells. Thus, in addition to cell polarity and the geometry of cell division, Dlkb1 directly or indirectly regulates the stability of spindle microtubules (MTs).

MATERIALS AND METHODS

Fly strains and genetic manipulations

The *dlkb1*^{315} mutant allele was isolated from a collection of 1600 third chromosome late lethals induced by ethylmethanesulfonate (EMS) in C. Zuker's laboratory (Koundakjian et al., 2004). The *dlkb1*^{7} allele is associated with the chromosome carrying *Df(3R)su(Hw)7*. This and all the deficiencies used for mapping were obtained from the Bloomington Stock Center. The *pins*^{P62} null allele and the *asl*^{2} mutation have been described previously (Bonaccorsi et al., 1998; Yu et al., 2000); *dlkb1*^{315} *pins*^{P62} and *dlkb1*^{315} *asl*^{2} double mutants were generated by recombination. All mutations were maintained over the *TM6B* balancer, and mutant larvae were identified based on their non-*Tubby* phenotype. Genetic markers and special chromosomes are described in FlyBase (http://www.flybase.org/). Germline transformation was performed as previously described (Vernì et al., 2004).

Antibodies and immunoblotting

The anti-Dlkb1 Antibody was generated in guinea pig using a Maltose Binding Protein (MBP)/Dlkb1 fusion protein. Expression of the fused protein in *E. coli,* and the production and purification of antibodies against this fusion was according to Vernì et al. (2004). Imunoblotting was performed as

described (Vernì et al., 2004); the anti-Dlkb1, anti-Pins and anti-Giotto (Giansanti et al., 2006) antibodies were diluted 1:2000, 1:1000 and 1:5000, respectively.

Cytology

Brains from third instar larvae were dissected and fixed according to Bonaccorsi et al. (2000). After several rinses in phosphate-buffered saline (PBS), brain preparations were incubated overnight at 4 ºC with a monoclonal anti-a tubulin antibody (Sigma-Aldrich), diluted 1:1000 in PBT (PBS with 0.1% TritonX-100), and any of the following rabbit antibodies, also diluted in PBT: anti-centrosomin (1:300; gift of T. Kaufman), anti-Deadpan (1:400; gift of Y. Jan), anti-Miranda (1:500; gift of Y. Jan), anti Bazooka (1:50; gift of F. Matsuzaki); anti-Gαi (1:200; gift of J. Knoblich); anti-Par-6 (1:1000; gift of J. Knoblich); anti-DaPKC (1:x100; Santa Cruz Biotechnology) and anti-Mud (1:200; gift of F. Matsuzaki). After two rinses in PBS, primary antibodies were detected by a 1 hour incubation at room temperature with FITC-conjugated anti-mouse IgG + IgM (1:20; Jackson Laboratories) and Alexa 555-conjugated anti-rabbit IgG (1:300; Molecular Probes), diluted in PBS.

For double Centrosomin/Pins immunostaining, brains were incubated overnight at 4 ºC with the rabbit anti-Centrosomin antibody (1:300) and a rat anti-Pins antiboby (1:100; gift of W. Chia) diluted in PBT. Detection was performed by 1 hour incubation at room temperature with Alexa 555-conjugated anti-rabbit IgG (Molecular Probes) and FITC-conjugated anti-rat IgG (Jackson Laboratories) diluted 1:300 and 1:20 in PBS, respectively.

For Dlkb1 immunostaining, brain preparations were incubated overnight at 4 ºC with the anti-Dlkb1 antibody (1:100 in PBT) and, after rinsing in PBS,

incubated 1 hour at room temperature with Alexa 555-conjugated anti-guinea pig IgG diluted 1:500 in PBS.

In all cases, immunostained preparations were mounted in Vectashield medium H-1200 (Vector Laboratories) containing the DNA dye DAPI (4,6 diamidino-2-phenylindole). Preparations were examined with a Zeiss Axioplan microscope, equipped with an HBO100W mercury lamp and a cooled charged-coupled device (CCD camera; Photometrics CoolSnap HQ). Grayscale images were collected separately, converted to Photoshop (Adobe Systems), pseudocolored and merged.

Spindle measurements were taken on enlarged digital images and scaled down to their size in mm. In preparations stained for Cnn, measurements were taken from centrosome-to-centrosome. In the absence of Cnn staining, measurements were taken from pole-to-pole in anastral spindles; in the presence of asters, measurements were taken from the center of the astral MT array.

RESULTS

Isolation and characterization of mutations in the *dlkb1* gene

In the course of a screen aimed at the isolation of mitotic mutants (see Materials and Methods), we identified a lethal mutation that causes frequent polyploid cells in larval brains (see below). Animals homozygous for this mutation die at the larval/pupal transition, as do most mitotic mutants; most probably, they exploit maternally supplied products to survive until late larval stages (Gatti and Baker, 1989). Deficiency mapping showed that this mutation is uncovered by both *Df(3R)urd* and *Df(3R)26c,* which define a map interval that contains only 16 annotated genes. During these mapping studies, we also

identified another mutant allele of this same mitotic gene. This allele is associated with the chromosome that carries *Df(3R)su(Hw)7,* but is independent of the deficiency. We next sequenced the candidate genes and found that both mutant stocks carry lesions in the *dlkb1* gene (also known as CG9374). This gene encodes a 567 amino acid serine/threonine kinase homologous to the Par-4 kinase of *C. elegans* and to the human LKB1 kinase mutated in the Peutz-Jeghers syndrome (Martin and St. Johnston, 2003). The $dlkb1^{315}$ mutant allele isolated in our screen carries a frameshift mutation resulting in a truncated Dlkb1 protein of 234 amino acids; the $dlkb1^{7}$ allele, associated with *Df(3R)su(Hw)7,* has a stop codon that truncates Dlkb1 to a 346 amino acid polypeptide (Figure A1.1). A genomic fragment including sequences that extend roughly 1 kb on either side of *dlkb1* (Figure 1A) rescued both the lethality and the mitotic phenotypes of $dlkb1^{315}/dlkb1^{315}$ and $dlkb1^{315}/dlkb^{7}$ mutants.

Mutations in the *dlkb1* gene affect spindle formation

Drosophila brains contain mostly two types of dividing cells: NBs and GMCs (Goodman and Doe, 1993). Wild type larval NBs are characterized by many asymmetries that develop during the course of mitosis. Prometaphases and metaphases of larval NBs exhibit centrosomes and asters of similar sizes at the two cell poles. However, as NBs progress through anaphase and telophase, the MTs of the basal aster shorten dramatically while those of the apical asters elongate slightly (Figure A1.1B). Concomitantly, the basal centrosome becomes smaller than the apical one (Bonaccorsi et al., 2000; see Figure A1.4A below).

Figure A1.1. Mutations in the *dlkb1* gene disrupt spindle organization of both NBs and GMCs.

(A) A molecular map of the *dlkb1* gene and its genomic region. P[dlkb1^{+}] designates the genomic fragment that rescues both the lethality and the cytological defects associated with the *dlkb1* mutation. Black boxes correspond to protein-coding exons of the genes, and the arrows indicate the direction of transcription. The positions of the stop codons causing the *dlkb1^{315}* and *dlkb1^{7}* mutations are indicated by vertical lines.

(B) Mitotic spindle morphology of NBs and GMCs from wild type (wt) and *dlkb1* brains. Cells were stained for tubulin (Tub, green) and DNA (blue).

(C) Spindle morphology of wild type (wt), *dlkb1, asl* and *asl dlkb1* metaphases stained for tubulin (green), DNA (blue) and centrosomin (red). Note that the spindle density in *asl dlkb1* double mutants is substantially lower than in *asl* single mutants. Scale bar for all panels, 5mm.

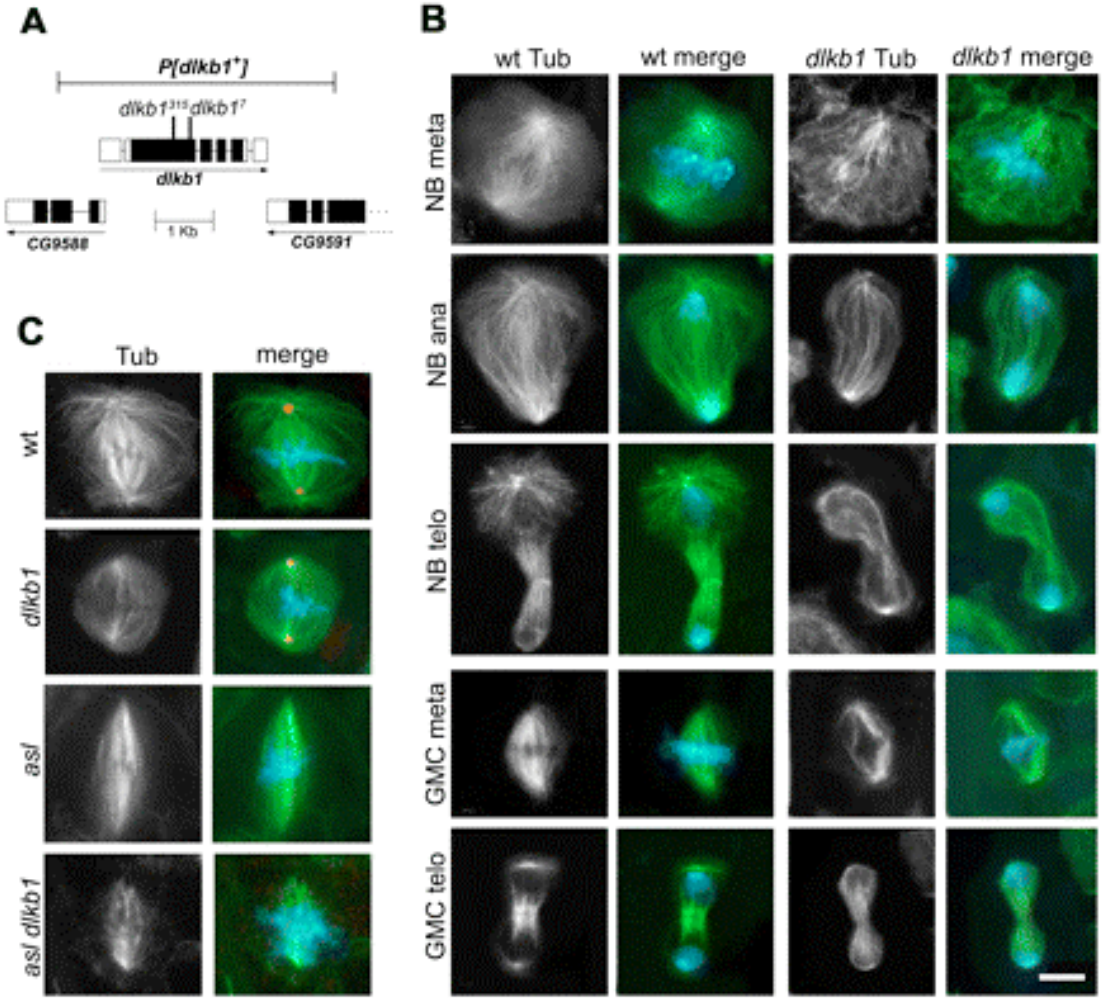
A
P[dlkb1+]
dlkb1315 dlkb17
dlkb1
CG9588
1 Kb
CG9591
B
wt Tub
wt merge
dlkb1 Tub
dlkb1 merge
NB meta
NB ana
NB telo
GMC meta
GMC telo
C
Tub
merge
wt
dlkb1
asl
asl dlkb1

These changes in aster and centrosome morphology are accompanied by a progressive displacement of the central spindle towards the basal pole, resulting in unequal cytokinesis (Giansanti et al., 2001). GMCs display equally-sized centrosomes and very small asters throughout mitosis, and divide symmetrically (Figure A1.1B; Bonaccorsi et al., 2000).

To determine the mitotic defect leading to polyploid cell formation in *dlkb1* mutants, we examined larval brain preparations from *dlkb1*^{315}/*dlkb1*^{315}, *dlkb1*^{315}/*Df(3R)urd* and *dlkb1*^{315}/*dlkb1*^{7} larvae stained for both tubulin and DNA. These mutant combinations showed identical mitotic aberrations. Most strikingly, mutant spindles showed an overall MT density that is substantially lower than that seen in wild type spindles (Figure A1.1B). In approximately 80% of mutant spindles, asters were absent or severely reduced; in control brains, the frequency of spindles without asters, or with very small asters, was 49% (Figure A1.1B; Table1). In addition, most mutant prometaphase and metaphase figures were characterized by low densities of both kinetochore and interpolar MTs, and ana-telophases displayed central spindles thinner than their wild type counterparts (Figures 1B and 3D below). Mutant brains also showed an increase in the relative frequency of metaphase figures with respect to wild type, suggesting that *dlkb1* mutations lengthen metaphase duration (Table A1.1).

Finally, mutant brains displayed approximately 20% polyploid cells (not shown); in wild type brains, the frequency of polyploid cells is virtually zero (Table A1.1). The phenotype of *dlkb1*^{315} homozygotes was qualitatively and quantitatively similar to that observed in *dlkb1*^{315}/*Df(3R)urd* hemizygotes, indicating that *dlkb1*^{315} is a null mutation (Table A1.1).

TableA1.1. Mitotic parameters in larval brains from *dlkb1* mutants.

Genotype (a)	# of cells (b)	metaphases %	anaphases %	telophases %	sym. telo (c) %	no asters (d) %	polyploid cells %
Oregon R	1,095	68.0	16.3	15.6	35	49	0.2
315/315	423	83.5	10.9	6.6	68	82	20.2
315/Df	1,120	81.3	13.0	5.7	65	81	22.5
315/7	547	79.7	13.9	6.4	63	78	18.6

(a) Oregon R, wild type stock used as control; *315/315*, *dlkb1*^{315}*/dlkb1*^{315}*; 315/Df, dlkb1*^{315}*/Df(3R)urd*; *315/7, dlkb1*^{315}*/dlkb1*^{7}. (b) The numbers of cells scored refer only to diploid mitotic figures; polyploid cells were recorded but not used for calculation of the frequencies of different types of mitotic figures. (c) sym telo, relative frequencies of symmetric telophases; (d) no asters, diploid cells without asters or with very small asters.

The spindle phenotypes observed in *dlkb1* mutants could be due either to a defect in MT elongation and/or stability, or to a defect in centrosome function. To distinguish between these possibilities, we sought to eliminate centrosome function in *dlkb1* mutants. We have previously shown that brain cells of *asterless (asl)* mutants fail to assemble functional centrosomes and nucleate astral MTs. Nonetheless, *asl* NBs and GMCs manage to form robust anastral spindles that are able to mediate chromosome segregation (Bonaccorsi et al., 2000: Giansanti et al., 2001). We thus constructed *dlkb1 asl* double mutants and compared their phenotype to those exhibited by *dlkb1* and *asl* single mutants. The anastral spindles from *asl* single mutants displayed a MT density comparable to wild type (Figure A1.1C). In contrast, in *dlkb1 asl* double mutants, the density of spindle MTs was substantially reduced with respect to wild type and similar to that observed in *dlkb1* single mutants (Figure A1.1C). These results strongly suggest that the low density of spindle MTs observed in *dlkb1* mutants does not depend on centrosome dysfunction. Thus, the spindle phenotype of *dlkb1* mutants is likely to be attributable to either a decreased rate of MT growth or an increased MT instability.

dlkb1 mutations disrupt the asymmetry of NB division leading to a reduction in NB size

Observation of mitotic divisions stained for tubulin and DNA revealed that the spindles of *dlkb1* mutant cells are generally smaller than in wild type (Figure A1.1). In addition, the frequency of asymmetric telophases in mutant brains (35-37%) was significantly lower than in wild type brains (65%) (Table A1.1). These phenotypes could reflect a partial loss of morphological asymmetry during NB division, resulting in smaller than normal daughter NBs.

We thus examined in greater detail the pattern of cell division in *dlkb1*^{315}*/Df(3R)urd* brains, and compared this pattern to those observed in wild type, *partner of inscuteable (pins)* and *asl* brains. Comparison between *dlkb1* and *pins* mutants was prompted by two previous findings. First, mutations in *pins* partially suppress the asymmetry of NB divisions, leading to a progressive reduction in NB size (Cai et al., 2003; Parmentier et al., 2000). Second, the *Drosophila* and the human LKB1 kinases interact with the orthologous proteins Pins and AGS3, respectively (Blumer et al., 2003). In addition, more detailed comparisons between *dlkb1* and *asl* mutants would allow us to assess more precisely the role of astral MTs in asymmetric NB divisions.

To unambiguously distinguish between NB and GMC spindles, we immunostained preparations from control and mutant brains for both tubulin and the NB marker Deadpan (Dpn), (Bier et al., 1992; Figure A1.3A below). The analysis of Dpn-positive cells showed that the *dlkb1* and *pins* NBs are indeed defective in aster formation. However, the two mutants displayed different patterns of spindle defects. In brains homozygous for the *pins*^{P62} null mutation (Yu et al., 2000), most NB prometaphases and metaphases showed normal asters but most ana-telophases were characterized by an abnormally small apical aster (Figure A1.2A-D). Despite this defect in astral MTs, the density of the spindle MTs in *pins* NBs was comparable to that observed in their wild type counterparts (compare Figure A1.2A-D with Figure A1.1B). In contrast, the spindles of *dlkb1* NBs not only showed a reduction in MT density but also displayed small asters in both metaphase and ana-telophase figures (Figures A1.1B and A1.2E).

Figure A1.2. Mutations in *pins* affect aster formation without altering the density of spindle MTs.

Cells were stained for tubulin (green), DNA (blue) and Deadpan (not shown, but see Figure A1.3A below) to identify NBs. (A) Prometaphase, (B) metaphase, (C) anaphase and (D) telophase from $pins^{P62}$ mutant brains. Scale bar, 5mm. (E) Frequencies of NBs displaying normal asters in wild type, *dlkb1* and *pins* brains.

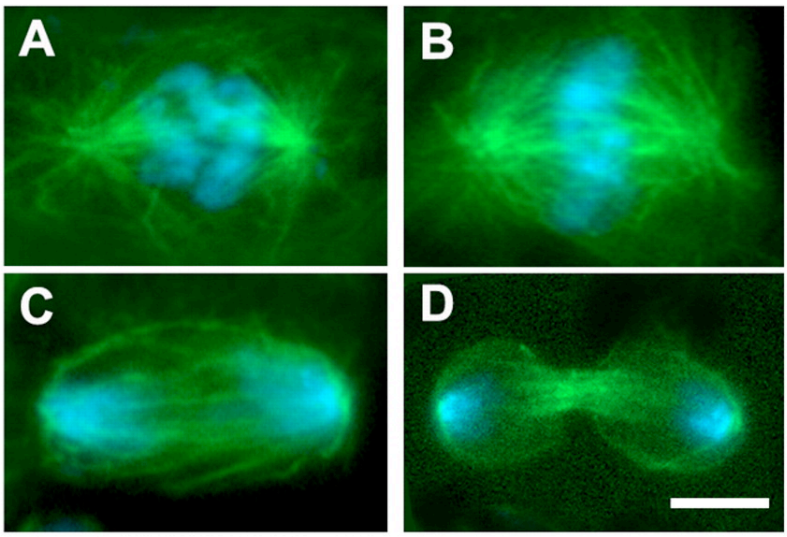
A
B
C
D

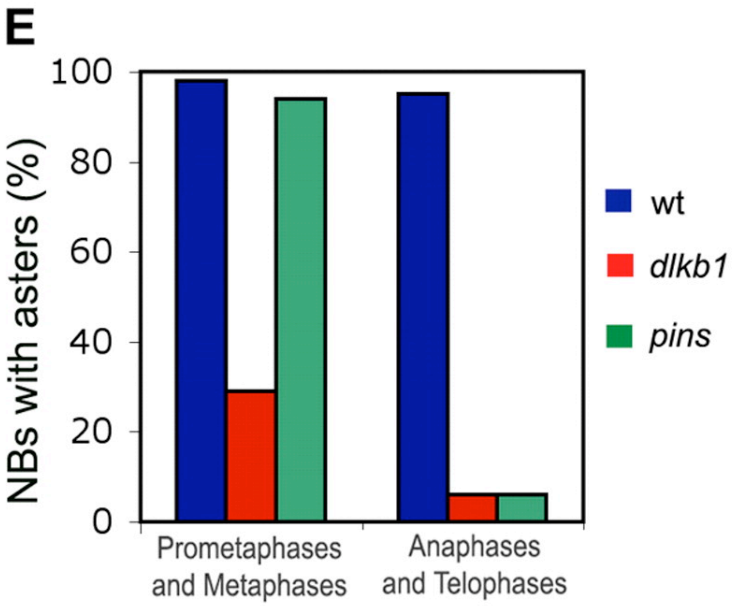
E
100
80
60
40
20
0
NBs with asters (%)
Prometaphases
and Metaphases
Anaphases
and Telophases
wt
dlkb1
pins

Figure A1.3. Mutations in *dlkb1* disrupt unequal cytokinesis and reduce the average size of NB population within mutant brains.

(A) Wild type and *dlkb1* metaphases stained for tubulin (Tub) DNA and Deadpan (Dpn). Note that the NBs are more intensely stained by the anti-Dpn antibody than GMCs. Scale bar, 5mm.

(B and C) Size distribution of metaphase (B) and ana-telophase (C) spindles in wild type, $dlkb1^{315}/Df(3R)urd$, $pins^{P62}/pins^{P62}$ and asl^{2}/asl^{2} brains. Dpn-positive (NB) and negative (GMC) spindles are depicted in red and green, respectively. Size (mm) classes in (B): A, 4.7-6.9; B, 7.0-9.2; C, 9.3-11.5; D, 11.6-13.8; E, 13.9-16.1; F, 16.2-18.4; G, 18.5-20.7; H, 20.8-23.0; I, 23.1-31.7. Size (mm) classes in (C): J, 6.7-11.2; K, 11.3-15.8; L, 15.9-20.4; M, 20.5-25.0; N, 25.1-29.6; O, over 29.7. The numbers on top of each column correspond to the number of cells observed in each size class.

(D) Criterion used for measuring the asymmetry index of NB divisions. The difference between the length of the long (a) and the short (b) spindle axis (a-b) was divided it by the total length of the two axes (a+b). Scale bar, 5mm.

(E) Asymmetry indexes in wild type, $dlkb1^{315}/Df(3R)urd$, $pins^{P62}/pins^{P62}$ and asl^{2}/asl^{2} NBs of different sizes. The bars correspond to the SEM. Size (mm) classes: P, 11.3-15.8; Q, 15.9-20.4; R, 20.5-25.0; S, 25.1-29.6; T, over 29.7.

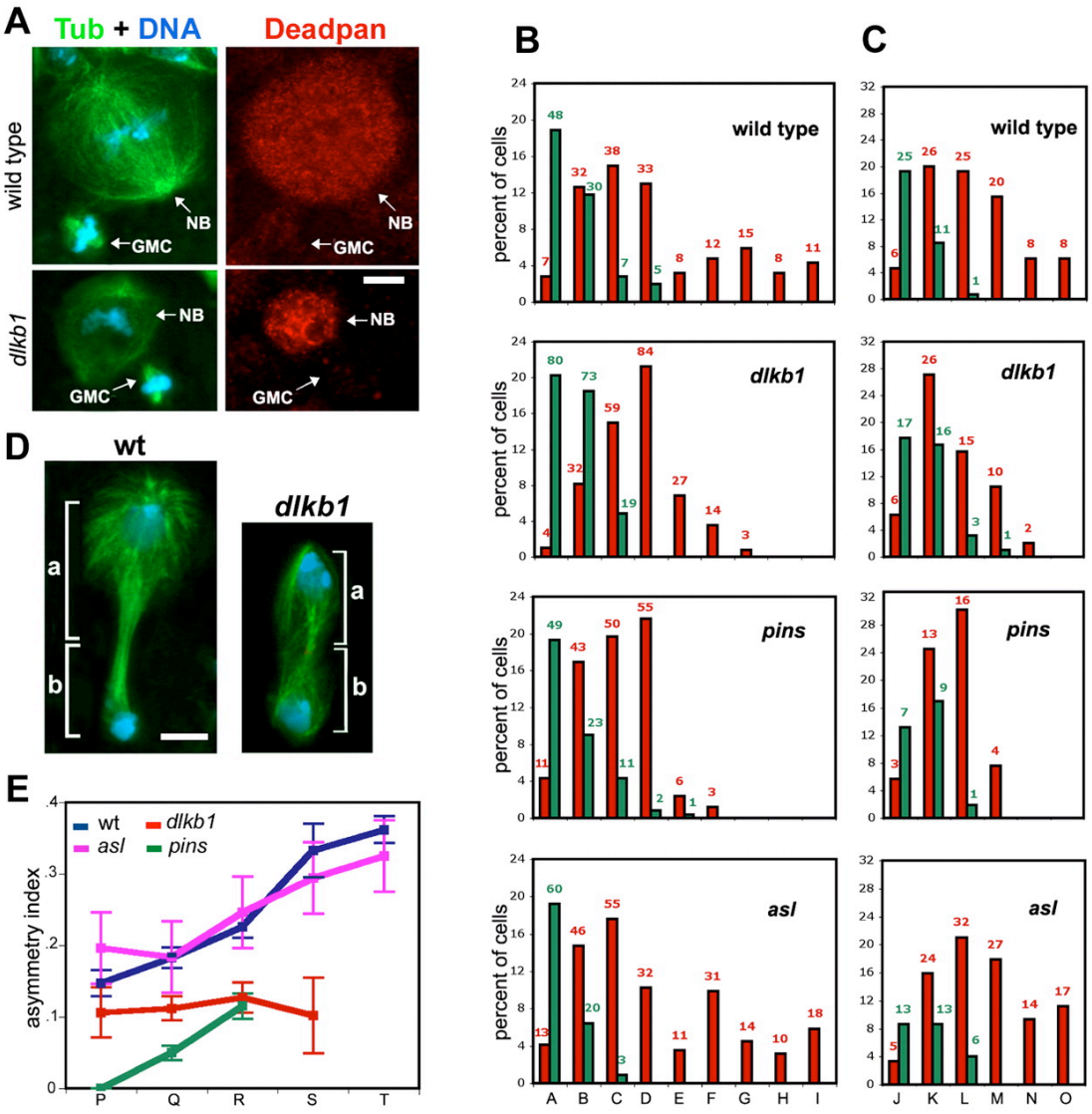
A
Tub + DNA
Deadpan
wild type
dlkb1
NB
GMC
B
C
wild type
dlkb1
pins
asl
percent of cells
D
wt
dlkb1
a
b
E
wt
dlkb1
asl
pins
asymmetry index
P
Q
R
S
T
A
B
C
D
E
F
G
H
I
J
K
L
M
N
O

In *pins* and *asl* mutants, the spindles of Dpn-negative GMCs displayed a normal morphology and were indistinguishable from their wild type counterparts (data not shown). However, in *dlkb1* mutants, GMC spindles were characterized by low MT density just as those of the NBs (Figure A1.1B). Thus, the wild type function of *dlkb1* is required for proper spindle formation in both NBs and GMCs.

We next measured the spindle length of metaphase and ana-telophase figures in both NBs (Dpn-positive) and GMCs (Dpn-negative). In *dlkb1* and *pins* mutant brains, the average sizes of NB spindles are substantially smaller than those measured in either *asl* or wild type brains. This is mainly due to the absence of large NBs, as both *dlkb1* and *pins* mutants lack NB metaphases and telophases longer than 19 and 26 mm, respectively; these large NBs represent approximately 20% of the NBs found in wild type or *asl* mutant brains. In contrast, the average sizes of the GMC spindles observed in *dlkb1*, *asl* and *pins* mutants were very similar and comparable to those of wild type controls (Figure A1.3B, C). An explanation for these results is that in both *dlkb1* and *pins* mutants NBs divide more symmetrically than either in *asl* or wild type. To test this possibility, we directly evaluated the degree of asymmetry of NB telophases showing strong Dpn staining. The asymmetry index was determined using the formula a-b/a+b, where a is the long axis of the spindle and b its short axis (Figure A1.3D). This analysis (Figure A1.3E) clearly shows that the NBs from *dlkb1* and *pins* mutants divide more symmetrically than those of either *asl* or wild type. Collectively, these results indicate that mutations in either *dlkb1* or *pins* partially suppress the asymmetry of NB division, leading to a reduction in the NB size at each cell division cycle.

To ask whether mutations in *dlkb1* and *pins* affect centrosome size, brain preparations were stained for centrosomin (Cnn), an integral component of *Drosophila* centrosomes (Megraw et al., 2001). Observations were restricted only to those cells that, according to our analysis of spindle size distribution (Figure A1.3B, C), were likely to be NBs (wild type, *dlkb1* and *pins* metaphases longer than 12 mm, and ana-telophases longer than 16 mm). This analysis (Figure A1.4A, B) revealed that 88% (n = 76) of wild type NBs displays centrosomes of different sizes at their poles. In contrast, only in 34% (n = 180) of *dlkb1* NBs and 39% (n = 100) of *pins* NBs is the centrosome at the apical pole larger than that at the basal pole. These results indicate that *dlkb1* and *pins* control asymmetry in centrosome size during NB division.

dlkb1 mutations affect Mira and Baz/Par-6/DaPKC but not Pins/Gαi localization in dividing NBs

We examined whether *dlkb1* and *pins* mutations affect the distribution of Miranda in dividing NBs. Larval brain preparations were simultaneously stained for both tubulin and Mira and analyzed for Mira localization (Figure A1.5A). We again restricted our analysis to large mitotic figures that are likely to be NBs by the criteria just employed. Both *dlkb1* and *pins* mutant NBs revealed abnormal Mira distributions, but the patterns of Mira mislocalization were different (Figure A1.5A, B). In wild type, 93% of NB metaphases and ana-telophases displayed a clear Mira crescent at the basal pole, while the remaining 7% showed diffuse Mira staining. In contrast, in *dlkb1* and *pins* mutants the frequencies of NBs with a basal Mira crescent were 47% and 26%, respectively. Most (97%) of *dlkb1* mutant NBs lacking a Mira crescent displayed a diffuse cytoplasmic localization of Mira.

Figure A1.4. Mutations in the *dlkb1* gene affect centrosome size during NB division.

(A) Metaphases and telophases from wild type and *dlkb1*^{315}*/Df(3R)urd* mutant brains stained for tubulin (green), DNA (blue) and centrosomin (red). Note the differently-sized and the equally-sized centrosomes at the poles of wild type and *dlkb1* mutant cells, respectively. Scale bar, 5mm.

(B) Frequency of NBs displaying differently-sized centrosomes in wild type (wt), *dlkb1*^{315}*/Df(3R)urd* and*, pins*^{P62}*/pins*^{P62} brains.

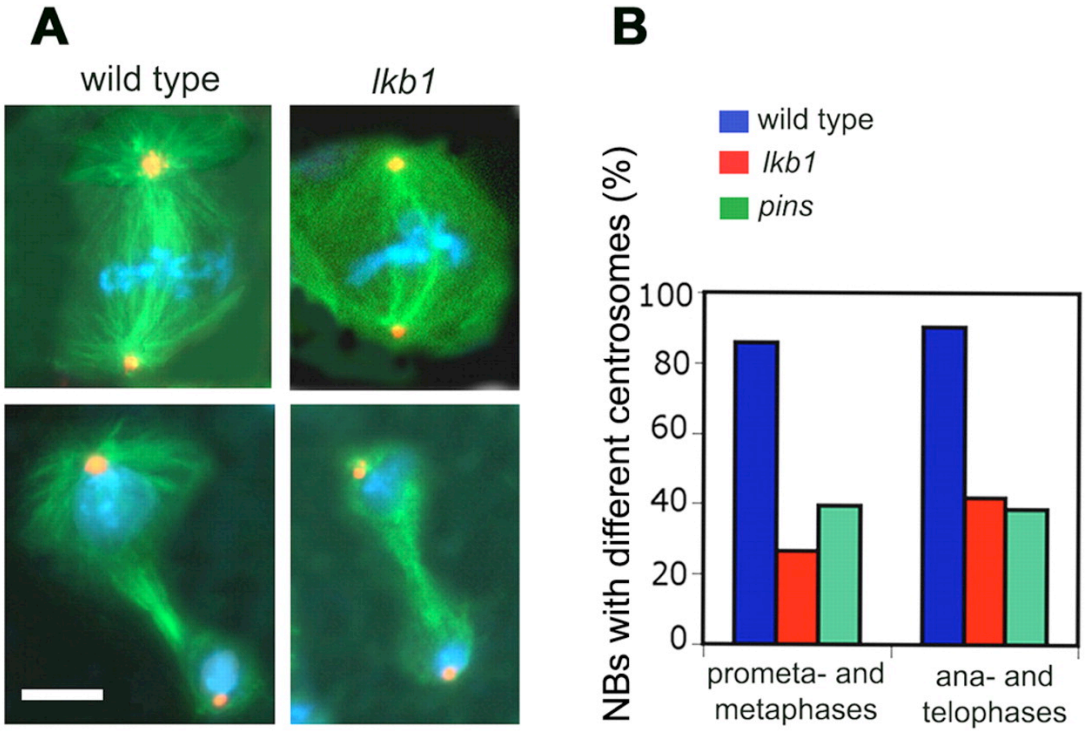
A
wild type
lkb1
B
wild type
lkb1
pins
NBs with different centrosomes (%)
100
80
60
40
20
0
prometa- and metaphases
ana- and telophases

Figure A1.5. Mutations in the *dlkb1* gene affect Mira localization at the NB basal pole

(A) Mira localization in wild type, $dlkb1^{315}/dlkb1^{315}$ and $pins^{P62}/pins^{P62}$ NBs. Cells were stained for tubulin (Tub), DNA and Mira. Scale bar, 5mm.

(B) Distribution of Mira in dividing NBs from wild type (wt), $dlkb1^{315}/dlkb1^{315}$ and $pins^{P62}/pins^{P62}$ brains; regular, regular Mira crescent at the basal pole; cortical, Mira associated with the entire cell cortex; diffuse, Mira dispersed in the cytoplasm.

A

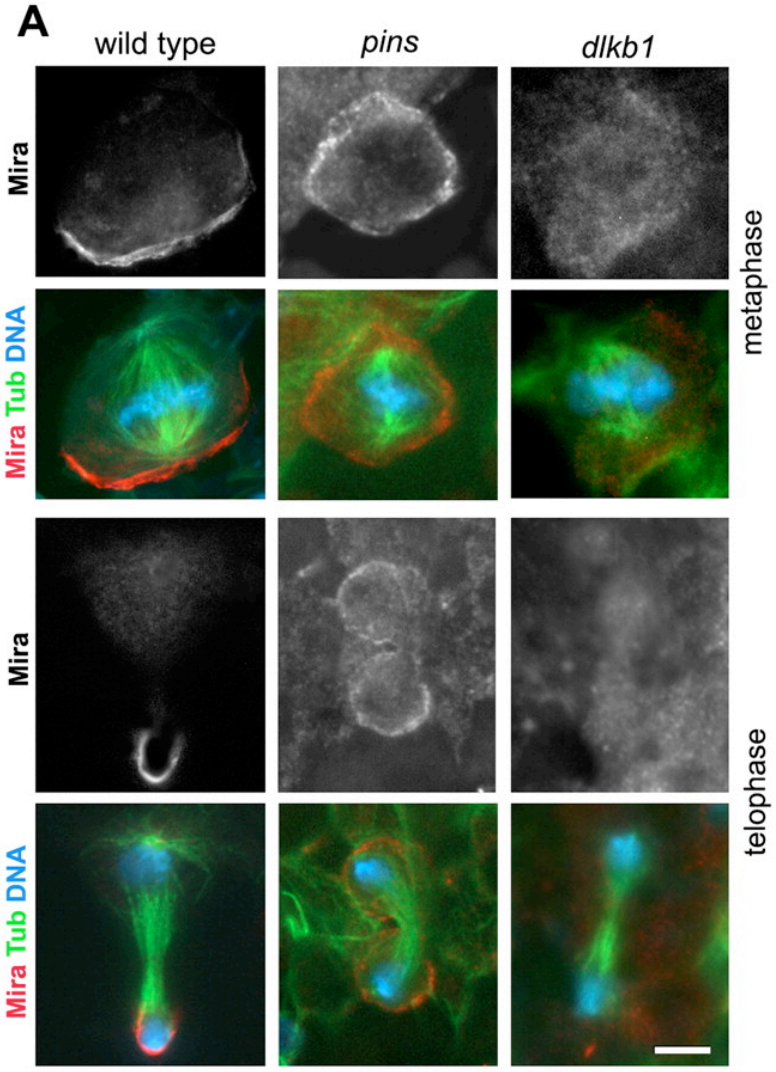

B

genotype	# of cells	regular %	cortical %	diffuse %
Metaphases and early anaphases				
wt	123	90	1	9
dlkb1	128	41	2	57
pins	116	25	26	49
Late anaphases and telophases				
wt	67	97	0	3
dlkb1	39	64	3	33
pins	30	30	20	50

However, while the majority (67%) of *pins* mutant NBs without a Mira crescent had this same pattern, a substantial minority (33%) of these cells showed a diffuse cortical distribution of Mira (Figure A1.5B).

We next determined whether *dlkb1* mutations affect the localization of Pins and Gαι at the apical cortex of dividing NBs (NBs were again identified by their size). A regular Pins signal was observed in 95% (n = 60) of the wild type NBs and in 84% (n = 145) of the *dlkb1* NBs (Figure A1.6A, B). Gαi formed a crescent at the apical pole of 96% of wild type NBs (n = 61) and 74% of *dlkb1* mutant NBs (n = 75) (Figure A1.6A, B). Consistent with previous results (Cai et al., 2003; Shaefer et al., 2001), we observed a Gαi apical crescent only in 4% (n = 50) of *pins* mutant NBs (data not shown). Thus, while *dlkb1* mutations affect Mira localization at the basal cortex, they have little or no effect on Pins and Gαi localization at the apical cortex.

We also analyzed Baz, DaPKC and Par-6 localization in both wild type and *dlkb1* mutant NBs. In wild type larval brains, the Baz signal was rather weak and only 48% (n = 63) of the dividing NBs displayed a clear Baz crescent at the apical pole. However, in *dlkb1* mutant brains, only 5 of the 106 NBs scored showed a discernible Baz crescent (Figure A1.6A, B). The DaPKC and Par-6 apical crescents were observed in 96% (n = 24) and 71% (n = 35) of wild type NBs, respectively, but most *dlkb1* NBs did not show apical accumulations of these proteins; DaPKC and Par6 crescents were detected only in 7% (n = 30) and 12% (n = 33) of *dlkb1* mutant NBs. These results suggest that the wild type function of *dlkb1* is required for the localization of the Baz, DaPKC and Par-6 at the NB apical pole.

Figure A1.6. Mutations in the *dlkb1* gene disrupt Baz/Par-6/DaPKC but not Pins/Gαi localization at the NB apical pole.

(A) Pins, Gαi, Baz, Par-6 and DaPKC localization in wild type and *dlkb1*^{315}/*dlkb1*^{315} mutants. NBs in the first row were simultaneously stained for Pins, centrosomin (Cnn) and DNA (blue). Cells shown in the subsequent rows were stained for tubulin (Tub), DNA (blue) and either Gαi, Baz, Par-6 or DaPKC. Scale bar, 5mm.

(B) Frequencies of NBs with Pins, Gαi, Baz, Par-6 and DaPKC crescents in wild type and *dlkb1*^{315}/*dlkb1*^{315} mutant brains.

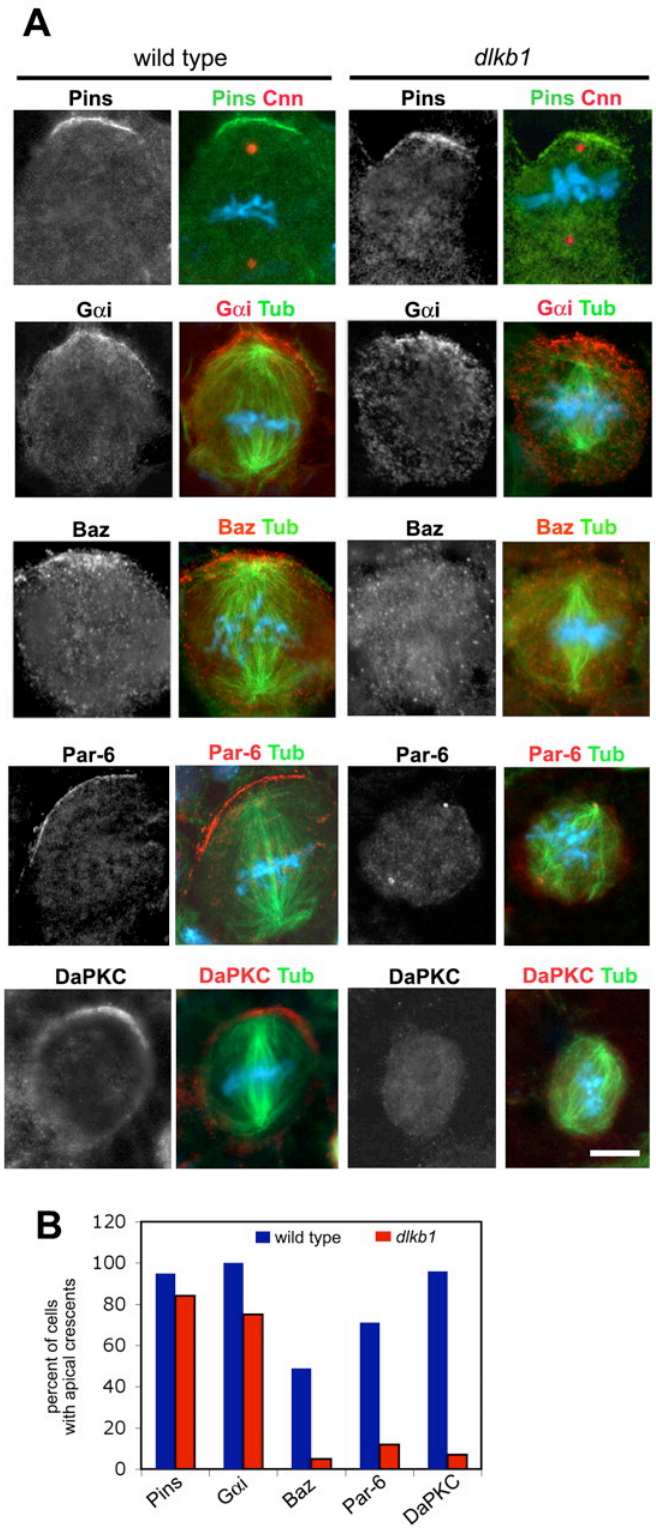
A
wild type
dlkb1
Pins
Pins Cnn
Pins
Pins Cnn
Gαi
Gαi Tub
Gαi
Gαi Tub
Baz
Baz Tub
Baz
Baz Tub
Par-6
Par-6 Tub
Par-6
Par-6 Tub
DaPKC
DaPKC Tub
DaPKC
DaPKC Tub
B
wild type
dlkb1
percent of cells with apical crescents
120
100
80
60
40
20
0
Pins
Gαi
Baz
Par-6
DaPKC

Recent work has suggested that DaPKC delocalization from the apical cortex can result in NB overproliferation (Lee et al., 2006b). Consistent with this idea, the brains from third instar larvae of *dlkb1* null mutants exhibit a dramatic hyperplasia of both the hemispheres and the ventral ganglion; this phenotype has been attributed to a reduction in developmental apoptosis during embryogenesis (Lee et al., 2006a). We observed a clear brain overgrowth in all our dlkb1 mutant alleles, confirming that Dlkb1 regulates *Drosophila* brain size (data not shown). It is likely that the brain hyperplasia elicited by dlkb1 mutations results from both defective apoptosis and DaPKC-related NB overproliferation

Dlkb1 is not required for NB spindle rotation

We examined 128 metaphases of *dlkb1* mutant NBs; 53 of them displayed a Mira crescent but only in one case was this crescent incorrectly oriented with respect to the spindle axis (Figure A1.5B). In contrast, this crescent was misoriented with respect to the spindle axis in 9 of the 29 *pins* NB metaphases with a Mira crescent (Figure A1.5B). These results confirm that Pins is required for proper spindle rotation during NB division and indicate that the Dlkb1 kinase is not involved in this process.

Recent work has shown that that spindle rotation is regulated by Mud (Mushroom body defect), a protein related to vertebrate NuMa that interacts with both Pins and the spindle microtubules. In embryonic NBs Mud forms an apical crescent and accumulates at the spindle poles; in larval NBs the cortical localization of Mud is weak or undetectable but the protein remains enriched at the spindle poles (Bowman et al., 2006; Izumi et al., 2006; Siller et al., 2006).

Figure A1.7. Mud localization in wild type and *dlkb1* mutant NBs. Cells were stained for Mud, tubulin (Tub) and DNA (blue).

(A and B) wild type prophase (A) and metaphase (B). (C and D) $dlkb1^{315}/dlkb1^{315}$ prophase (C) and metaphase (D). Scale bar, 5mm.

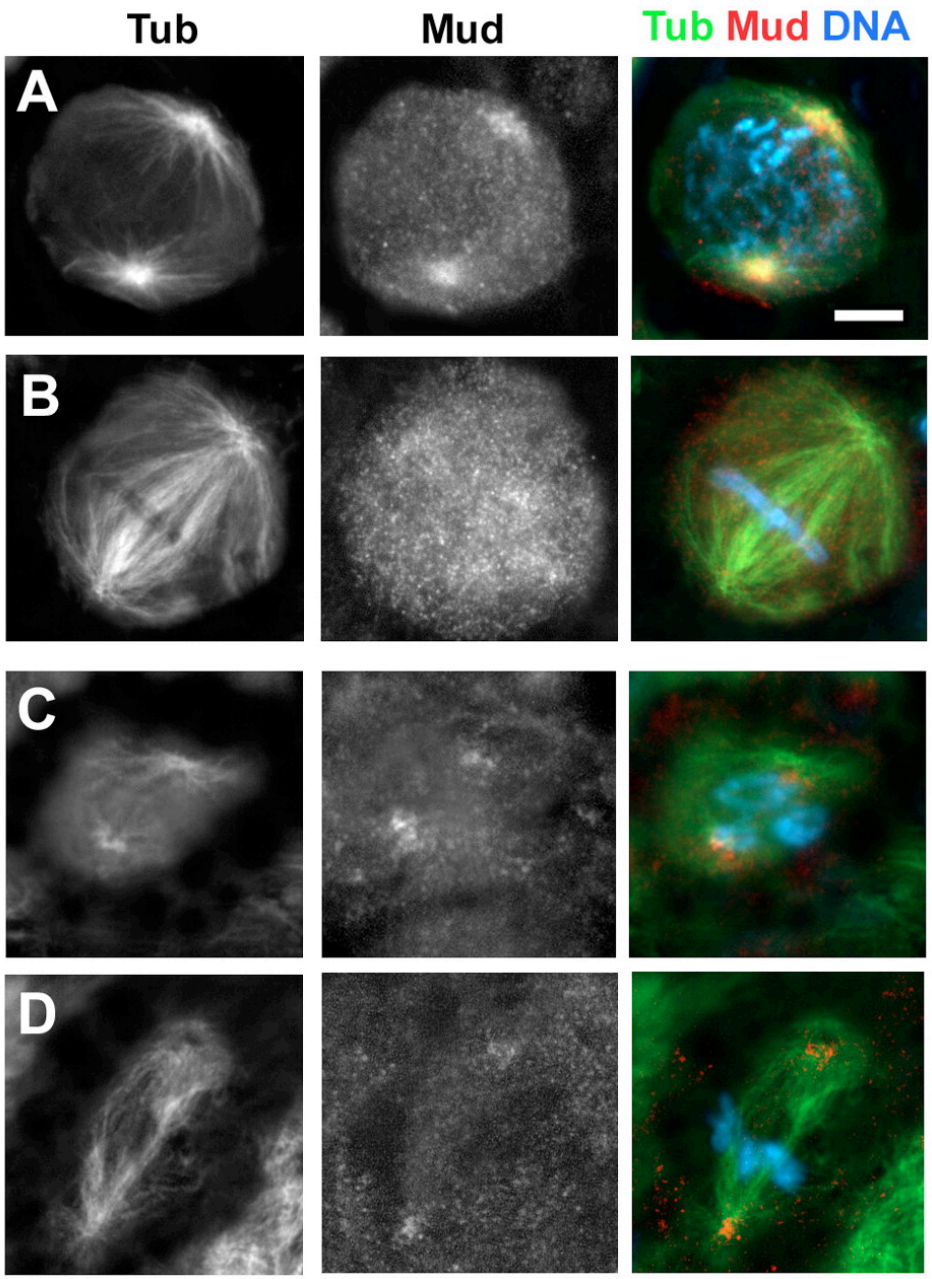
Tub
Mud
Tub Mud DNA
A
B
C
D

Immunostaining for Mud revealed that the protein is enriched at the centrosomes and the astral MTs in 93% (n = 45) of prophase and early prometaphase NBs (Figure A1.7A). With progression through mitosis, Mud localization becomes more diffuse and 62% (n = 45) of NB metaphase figures do not exhibit clear Mud accumulations at the spindle poles (Figure A1.7A); however, Mud relocalizes at the pericentrosomal regions of most anaphases and telophases (83%, n = 30; not shown). In *dlkb1* mutant NBs, Mud accumulates at the centrosomes/asters in 91% (n = 35) of prophase and early prometaphase NBs (Figure A1.7C), and remains associated with the spindle poles in 78% (n =37) of the metaphases (Figure A1.7D) and 85% (n = 20) of the ana-telophases (not shown). Thus, mutations in *dlkb1* do not affect Mud localization during metaphase and ana-telophase but appear to increase Mud concentration at the spindle poles during metaphase.

Subcellular localization of Dlkb1

To determine the subcellular localization of Dlkb1, we raised a guinea pig antibody against the entirety of Dlkb1. Western blot analysis showed that this antibody recognizes a band of the expected size (~ 63 kDa) in larval, embryonic and S2 cell extracts. This band is absent in both $dlkb1^{315}/Df(3R)urd$ and $dlkb1^{315}/dlkb1^{7}$ larvae (Figure A1.8A), demonstrating that it corresponds with Dlkb1. Since the truncated forms of Dlkb1 encoded by the $dlkb1^{315}$ and $dlkb1^{7}$ mutant alleles were not observed in mutant animals, either the mutant transcripts or the truncated proteins are unstable. These findings provide a strong support for the genetic data (Table A1.1), indicating that the $dlkb1^{315}$ mutant allele is functionally null.

Figure A1.8. Expression and intracellular localization of the Dlkb1 kinase.

(A) Western blot showing that our anti-Dlkb1 antibody recognizes a band of approximately 63 kDa**.** This band is absent in extracts from either *dlkb1*^{315}*/Df(3R)urd* or *dlkb1*^{315}*/dlkb1*^{7} mutant larvae. α-tubulin was used as a loading control (LC).

(B) Immunostaining of wild type dividing NBs for Dlkb1. Note that Dlkb1is diffuse in the cytoplasm. Scale bar, 5mm.

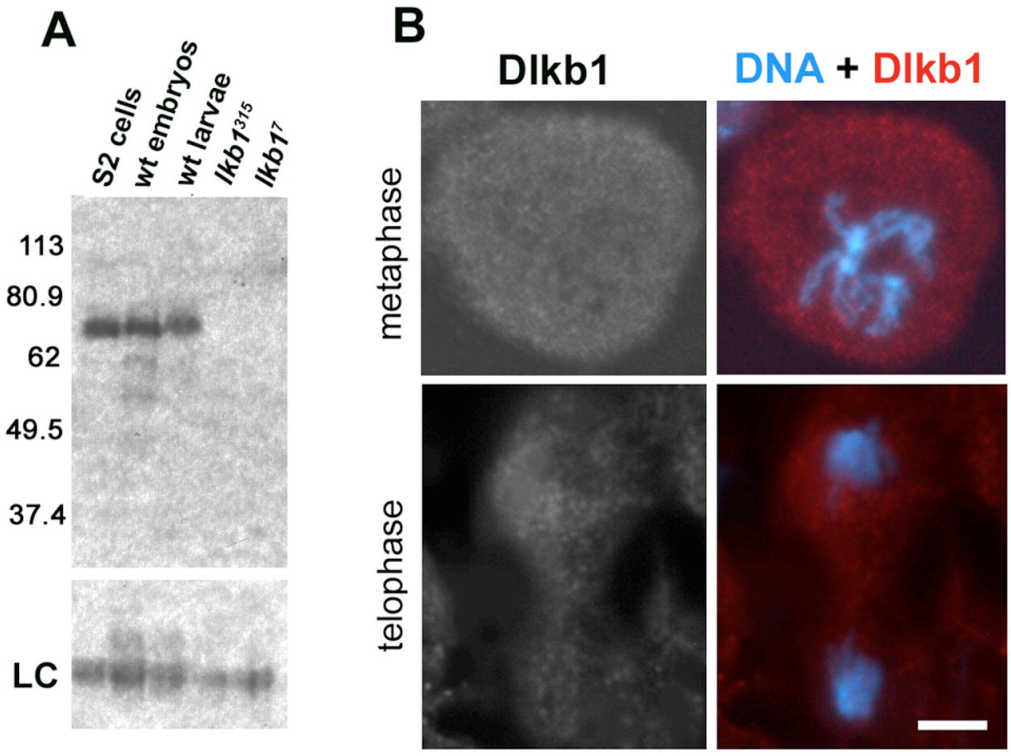
A
S2 cells
wt embryos
wt larvae
lkb1315
lkb17
113
80.9
62
49.5
37.4
LC
B
Dlkb1
DNA + Dlkb1
metaphase
telophase

Immunolocalization experiments revealed that Dlkb1 is dispersed in both the nucleus and the cytoplasm of interphase larval brain cells, and in the cytoplasm of both NBs and GMCs undergoing mitotic division. Immunostaining of *dlkb1*^{315}/Df(3R)*urd* mutant cells did not reveal any clear cytoplasmic signal, confirming the specificity of the antibody (Figure A1.8B and data not shown). The diffuse localization of Dlkb1 in brain cells is not consistent with its cortical localization in Drosophila oocytes (Martin and St. Johnston, 2003). However, the Dlkb1 localization pattern in brain cells does not depend on the quality of our antibody, as the same antibody revealed a cortical accumulation of Dlkb1 in oocytes (data not shown).

Dlkb1 and Pins function in different pathway controlling NB division

The findings that Dlkb1 and Pins co-precipitate (Blumer et al., 2003), and that *dlkb1* and *pins* mutations cause similar (but not identical) phenotypes, prompted us to perform an epistasis analysis. We thus compared the phenotype of the *dlkb1*^{315} *pins*^{P62} double mutant with those of the single mutants by examining brain preparations stained for tubulin, Dpn and DNA. In *dlkb1 pins* mutant brains, the spindles of both NBs and GMCs are much more defective than those observed in either of the single mutants (Compare Figure A1.9 with Figures 1 and 2). In addition to cells with severely defective spindles (Figure A1.9A, C, F, G, I), we also observed many (50%, n = 300) mitotic figures in which the spindle morphology was barely recognizable (Figure A1.9B, D, E, H); the frequency of the latter type of cells was only 4% (n = 201) in the *dlkb1* single mutant.

Figure A1.9. *dlkb1* and *pins* function in different pathways controlling the stability of spindle MTs.

Mitotic figures from brains of *dlkb1*^{315} *pins*^{P62} double mutants were stained for tubulin (Tub, green), DNA (blue) and centrosomin (red). (A – F) NBs, (G – I) GMCs. (A, B) metaphases; (C – E) anaphases; (F) telophase (G) metaphases; (H) anaphase; (I) telophase. The arrow in (E) points to a lagging X chromosome with unseparated sister chromatids. Note the extremely defective spindle structures of the NBs shown in (B, D, E and H). Scale bar, 5mm.

(J) Size distribution of metaphase spindles in wild type and *dlkb1 pins* brains. Dpn-positive (NB) and negative (GMC) spindles are depicted in red and green, respectively. Size (mm) classes: A, 4.7-6.9; B, 7.0-9.2; C, 9.3-11.5; D, 11.6-13.8; E, 13.9-16.1; F, 16.2-18.4; G, 18.5-20.7.

(K) Expression of Pins and Dlkb1 in brains from third instar larvae of *dlkb1*, *pins* and *dlkb1 pins* mutants. Note that the Dlkb1 protein is undetectable in larval brain extracts of both *dlkb1*^{315} homozygotes and *dlkb1*^{315} *pins*^{P62} double mutants. Similarly, Pins cannot be detected in brain extracts of both *pins*^{P62}/*pins*^{P62} mutants and *dlkb1*^{315} *pins*^{P62} double mutants. The Giotto proteins (Giansanti et al., 2006) was used as a loading control (LC).

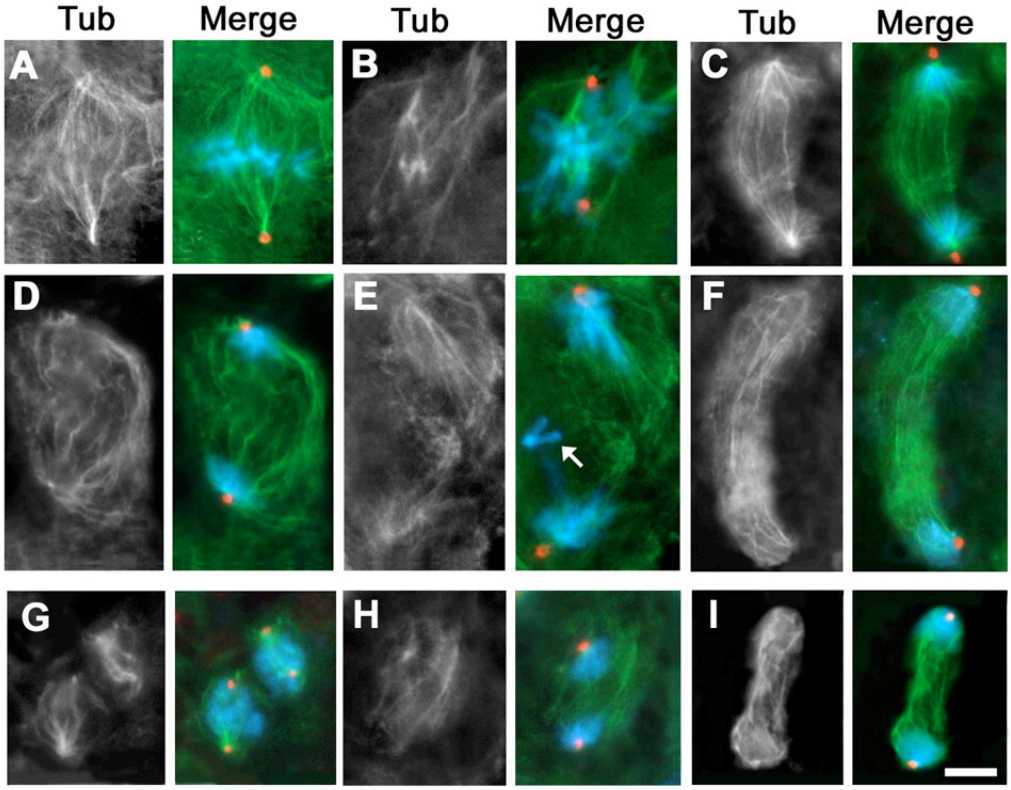
Tub
Merge
Tub
Merge
Tub
Merge
A
B
C
D
E
F
G
H
I

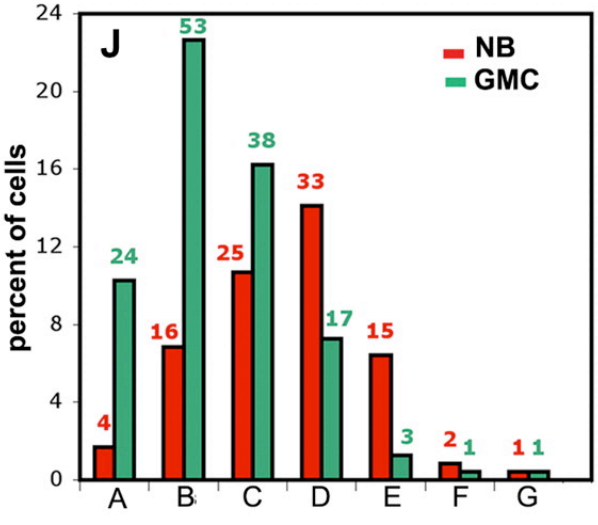
J
NB
GMC
percent of cells
24
20
16
12
8
4
0
A
B
C
D
E
F
G
4
24
16
53
25
38
33
17
15
3
2
1
1
1

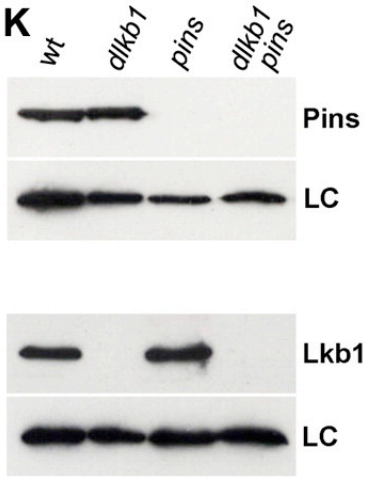
K
wt
dlkb1
pins
dlkb1 pins
Pins
LC
Lkb1
LC

In *dlkb1 pins* metaphases, the MT density is extremely low, the spindle poles have a characteristic pointed appearance and the asters are completely absent (Figure A1.9A). The ana-telophases are also devoid of asters and display few and sparse central spindle MTs, which are never pinched in the middle (Figure A1.9C, F). These results indicate that *dlkb1* and *pins* function in parallel pathways to control spindle formation. The absence of central spindle pinching, which suggests an accompanying failure of cytokinesis, prevented a reliable assessment of the degree of asymmetry of NB divisions. However, NB spindles of the double mutant are smaller than in wild type (Figure A1.9J). In addition, the analysis of centrosome size in large metaphase figures (longer than 14 mm), most of which are likely to be NBs, revealed that 90% (n = 106) of them have equally sized centrosomes. In wild type, *dlkb1* and *pins* the frequencies of NB metaphases with centrosomes of equal size were 12%, 72% and 61%, respectively (Figure A1.4B). Finally, only 3% (n = 120) of the *dlkb1 pins* NB metaphases were characterized by a Mira crescent; in the remaining cells, Mira was either diffuse in the cytoplasm (85%) or associated with the entire cell cortex (12%). Thus, the Mira mislocalization phenotype observed in *dlkb1 pins* double mutants is stronger than that seen in the single mutants (see Figure A1.5B).

Although the $dlkb1^{315}$ and $pins^{P62}$ alleles are both functionally null, it cannot be excluded that the brains of the $dlkb1^{315}$ $pins^{P62}$ double mutants retain residual amounts of the maternally supplied Dlkb1 and Pins proteins. We thus performed a Western blotting analysis of extracts from third instar larval brains of $dlkb1^{315}$, $pins^{P62}$ and $dlkb1^{315}$ $pins^{P62}$ mutants. As shown in Figure A1.9K, $dlkb1^{315}$ and $dlkb1^{315}$ $pins^{P62}$ brains do not exhibit detectable amounts of the Dlkb1 kinase, consistent with the results shown in Figure A1.8A. Similarly, the

Pins protein appears to be completely absent in *pins*^{P62} and *dlkb1*^{315} *pins*^{P62} brains. Thus, the phenotypes observed in the single and double mutants reflect a complete loss of the wild type function of either Dlkb1 or Pins or both.

Collectively, our results suggest that *dlkb1* and *pins* act in different pathways to control the asymmetry of NB division. These genes also function in parallel pathways involved in MT stability and spindle formation. Whether the latter pathways are the same that control the asymmetry of NB mitosis remains to be determined.

DISCUSSION

Dlkb1 controls the stability of spindle MTs

Our results indicate that mutations in the *dlkb1* gene disrupt spindle formation in both NBs and GMCs. In addition, the finding that the imaginal discs of *dlkb1* mutant larvae are small and misshapen suggests a defect in imaginal cell mitosis. Previous studies have shown that late larval lethality and small imaginal discs are diagnostic of abnormalities in mitotic divisions (Gatti and Baker, 1989). Thus, the *dlkb1* phenotype strongly suggests that the Dlkb1 kinase plays an important mitotic role not only in NBs, but also in other somatic cell types. Despite the low density of spindle MTs, most mutant metaphases enter anaphase (the frequency of anaphases in *dlkb1* mutants and in wild type controls was 10-13% and 16%, respectively; see Table A1.1), suggesting that in a substantial fraction of mutant cells the spindle checkpoint is either not induced or only transiently activated. However, the defects in NB spindles are likely to lead to the formation of polyploid cells. These cells could arise through two different mechanisms. Cells blocked in metaphase due to either reduced MT density or activation of the spindle checkpoint could revert

to interphase and become polyploid after an additional round of DNA replication. Alternatively, cells that enter anaphase but assemble an abnormally thin central spindle may be unable to undergo cytokinesis and thus produce polyploid cells (Vernì et al., 2004).

The precise function of Dlkb1 in spindle formation and/or maintenance is currently unclear. However, the finding that the spindles of *dlkb1 asl* double mutants display a lower MT density than *asl* single mutants argues for a defect in MT stability and not in centrosome function. Studies in mammalian cells have shown that LKB1 is a master kinase that phosphorylates at least 14 kinases all related to AMP-activated kinases (AMPK). Kinases of the AMPK family include regulators of cellular energy levels, as well as four Microtubule Affinity Regulating Kinases (MARK; reviewed by Alessi et al., 2006; Baas et al., 2004b). The MARK enzymes are the mammalian homologues of *C. elegans* and *Drosophila* Par-1. However, *Drosophila* Par-1, which controls MT stability in oocytes (Shulman et al., 2000), appears to act upstream of Dlkb1/Par4 (Martin and St. Johnston, 2003). It is therefore unlikely that the Dlkb1 substrate required for the stability of spindle MTs is Par-1. Further evidence that Dlkb1 does not act via Par-1 phosphorylation comes from RNAi experiments showing that Dlkb1 depletion, but not Par-1 depletion, causes defects in spindle morphology (Bettencourt-Dias et al., 2005). Thus, current data indicate that the Dlkb1 kinase regulates the activity of an unknown factor required for the stability of the spindle MTs; this factor could either be a direct substrate of Dlkb1 or a substrate for one of the kinases acting downstream Dlkb1.

Our cytological analyses have shown that the spindles of *dlkb1 pins* double mutants display a MT density that is substantially lower than that

observed in either single mutant. Here again, highly defective spindles were observed in both NBs and GMCs. In addition, doubly mutant larvae showed extremely reduced imaginal discs, suggesting an underlying mitotic defect. Given that the *dlkb1*^{315} and *pins*^{P62} alleles used in the analysis are both functionally null and that the corresponding proteins were undetectable in mutant brains (Yu et al., 2000; this study), these results indicate that Pins and Dlkb1 function in different pathways for the control of MT stability. The observation that the spindles of *pins* mutants display a normal MT density further suggests that Pins plays a redundant role in the maintenance of MT stability. A role of Pins in spindle formation and/or stability has never been demonstrated in *Drosophila*. However, the mammalian homologue of Pins binds NuMa and regulates mitotic spindle organization and positioning (Du et al., 2001).

Dlkb1 controls the asymmetry of NB division

We have analyzed the phenotypic consequences of *dlkb1* mutations in larval brain NBs. In contrast with embryonic NBs that display small, regularly-sized spindles (their metaphase spindles are approximately 5 mm long), brain NBs exhibit spindles of very different sizes (ranging from 5 to 32 mm for metaphase spindles). Nonetheless, dividing brain NBs exhibit the same asymmetries of their embryonic counterparts, including asymmetries in aster and centrosome size, localization of specialized protein complexes and positioning of the cleavage furrow (Bowman et al., 2006; Giansanti et al., 2001; Lee et al., 2006b; Parmentier et al., 2000; Rolls et al., 2003; Siller et al., 2006; this study). However, the degree of asymmetry of brain NB division is directly related to the cell size, so that large NBs divide more asymmetrically

than the small ones (Figure A1.3E). This is likely to render large brain NBs particularly sensitive to mutations that affect cleavage furrow positioning. Consistent with this hypothesis, mutations in *pins* have mild effects on the asymmetry of embryonic NB divisions (Cai et al., 2003) but disrupt unequal cytokinesis in most larval brain NBs (Parmentier et al., 2000; Figure A1.3E). *dlkb1* larval NBs also divide more symmetrically than their wild type counterparts, leading to larval brains devoid of large NBs. In addition, most *dlkb1* NBs display centrosomes of equal size and very small asters at both poles. However, the symmetric cytokinesis of *dlkb1* NBs cannot result from their short astral MTs, as *asl* NBs divide asymmetrically in the complete absence of asters (Figure A1.3B, C, E).

dlkb1 mutant NBs are also characterized by the abnormal distribution of several components of the apical and basal complexes. In *dlkb1* mutant brains, most NBs display normal Pins and Gαi crescents at their apical pole but fail to accumulate Baz, DaPKC and Par-6 at the same pole. In addition, most *dlkb1* mutant NBs fail to exhibit a normal Mira crescent at the basal pole cortex. A normal localization of Pins and Gαi has been already observed in most embryonic NBs defective in the Baz/Par6 pathway (Cai et al., 2003; Izumi et al., 2004; Schaefer et al., 2000; Yu et al., 2000; 2003). Moreover, studies on embryonic NBs have suggested that Baz, Par-6 and DaPKC function as a complex, are interdependent for their localization at the NB apical pole, and required for the formation of the Mira crescent at the basal pole (Petronczki and Knoblich, 2000; Wodarz et al., 2000). However, subsequent work on second instar larval NBs has shown that these proteins are not mutually dependent for the formation of the Baz/Par-6/DaPKC apical crescent; they accumulate at the apical cortex in a hierarchical fashion, with

Baz and Par-6 mediating proper DaPKC localization (Rolls et al., 2003). Mutations that disrupt the Pins/Gαi pathway prevent asymmetrical localization of either Pins or Gαi in embryonic NBs but do not substantially affect Mira accumulation at the basal pole (Cai et al., 2003). However, it should be noted that mutations in *pins* partially disrupt asymmetric Mira localization in larval brain NBs (Parmentier et al., 2000; this study), suggesting that larval NBs differ from embryonic NBs in some aspects of the control of Mira localization. Thus, taking into account the differences between embryonic and larval NBs, our results indicate that mutations in the *dlkb1* gene and those that disrupt the Baz/Par6 pathway affect similar aspects of NB mitotic division.

Our analyses have shown that in *dlkb1 pins* double mutants the NBs divide more symmetrically than in the corresponding single mutants. This indicates that the *dlkb1* and *pins* genes act in different pathways that mediate unequal cytokinesis. Previous studies have shown that the asymmetry of NB cytokinesis depends on the Baz/Par6 and the Pins/Gαi redundant pathways. When only one of these pathways is impaired, NBs still divide asymmetrically, but they divide symmetrically when both are disrupted (Cai et al., 2003). The simplest interpretation of our findings is that *dlkb1* acts in the Baz/Par6 pathway. In addition, the observation that Dlkb1 is required for proper localization of Baz, Par-6 and DaPKC suggest that this kinase acts at the top of the hierarchical mechanism that mediates accumulation of the Baz/Par6 complex at the apical cortex. However, although we favor the hypothesis that Dlkb1 acts in the Baz/Par6 pathway, we cannot exclude the possibility that this kinase functions in both the Baz/Par6 and Pins/Gαi pathways, or in a third pathway different from the Baz/Par6 pathway.

In this context, it is important to note that our results exclude the possibility that *dlkb1* acts via Pins phosphorylation. Previous studies have shown that mammalian LKB1 coprecipitates and phosphorylates AGS3, the mammalian orthologue of Pins. Dlkb1 and Pins coimmunoprecipitate as well, but it is currently unclear whether Pins is phosphorylated by Dlkb1 (Blumer et al., 2003). Regardless of whether Pins is a substrate of Dlkb1, the phenotypes elicited by *dlkb1* mutations cannot be the consequence of an impairment of Pins function. *dlkb1* and *pins* mutant NBs do in fact differ in a number of phenotypic traits, including spindle organization and the pattern of Mira localization, and do not belong to the same epistasis group.

Dlkb1 is not required for NB spindle rotation

In vivo imaging has shown that the spindles of embryonic NBs rotate during metaphase to become aligned with the center of the Pins apical crescent (Kaltschmidt et al., 2000). In contrast, the spindles of larval NBs align with the Pins crescent at prophase (Siller et al., 2006). Failure of proper rotation of larval NB spindles results in spindles that are misoriented with respect to the apical (Pins) and basal (Mira) crescents (Giansanti et al., 2001; Siller et al., 2006). There is also evidence that proper positioning of larval NB spindles depends on astral MTs, since in approximately 50% of *asl* NB metaphases the Mira crescent is misoriented with respect to the spindle axis (Giansanti et al., 2001; this study).

Our results indicate that spindle rotation occurs normally in *dlkb1* mutant NBs. In addition, we have shown that prophase/prometaphase larval NBs of *dlkb1* mutants normally accumulate the Mud protein, which mediates proper spindle alignment in both embryonic and larval NBs (Bowman et al.,

2006; Izumi et al., 2006; Siller et al., 2006). Together, these results indicate that the Dlkb1 kinase is not required for spindle rotation and that the short astral MTs of *dlkb1* mutant NBs can mediate proper spindle positioning. These results are consistent with the idea that the Pins/Gαi, but not the Baz/Par6 pathway is involved in spindle rotation (Izumi et al., 2004; Siegrist and Doe, 2005) and provide further support for the hypothesis that Dlkb1 functions in the latter pathway.

Recent work has shown that in the absence of the Baz/Par6 pathway, astral MTs can mediate the localization of Pins/Gαi at the basal cortex (Siegrist and Doe, 2005). Assuming that Dlkb1 acts in the Baz/Par6 pathway, the finding that this kinase is not required for the formation of Pins/Gαi crescents indicates that the short astral MTs of *dlkb1* NBs retain the ability to mediate Pins/Gαi cortical localization.

Conclusions and perspectives

Our results indicate that Dlkb1 and Pins function in partially redundant pathways controlling the stability of spindle MTs. These proteins are also required for the asymmetry of NB divisions and, here again, they appear to function in different pathways. Pins acts in a common pathway with Gαi, while Dlkb1 is likely to function in the Baz/Par6 pathway. Intriguingly, recent work has shown that simultaneous loss of *pins* and *baz* functions results in the formation of abnormally small embryonic NB spindles that lack astral MTs at both poles (Fuse et al., 2003). Thus, the embryonic NBs of *baz pins* double mutants have a spindle phenotype reminiscent of that observed in *dlkb1* larval NBs. These findings raise the question of whether the Pins/Gαi and Baz/Par6 pathways redundantly control spindle organization as they do for the

asymmetry of NB divisions. The extant data do not provide a clear answer for this question. The analysis of the roles of the two pathways in spindle formation and their precise relationships with the Dlkb1 kinase will be an interesting problem to be addressed in future studies.

Previous studies in *Drosophila* and mammalian cells have led to the suggestion that loss of epithelial cell polarity is ultimately responsible for the Peutz-Jeghers cancer syndrome (Martin and St. Johnston, 2003; Baas et al., 2004b). Here, we have shown that Dlkb1 plays an essential mitotic role and is required for the asymmetry of NB division. These results lead us to propose that tumor development in Peutz-Jeghers patients depends on the impairment of multiple processes, including cell polarity, the asymmetry of stem cell division and the fidelity of chromosome segregation during mitosis.

ACKNOWLEDGEMENTS

We thank W. Chia, Y. Jan, T. Kaufman, J. Knoblich and F. Matsuzaki for antibodies and fly stocks. This work was supported by grants from Centro di Eccellenza di Biologia e Medicina Molecolare (BEMM) to MG, and by the NIH grant GM48430 to MLG.

LITERATURE CITED

Alessi, D. R., Sakamoto, K. and Bayascas, J.R. (2006). LKB1-dependent signaling pathways. *Annu. Rev. Biochem.* **75,** 137-163.

Baas, A. F., Kuipers, J., van der Wel, N. N., Batlle, E., Koerten, H. K., Peters, P. J. and Clevers, H. C. (2004a). Complete polarization of single intestinal epithelial cells upon activation of LKB1 by STRAD. *Cell* **116,** 457-466.

Baas, A. F., Smit, L. and Clevers, H. (2004b). LKB1 tumor suppressor protein: PARtaker in cell polarity. *Trends Cell Biol.* **14,** 312-319.

Betschinger, J. and Knoblich, J. A. (2004). Dare to be different: asymmetric cell division in *Drosophila, C. elegans* and vertebrates. *Curr. Biol.* **14,** R674-R685.

Bettencourt-Dias, M., Giet, R., Sinka, R., Mazumdar, A., Lock, W. G., Balloux, F., Zafiropoulos, P. J., Yamaguchi, S., Winter, S., Carthew, R. W., et al. (2004). Genome-wide survey of protein kinases required for cell cycle progression. *Nature* **432,** 980-987.

Bier, E., Vaessin, H., Younger-Shepherd, S., Jan, L. Y. and Jan, Y. N. (1992). *deadpan*, an essential pan-neural gene in *Drosophila*, encodes a helix-loop-helix protein similar to the *hairy* gene product. *Genes Dev.* **6,** 2137-2151.

Blumer, J. B., Bernard, M. L., Peterson, Y. K., Nezu, J., Chung, P., Dunican, D. J., Knoblich, J. A. and Lanier, S. M. (2003). Interaction of activator of G-protein signaling 3 (AGS3) with LKB1, a serine/threonine kinase involved in cell polarity and cell cycle progression: phosphorylation of the G-protein regulatory (GPR) motif as a regulatory mechanism for the interaction of GPR motifs with Galphai. *J. Biol Chem.* **278,** 23217-23220.

Bonaccorsi, S., Giansanti, M. G. and Gatti, M. (1998). Spindle self-organization and cytokinesis during male meiosis in *asterless* mutants of *Drosophila melanogaster. J. Cell Biol.* **142,** 751-761

Bonaccorsi, S., Giansanti, M. G. and Gatti, M. (2000). Spindle assembly in *Drosophila* neuroblasts and ganglion mother cells. *Nat. Cell Biol.* **2,** 54-56.

Bowman, S. K., Neumuller, R. A., Novatchkova, M., Du, Q. and Knoblich, J. A. (2006). The *Drosophila* NuMA Homolog Mud regulates spindle orientation in asymmetric cell division. *Dev. Cell* **10,** 731-742.

Cai, Y., Yu, F., Lin, S., Chia, W. and Yang, X. (2003). Apical complex genes control mitotic spindle geometry and relative size of daughter cells in *Drosophila* neuroblast and pI asymmetric divisions. *Cell* **112,** 51-62.

Du, Q., Stukenberg P. T. and Macara, I. G. (2001). A mammalian Partner of Inscuteable binds NuMa and regulates mitotic spindle organization. *Nat. Cell Biol.* **3,** 1069-1075.

Fuse, N., Hisata, K., Katzen, A. L. and Matsuzaki, F. (2003). Heterotrimeric G proteins regulate daughter cell size asymmetry in *Drosophila* neuroblast divisions. *Curr. Biol.* **13,** 947-954.

Gatti, M. and Baker, B. S. (1989). Genes controlling essential cell-cycle functions in *Drosophila melanogaster*. *Genes Dev.* **3,** 438-453.

Giansanti, M.G, Bonaccorsi, S., Kurek, R., Farkas, R. M., Dimitri, P., Fuller, M.T. and Gatti, M. (2006). The class I PITP Giotto is required for *Drosophila* cytokinesis. *Curr. Biol.* **16,** 195-201.

Giansanti, M. G, Gatti, M. and Bonaccorsi, S. (2001). The role of centrosomes and astral microtubules during asymmetric division of *Drosophila* neuroblasts. *Development* **128,** 1137-1145.

Goodman, C. S. and Doe, C. Q. (1993). Embryonic development of the *Drosophila* central nervous system. In *The Development of Drosophila melanogaster* (ed. M. Bate and A. Martinez Arias), pp. 1131-1206. New York Cold Spring Harbor Laboratory Press.

Izumi, Y., Ohta, N., Itoh-Furuya, A., Fuse, N. and Matsuzaki, F. (2004). Differential functions of G protein and Baz-aPKC signaling pathways in *Drosophila* neuroblast asymmetric division. *J. Cell Biol.* **164,** 729-738.

Izumi, Y., Ohta, N., Hisata, K, Raabe, T. and Matsuzaki, F. (2006). *Drosophila* Pins-binding protein Mud regulates spindle-polarity coupling and centrosome organization. *Nat. Cell Biol.* **8,** 586-593.

Kaltschmidt, J. A., Davidson, C. M., Brown, N. H. and Brand, A. H. (2000). Rotation and asymmetry of the mitotic spindle direct asymmetric cell division in the developing central nervous system. *Nat. Cell Biol.* **2,** 7-12.

Koundakjian, E. J., Cowan, D. M., Hardy, R. W. and Becker A. H. (2004). The Zuker collection: a resource for the analysis of autosomal gene function in *Drosophila melanogaster*. *Genetics* **167,** 203-206.

Lee, J. H., Koh, H., Park, J., Lee, S. Y., Lee, S., and Chung, J. (2006a). JNK pathway mediates apoptotic cell death induced by tumor suppressor LKB1 in *Drosophila. Cell Death and Diff.* **13,** 1110-1122.

Lee, C-Y., Robinson K. J. and Doe, C. Q. (2006b). Lgl, Pins, and aPKC regulate neuroblast self-renewal versus differentiation. *Nature* **439,** 594-598.

Martin, S. G. and St. Johnston, D. (2003). A role for *Drosophila* LKB1 in anterior-posterior axis formation and epithelial polarity. *Nature* **421,** 379-384.

Megraw, T. L., Kao, L. R. and Kaufman, T. C. (2001). Zygotic development without functional mitotic centrosomes. *Curr Biol.* **11,** 116-120.

Parmentier, M. L., Woods, D., Greig, S., Phan, P. G., Radovic, A., Bryant, P. and O'Kane, C. J. (2000). Rapsynoid/partner of inscuteable controls asymmetric division of larval neuroblasts in *Drosophila*. *J. Neurosci*. **20,** RC84.

Petronczki, M. and Knoblich, J. A. (2000). DmPar-6 directs epithelial polarity and asymmetric cell division of neuroblasts in *Drosophila*. *Nature Cell Biol.* **3,** 43-49.

Rolls, M. M., Albertson, R., Shih, H-P, Lee, C-Y and Doe, C. Q. (2003). *Drosophila* aPKC regulates cell polarity and cell proliferation in neuroblasts and epithelia. *J. Cell Biol.* **163,** 1089-1098.

Schaefer, M., Shevchenko, A., Shevchenko, A. and Knoblich, J.A. (2000). A protein complex containing Inscuteable and the Ga-binding protein Pins orients asymmetric cell divisions in *Drosophila. Curr. Biol.* **10,** 353-362.

Shulman, J. M., Benton, R, and St. Johnston, D. (2000). The *Drosophila* homolog of *C. elegans* PAR-1 organizes the oocyte cytoskeleton and directs oskar mRNA localization to the posterior pole.
Cell **101,** 377-388.

Siegrist, S. E. and Doe, C. Q. (2005). Microtubule-induced Pins/Galphai cortical polarity in *Drosophila* neuroblasts. *Cell* **123,** 1323-1335.

Siller, K. H., Cabernard, C. and Doe, C. Q. (2006). The NuMA-related Mud protein binds Pins and regulates spindle orientation in *Drosophila* neuroblasts. *Nat. Cell Biol.* **8,** 594-600.

Vernì, F., Somma, M. P., Gunsalus, K. C., Bonaccorsi, S., Belloni, G., Goldberg, M. L., and Gatti, M. (2004). Feo, the *Drosophila* homolog of PRC1, is required for central-spindle formation and cytokinesis. *Curr Biol.* **14,** 1569-1575.

Watts, J. L., Morton, D. G., Bestman, J. and Kemphues, K. J. (2000). The *C. elegans par-4* gene encodes a putative serine-threonine kinase required for establishing embryonic asymmetry. *Development* **127,** 1467-1475.

Wodarz, A. (2005). Molecular control of cell polarity and asymmetric cell division in *Drosophila* neuroblasts. *Curr. Opin. Cell Biol.* **17,** 1-7.

Wodarz, A, Ramrath, A., Grimm, A., and Knust, E. (2000). *Drosophila* Atypical Protein Kinase C associates with Bazooka and controls polarity of epithelia and neuroblasts. *J. Cell Biol*. **150,** 1361-1374

Yu, F., Morin, X., Cai, Y., Yang, X., and Chia, W. (2000). Analysis of *partner of inscuteable,* a novel player of *Drosophila* asymmetric divisions, reveals two distinct steps in *inscuteable* apical localization. *Cell* **100,** 399-409.

Yu, F., Cai, Y., Kaushik, R., Yang, X., and Chia, W. (2003). Distinct roles of Gai and Gb13F subunits of the heterotrimeric G protein complex in the mediation of *Drosophila* neuroblast asymmetric divisions. *J. Cell Biol.* **162,** 623-633.

APPENDIX 2

CHARACTERIZATION OF SIX CELL CYCLE MUTATIONS IN *DROSOPHILA*

INTRODUCTION

Cell division is an essential, highly regulated process that allows every living organism to grow, develop, and produce progeny. The cell cycle is simply described as containing of G1 (gap 1 phase), S (DNA Synthesis), G2 (gap 2), and M (mitosis). G1, S, and G2 together constitute interphase, the period that separates successive mitotic divisions, and during which cells grow and replicate their DNA. Mitotic cell division is the intricate process by which the replicated DNA and cellular components of one parental cell are equally divided to become two daughter cells.

Although mitosis is a continuous process, it is often split into more specific stages for the sake of discussion. Cells exit interphase and enter prophase, when the chromosomes begin to condense mostly because of the phosphorylation of certain histones. Prometaphase is characterized by further condensation of the chromosomes, nuclear envelope breakdown, and the initial stages of the attachment of microtubules to the kinetochores of the chromatids. Metaphase is considered to have begun when the sister chromatids are bidirectionally attached to microtubules so that the chromosomes align along the metaphase plate. A checkpoint exists which holds a cell in metaphase until all chromatids are aligned properly and kinetochore microtubules achieve a proper amount of tension across the

chromosomes. Separation of the sister chromatids occurs during anaphase, allowing the individual chromatids to move along the kinetochore microtubules to opposite poles of the cell. When the chromatids are fully separated, the cells enter telophase and the nuclear envelopes are reformed while the chromosomes decondense. The two daughter cells are physically separated during cytokinesis, which occurs (in animal cells) by the formation of a cleavage furrow between the asters of the spindle apparatus. With mitosis complete, the cells then re-enter interphase. The length of time spent in interphase depends on the cell type and developmental stage of the organism, but it can be as short as a couple of minutes, as occurs during early *Drosophila* embryogenesis (Foe and Alberts, 1983) or as long as forever, since a newly formed cell may remain quiescent for the rest of the life of the organism.

Drosophila and mitosis

Drosophila is an ideal model organism for studying mitosis, in large part because maternal contributions can allow certain mutants to live to a stage in development at which mitosis can be examined by high-resolution cytological techniques. In *Drosophila* larvae only three cell types are undergoing mitosis: the imaginal discs, abdominal histoblasts and the neuroblasts (Gatti and Goldberg, 1991). By comparing the development of these tissues and mitosis of these dividing cells in mutant and wild type flies, the role of individual proteins in mitosis can be elucidated.

Many proteins important for cell division in *Drosophila* are provided in sufficient concentrations within the egg for homozygote mutant zygotes to develop to the third instar larval stage, when the maternally supplied stores of

the protein are depleted (Baker et al., 1982). These late larval lethal mutants can show many types of aberrant behavior during cell division, resulting in an increase or decrease in the mitotic index in mitotically active tissues, small or absent imaginal discs, and cells that are anueploid or polyploid, or that show defects in chromosome condensation (Gatti and Goldberg, 1991).

In this Appendix, I will describe my initial characterization of six different mutant strains that were provided to us by Dr. Fiammetta Verní in the laboratory of Professor Maurizio Gatti at the University of Rome. Dr. Verní screened the Zucker collection of EMS-induced mutants (Koundakjian et al., 2004) for strains showing late larval lethality that also displayed potential chromosome condensation defects (see Chapter 2 for more details). My characterization involved genetic mapping of the mutation in question as well as a preliminary cytological analysis of the mutant phenotype. The *toys are us (trus)* mutation described in Chapter 3 is a seventh mutant stock uncovered from this same screen.

MATERIALS AND METHODS

Wild Type Flies

All wild type (WT) flies discussed in this Appendix are from the *Drosophila melanogaster* laboratory stock OregonR (OR). The mitotic index is defined as the number of mitotic cells visualized per field of view at 1000 X. In a WT third instar larval brain, the average mitotic index is 0.62 +/- 0.06 Images of WT brain squashes showing normal mitotic figures are provided (Figure A2.1 A-D) for comparison to the mutants that will be discussed in this chapter.

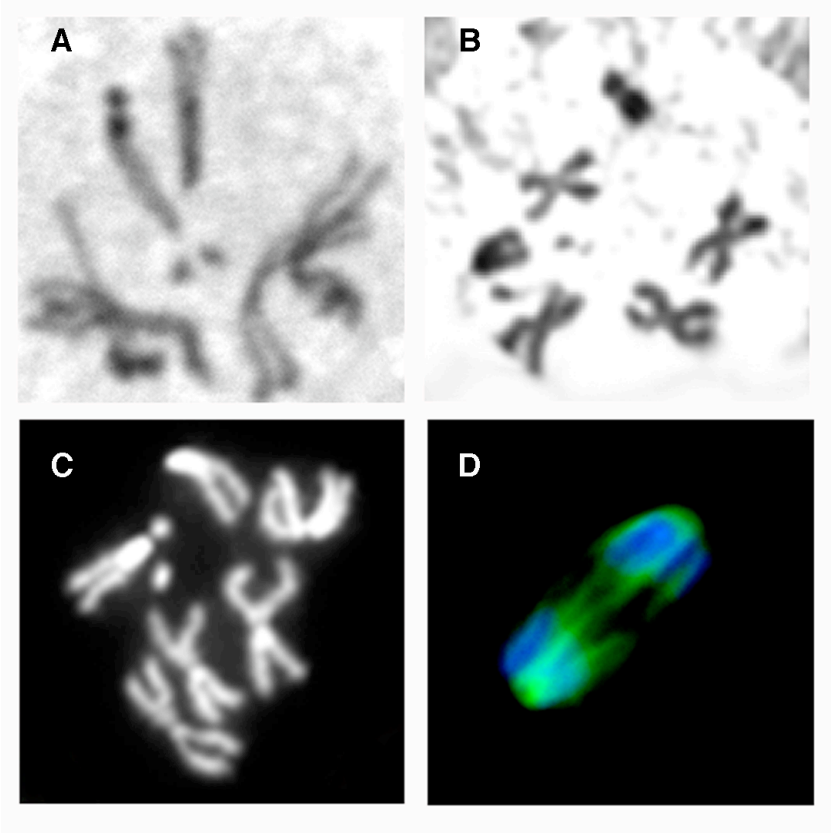

Figure A2.1 Phenotype of wild type brains

(A-B) Orcein-stained brain squashes showing the range of normally condensed mitotic chromosomes in metaphase. (C) DAPI stained mitotic chromosomes are condensed and identifiable as individual chromosomes. (D) A wild type anaphase showing DNA stained with Hoerst (blue) and spindles stained with anti-Tubulin (green).

Cytology of brains for analysis of mitosis

Larval brains were dissected, fixed, and squashed as described in Williams *et al*. (1992), except that incubation in 3.7% formaldehyde was decreased to 20 min. Incubations with antibodies were done overnight at 4°C in phosphate saline buffer (PBS) containing 0.1% Triton X (PBT). Primary antibodies were rabbit anti-Phosphohistone H3 (Upstate, Charlottesville, VA) used at a 1:500 dilution and mouse anti-α-Tubulin (Upstate, Charlottesville, VA) at a 1:100 dilution. Brains were incubated in primary antibody overnight at 4˚C. These primary antibodies were detected by the following secondary antibodies: TRITC (tetrarhodamineisothiocyanate)-conjugated anti-rabbit IgG (Jackson Immunoresearch, West Grove, PA) and Cy2 (cyanine 2) conjugated anti-mouse IgG (Jackson Immunoresearch), both at a 1:500 dilution for 3 hrs at room temperature. DNA was detected by staining with 0.05 μg/ml Hoechst 33742 (Sigma, St. Louis, MO) in PBS for 5 minutes. Imaging was performed on an Olympus BX-50 microscope equipped with a Qimaging Retiga Exi CCD camera (Burnaby, BC, Canada) and MetaMorph 6.1 software (Universal Imaging, Downington, PA).

For aceto-orcein staining, larval brains were dissected in 0.7% NaCl and transferred immediately to a drop of aceto-orcein stain (2% orcein in 45% acetic acid) on a cover slip and squashed onto a glass slide (Gatti and Goldberg, 1991). In some experiments, brains were incubated in 0.5 x 10^{-5} M colchicine in 0.7% NaCl for 0.5, 1, or 2 hours after dissection prior to transfer to aceto-orcein. Mitotic indices were determined as previously described (Williams et al., 1992); briefly, the mitotic index of a sample was defined as the number of PH3-staining mitotic cells per standard field of view at 1000X.

RNAi

RNAi was done in Kc cells as described by Clemens *et al*. (Clemens et al.). Briefly, with a few minor changes, dsRNA was produced using the MEGAscript T3 & T7 High Yield Transcription Kits (Ambion, Austin, TX) according to the manufacturer's instructions. Primers used to amplify the cdc6 cDNA LD25083 clone were the same used by Kiger and colleagues (2003). This primer pair contained both T7 and T3 promoter sequence and gene specific sequences. Kc cells were propagated in HyQ-CCM3 media (HyClone, Logan, UT) and were diluted to a concentration of 1 x 10^6 cells/mL before plating 1 mL per well in 6 well plates. dsRNA was added to the cells to a concentration of 30 nM and immediately swirled for mixing. A final 2 mL of media were added, and the cells were allowed to grow for 3 days to allow for the turnover of protein products.

Cytology for analysis of Kc cells and RNAi

Cells were spun down in Eppendorf tubes and the excess supernatant aspirated away between each step before transfer to slides. One mL of cells in media was fixed in 3.7% formaldehyde in PBS for 15 min. Cells were then dehydrated by treating with 45% acetic acid for 30 sec, followed by 60% acetic acid for 3 min. All but 45 μL of the acetic acid was removed, and 20 μL of the resuspended solution was pipeted onto a clean coverslip. A slide was inverted onto the coverslip, and the sandwich was then squashed between filter paper to spread cells and chromosomes. Slides were placed in liquid nitrogen after squashing and then refixed in methanol for 2 min before being staining with Hoechst 33742 as described above.

RESULTS AND DISCUSSION

The B38 mutant phenotype is caused by mutations in the *Drosophila* homologue of *cell division cycle 6 (dcdc6)*

Initial mapping by our collaborators in the Gatti laboratory localized the mutation in the B38 stock to a 217.5 kb region between 66D8 and 66E2. Using recently created Exelexis and Drosdel deletions, which have well defined breakpoints, I was able to delimit this area to a region containing 21 genes (Figure A2.2 A). Lethal mutations in three of these genes complemented the B38 mutation, decreasing the number of possible genes to 18. Of these genes, CG5971 (*Drosophila melanogaster* homologue of *cell division cycle 6* (*cdc6)*) was chosen as a candidate gene and sequenced; this analysis revealed two missense mutations, E33K and Q222R in the B38-bearing chromosome. The E33K mutation is located in the cdc binding domain and is next to a possible site of phosphorylation, Serine 32 (Figure A2.3A,B). The change of a carboxyl group to an amine at amino acid position 33 conceivably could alter both charge and steric shape so as to disrupt phosphorylation of S32 and thus the function of cdc6.

In yeast, Cdc6 is known to bind the Origin Recognition Complex (ORC) and is thus regarded as one of the factors involved in replication initiation (Diffley, 1994; Lisziewicz et al., 1988). When bound by Clb2/Cdc28 at the cdc binding domain, Cdc6 becomes unable to assemble the pre-replication complex (pre-RC) and thus prevents over-replication (Mimura et al., 2004). Cdc6 also functions in the G2-mitosis checkpoint (Figure A2.3C) in combination with other proteins monitoring DNA damage (Lau et al., 2006; Lydall and Weinert, 1997). Cdc6 inhibits Cdc2 though the Wee1 pathway and must be degraded for entry into mitosis (Bueno and Russell, 1992).

Figure A2.2 B38 map and mitotic phenotype

(A) Modified from Flybase 2007. A gene map of the cytological region 66D8 to 66D15 of chromosome 3, the region containing the *cdc6* gene (CG5971). Deficiencies and genes in green represent deletions that complemented the B38 mutation, while ones in red represent deletions that failed to complement. The blue vertical lines delineate the region to where the mutation was delimited. Cdc6 is highlighted in pink. (B-D) Orcein staining of B38 brains showing precocious sister chromatid separation and lagging chromosomes in anaphase (arrow).

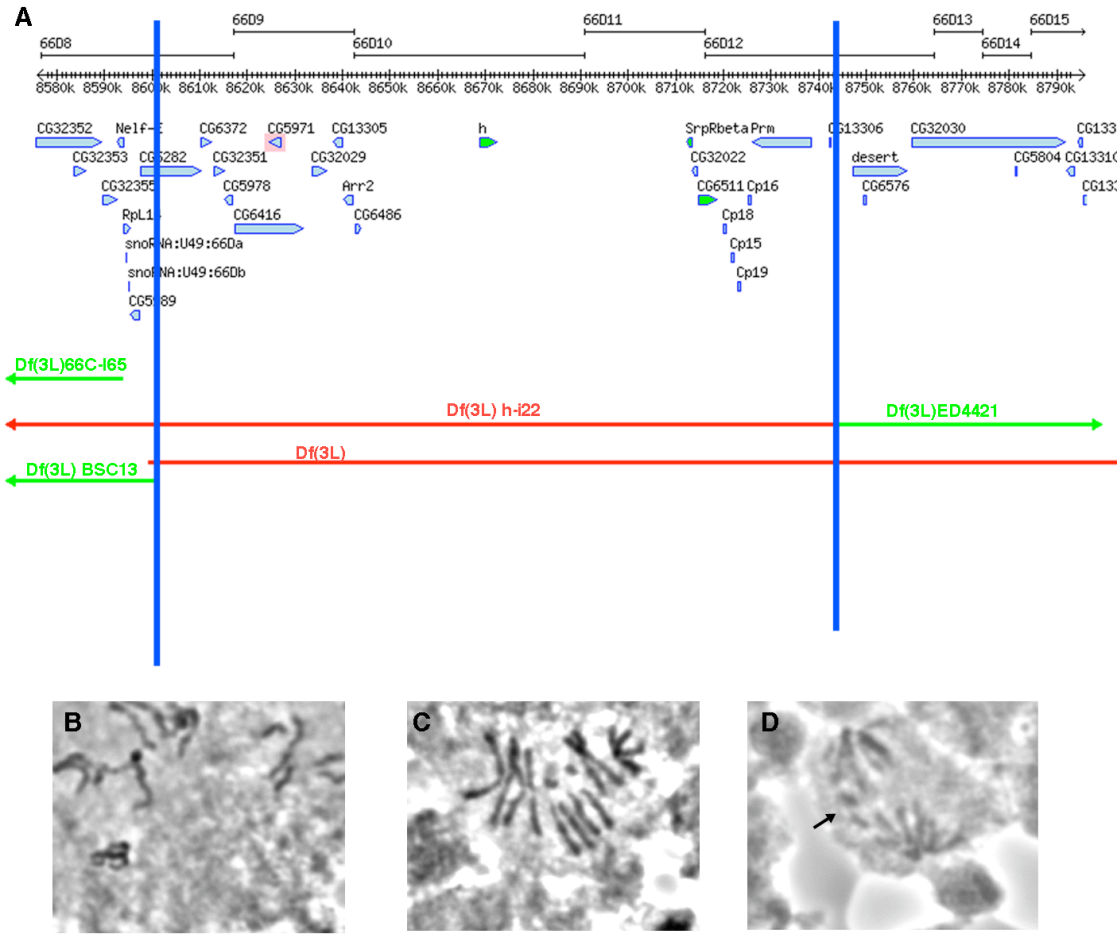
A
66D8
66D9
66D10
66D11
66D12
66D13
66D14
66D15
CG32352
CG32353
CG32355
RpL14
CG6282
CG32351
CG5978
CG6416
CG6372
CG5971
CG13305
CG32029
Arr2
CG6486
snoRNA:U49:66Da
snoRNA:U49:66Db
h
SrpRbeta
Prm
CG32022
CG6511
Cp16
Cp18
Cp15
Cp19
CG13306
CG32030
desert
CG6576
CG5804
Df(3L)66C-l65
Df(3L) h-i22
Df(3L)ED4421
Df(3L)
Df(3L) BSC13
B
C
D

Figure A2.3 Homologs of *cdc6* and the nature of the B38 mutation

(A) Homologs of the cdc6 gene. Regions in purple show the highly conserved cdc6 binding domain. Red lines mark known sites of phosphorylation and the red triangle represents a putative site of phosphorylation in *Drosophila*. Positions of the two amino acid substitutions associated with the B38 allele are shown. (B) The glutamic acid to lysine substitution caused by the B38 mutation could be sufficient to disrupt the S32 putative phosphorylation site. (C) cdc6 acts both in the G2-M checkpoint maintenance and clamp loading of the DNA replication machinery at the beginning of S phase.

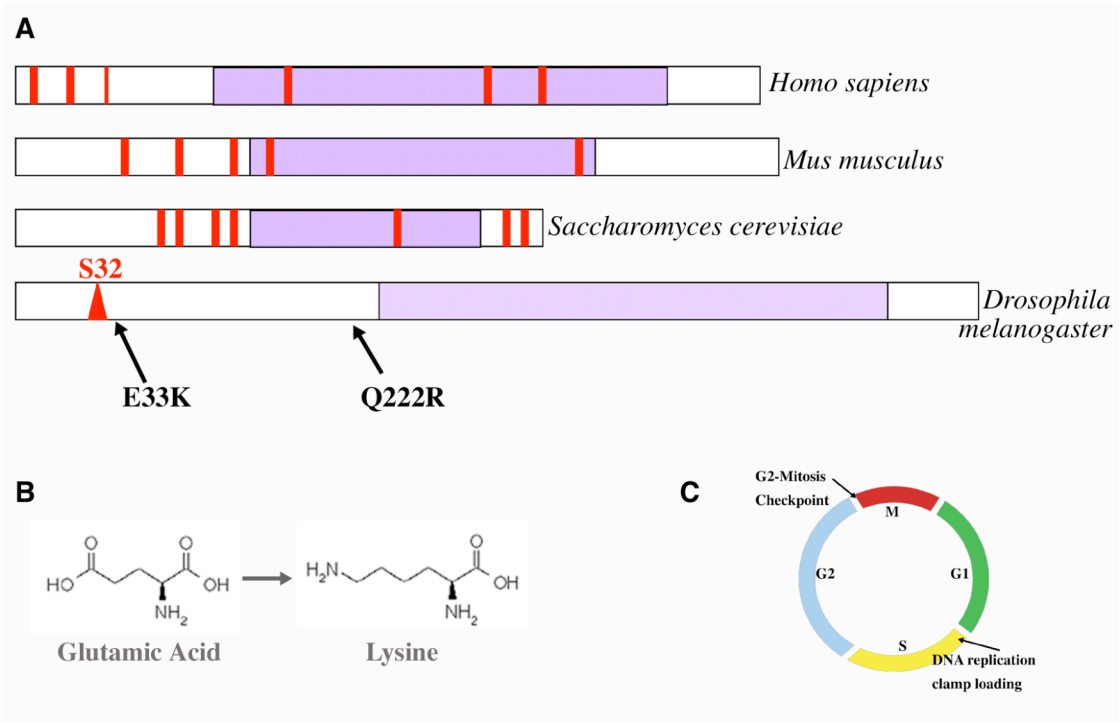
A
Homo sapiens
Mus musculus
Saccharomyces cerevisiae
S32
Drosophila melanogaster
E33K
Q222R
B
Glutamic Acid
Lysine
C
G2-Mitosis Checkpoint
M
G1
S
G2
DNA replication clamp loading

In *Drosophila* no research has been published on *cdc6*; B38 thus appears to be the first known mutant allele of this gene. Our observations show that this allele is third instar lethal and results in brains with a high mitotic index. Even though the mitotic index is almost double that of WT at $1.17_{+/-0.24}$, the size of the brains is essentially normal, suggesting that the cells are not over-proliferating but are instead becoming arrested in mitosis. When individual mitotic cells are observed, it is not a surprise that they are unable to undergo proper mitotic divisions. Many neuroblasts in mutant brains are highly aneuploid and have under-condensed DNA (Figure A2.2 B-D). Even in cells that have proper chromosomal numbers (Figure A2.2B), the chromosomes appear under-condensed. Usually cells get arrested in metaphase, but I presume that in this case, the cells are arrested in a G2/prophase-like state. Also, when dissected brains are treated with colchicine (a mitotic drug which arrests cells in metaphase), it becomes apparent that sister chromatids have separated precociously. Not surprisingly (given the apparent G2/prophase arrest), less than half of the normal frequency of anaphases was observed, and 86% of these anaphases showed clear evidence of misbehavior such as lagging chromosomes (Figure A2.2D).

To look further at the function of Cdc6 in *Drosophila*, we utilized RNAi to eliminate the protein in Kc cells. Three days of this treatment resulted in a high level of cell death.

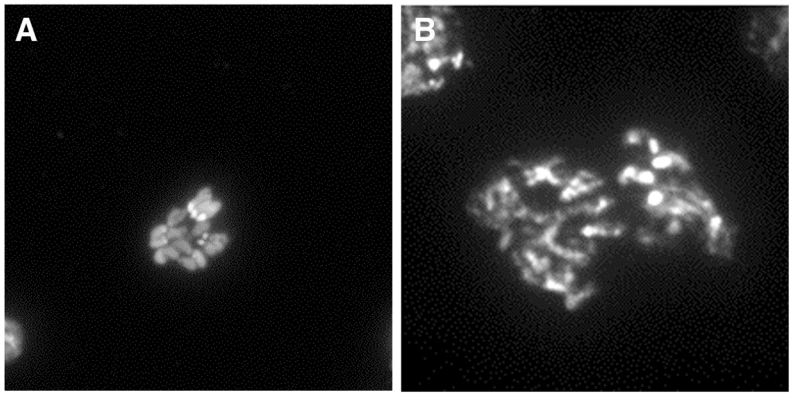

Figure A2.4 *cdc6* RNAi causes under-condensation in Kc cells.

(A) Wild type cells stained with DAPI for DNA show normal DNA condensation in mitosis. (B) Kc cells treated with *cdc6* RNAi fail to condense properly and are likely also polyploid.

Although we do not have an antibody to verify the knockdown of dCdc6, the extreme phenotype suggests a severe decrease in protein levels, since no other control RNAi done at the same time caused cellular lethality. Cells that remained alive showed a high level of aneuploidy and under-condensed chromosomes (Figure A2.4A-B), consistent with the phenotype observed in brain neuroblasts. This finding strengthens the argument that mutation of the *dcdc6* gene indeed causes the mitotic effects observed in the B38 mutant stock.

The MA41 mitotic phenotype is likely caused by a mutation in *DNA polymerase-delta*

My results indicate that, similar to the B36 mutation, MA41 is caused by a mutation in a gene whose product is essential for DNA replication. The MA41 mutant was characterized as a mitotic mutant due to its low mitotic index of $0.37_{+/- 0.11}$ [slightly over half of the wild type value ($0.67_{+/- 0.06}$)], a high frequency of anueploid cells, under-condensed chromosomes, and a high frequency of chromosomes with broken arms. By deficiency mapping, I narrowed the region containing the causative mutation to 71F1-72D10, a 540 kd region containing 19 genes (Figure A2.5A). Of these genes, DNA Polymerase delta (DNApol-δ) was a logical candidate for involvement with the phenotype. Sequencing confirmed that the MA41-bearing chromosome contains a point mutation within this gene that causes a C496Y amino acid replacement.

Drosophila DNApol-δ shares high homology with, and probable orthology to, its mammalian counterpart (Aoyagi et al., 1994). Using purified DNApol-δ in biochemical assays, Aoyagi and colleagues (1994) proposed that in

Drosophila DNApol-δ is essential for leading strand elongation during replication; they also concluded that it functions also as a proofreading exonuclease. Since the MA41 mutants are not embryonic lethal, it is unlikely that this allele of *DNApol-δ* is completely non-functional. Also, the broken chromosome morphology as well as anueploidy in mutants (Figure A2.5B-F) suggests that the lesion more likely disrupts the proofreading activity of DNApol-δ. As DNA breaks and mutations build up in the cells, loss of chromosome arms would become visible and would also affect the ability of chromosomes to properly segregate to their respective daughter cells (Figure A2.5A,C). Checkpoints for DNA damage during replication would also explain the low level of cells entering mitosis. Presumably the operative checkpoint in this case would be that regulating the transition between the S and G2 phases of the cell cycle.

Also of note, I found that the previously identified mutation *l(3)72Ac*^{10}, which maps to the same region, failed to complement MA41, suggesting that it constitutes a second allele of *DNApol*-δ. No sequencing of the gene in this mutant strain has yet been done, but if an additional aberration in the gene is found, this would constitute strong evidence for the identity of the mutant phenotypes with *DNApol*-δ.

Future characterizations of the putative *DNApol*-δ mutations as well as *cdc6(B38)* are being conducted by Dr. Tim Christensen (East Carolina University) in connection with their effect on the replication initiation factor Mini chromosome maintenance 10 (Mcm10).

Figure A2.5 MA41 map and mitotic phenotype

(A) Modified from Flybase 2007. A gene map of the cytological region 72A5 to 72D1 of chromosome 3, the region containing the *DNApol-δ* gene. Deficiencies and genes in green complemented the MA41 mutation, while deletions in red failed to complement MA41. The blue vertical lines delineate the region to where the mutation was delimited. *DNApol-δ* is highlighted in pink. (B,C) Orcein stained MA41 brains show lagging chromosomes in anaphase (arrows) and over condensed and polyploid DNA in metaphase. (D,E) DNA staining shows a similar phenotype to orcein staining, but Tubulin staining appears normal, suggesting that improper spindle formation is not the cause for the mitotic arrest seen in the MA41 mutant strain.

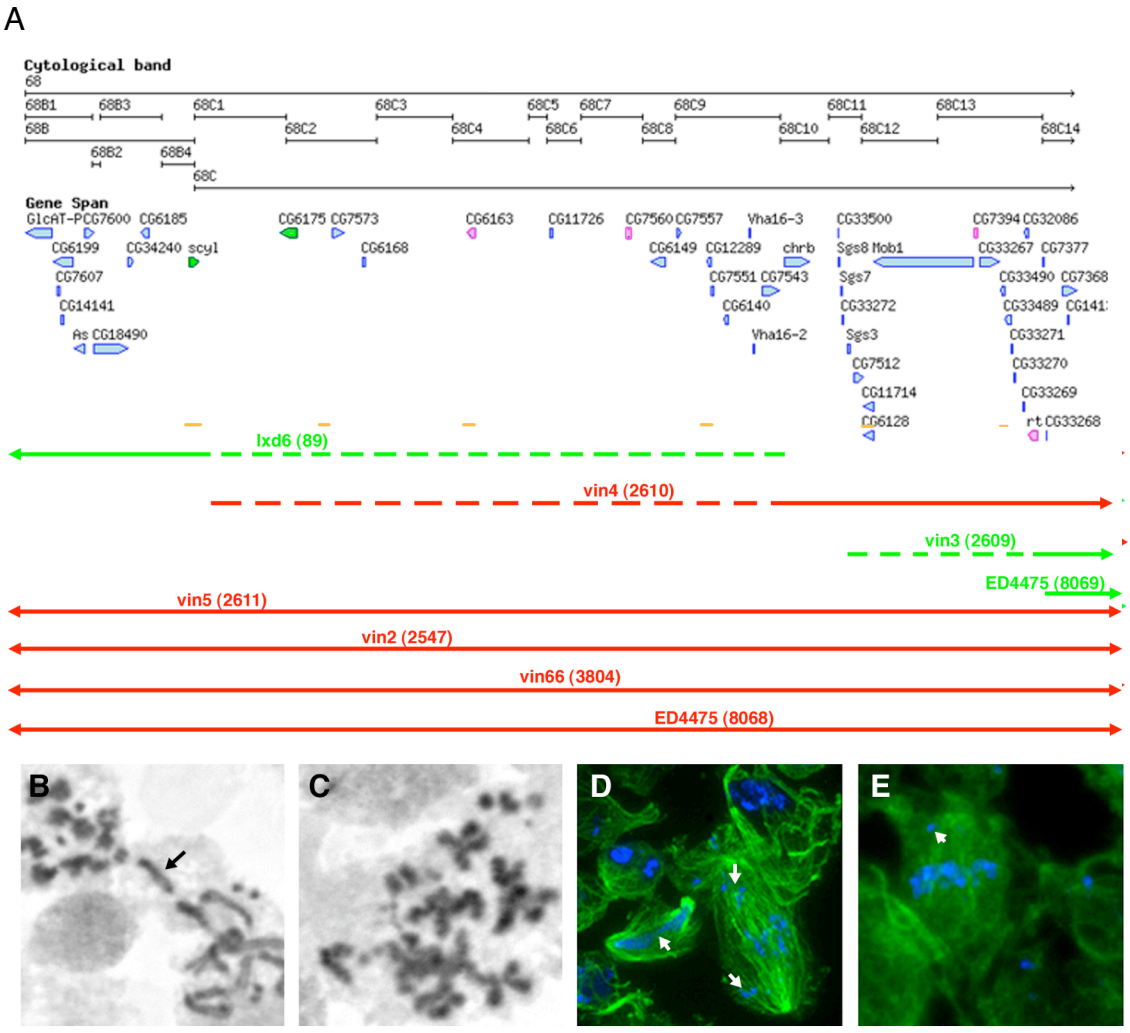
A
Cytological band
68
68B1
68B3
68C1
68C3
68C5
68C7
68C9
68C11
68C13
68B
68C2
68C4
68C6
68C8
68C10
68C12
68C14
68B2
68B4
68C
Gene Span
GlcAT-PCG7600
CG6185
CG6175
CG7573
CG6163
CG11726
CG7560
CG7557
Vha16-3
CG33500
CG7394
CG32086
CG6199
CG34240
scyl
CG6168
CG6149
CG12289
chrb
Sgs8
Mob1
CG33267
CG7377
CG7607
CG7551
CG7543
Sgs7
CG33490
CG7368
CG14141
CG6140
CG33272
CG33489
As
CG18490
Vha16-2
Sgs3
CG33271
CG7512
CG33270
CG11714
CG33269
CG6128
rt
CG33268
lxd6 (89)
vin4 (2610)
vin3 (2609)
ED4475 (8069)
vin5 (2611)
vin2 (2547)
vin66 (3804)
ED4475 (8068)
B
C
D
E

The M374 mutation causes high levels of polyploidy

The M374 mutation maps somewhere between 68A8 and 68C6 (Figure A2.6A). Unfortunately, this 470 kb region is sparse in deficiencies, known lethal genes, and even known transcriptional units. We first tested candidate genes in the *no optic lobe* family, since they have known alleles exhibiting mitotic defects that prevent proliferation of the optic lobes (Koizumi, 1995); however, none of these genes contained mutations in their coding sequences in the M374 strain. Of course, it is still possible that one of these genes is responsible for the phenotype and that the mutation is in a regulatory region; however, this possibility is difficult to determine from sequence information alone. In the future, fine scale P-element mapping might be used to narrow down the region responsible, perhaps to a single gene.

Despite our failure to locate the gene responsible for the M374 phenotype, the mutant deserves mention due to the extreme polyploidy seen in brain cells (Figure A2.6B-D). Cells with a hundred or more chromosomes are common, and the majority of cells display at least some degree of polyploidy and chromosomes that appear over-condensed. The extreme polyploidy suggests that these cells are capable of exiting mitosis without completing cell division and yet are competent to complete another round of the cell cycle; it is likely that cytokinesis is affected. Over-condensation is common in mutants that arrest in metaphase, since the chromosomes continue to condense throughout this stage. In the future, visualizing the spindle with antibodies against Tubulin will allow us to get a better idea of how mitosis is progressing, particularly during telophase and cytokinesis. Similarly, the use of GFP marked histones and live imaging (Yu et al., 2004) would provide more clues to mitotic progression in this mutant.

Figure A2.6 M374 map and mitotic phenotype

(A) Modified from Flybase 2007. A gene map of the cytological region 68A7 to 68C7 of chromosome 3, the region containing the as-yet unidentified M374 mutation. Deficiencies and genes in green complemented the M374 mutant, while deletions in red failed to compliment. The blue vertical lines delineate the region to where the mutation was delimited. (B-D) Orcein staining of M374 brains showing the high levels of polyploidy in most of the mitotic cells.

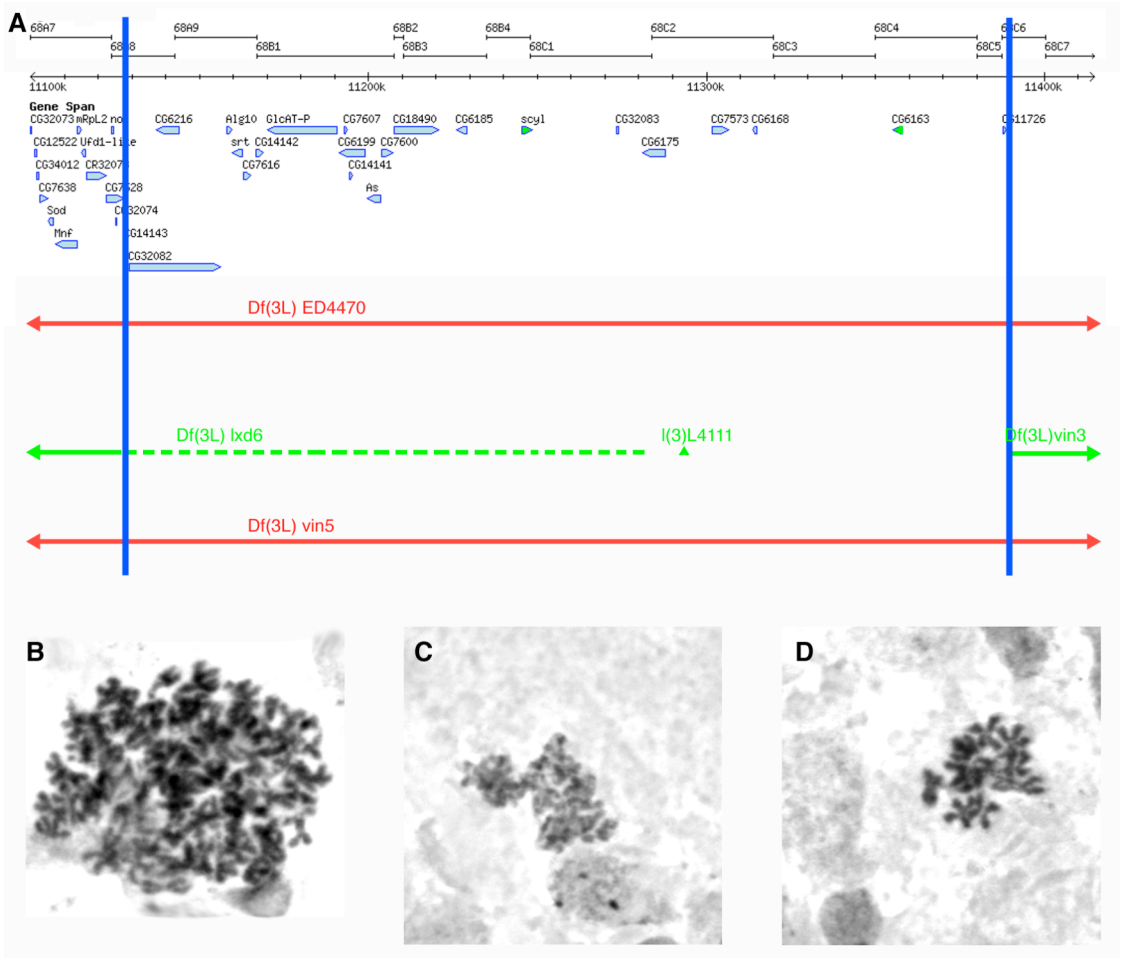
A
68A7
68A8
68A9
68B1
68B2
68B3
68B4
68C1
68C2
68C3
68C4
68C5
68C6
68C7
11100k
11200k
11300k
11400k
Gene Span
CG32073 mRpL2 no
CG12522 Ufd1-like
CG34012 CR32075
CG7638
CG7628
Sod
CG32074
Mnf
CG14143
CG32082
CG6216
Alg10
GlcAT-P
CG7607
CG18490
CG6185
scyl
srt
CG14142
CG7616
CG6199
CG7600
CG14141
As
CG32083
CG6175
CG7573
CG6168
CG6163
CG11726
Df(3L) ED4470
Df(3L) lxd6
l(3)L4111
Df(3L)vin3
Df(3L) vin5
B
C
D

MA9 mutants have small fragile brains with very few cells in mitosis

Originally, the MA9 mutation appeared to map to the region between 87F12-F15 and 88A1 on chromosome 3. However, using newly developed deficiencies with more precise endpoints, I was able to remap the gene to the region 88B1-88C1 (Figure A2.7B). This region is 110 kb long and contains 12 genes (Figure A2.7A). No candidate genes were sequenced in this region, and the identity of MA9 remains unknown.

The MA9 homozygous mutants have small brains that are very fragile when dissected. In squashed preparations, orcein staining revealed a mitotic index of only 0.19, less than 1/3 of the wild-type value. The cells that were in M-phase appeared morphologically normal, although I observed some apparently improper chromosome condensation. Interestingly, similar to the *trus* mutants, these larvae spend an extended time as larvae, although this delay has never been quantified. It is possible that these mutants also have a developmental hormone signaling deficiency, thus explaining their low mitotic index and lack of imaginal discs. If the developmental delay is indeed suggestive of a problem in the ecdysone pathway, it will be interesting to determine whether the phenotype can be rescued by feeding with ecdysone.

Figure A2.7 MA9 map and mitotic phenotype

(A) Modified from Flybase 2007. A gene map of the cytological region 88B1 to 88C1 of chromosome 3, the region containing the currently unidentified MA9 mutation. Deficiencies and genes in green complemented the MA9 mutation, while deletions in red failed to complement. The blue vertical lines delineate the region to where the mutation was delimited. (B) Map of a larger area of chromosome 3 showing deletions that were used for complementation analysis to narrow MA9 to the region shown in panel A. (C-D) Orcein staining of MA9 brains showing the over-condensation phenotype.

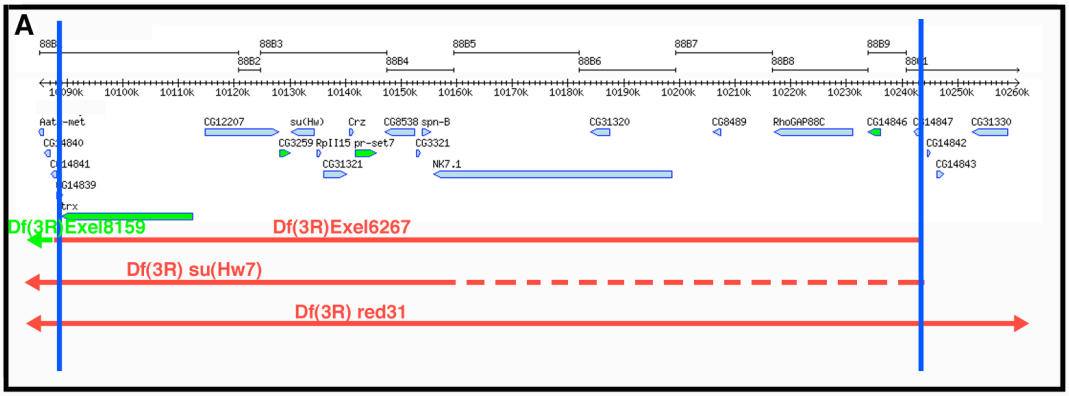
A
Df(3R)Exel8159
Df(3R)Exel6267
Df(3R) su(Hw7)
Df(3R) red31

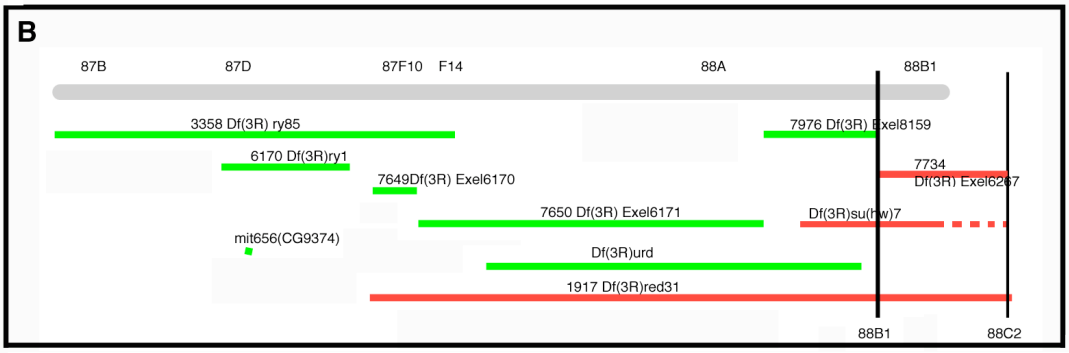
B
87B
87D
87F10
F14
88A
88B1
3358 Df(3R) ry85
7976 Df(3R) Exel8159
6170 Df(3R)ry1
7734
Df(3R) Exel6267
7649Df(3R) Exel6170
7650 Df(3R) Exel6171
Df(3R)su(hw)7
mit656(CG9374)
Df(3R)urd
1917 Df(3R)red31
88B1
88C2

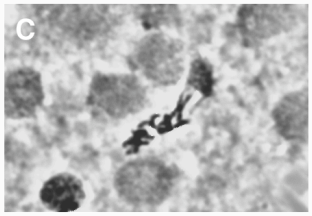
C

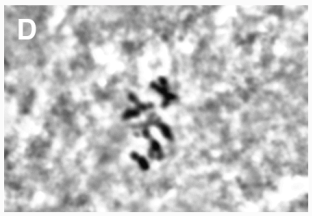
D

Mit1174 and M370x are likely alleles of Polo kinase

Dr. Verní previously mapped both Mit1174 and M370x to 77B2-6, a region of chromosome 3 containing 9 transcriptional units including the well-known mitotic gene *polo*. Both of these mutations complemented lethal alleles of *polo* in terms of viability, so it was originally believed that *polo* was not the gene responsible for the mutant phenotype. However, I repeated this complementation analysis and found that the transheterozygotes for either of the mutations and strong *polo* alleles were female sterile. Since alleles of *polo* can have separable functions (Riparbelli et al., 2000), it is likely that these two mutations represent new alleles of *polo.* However, the chromosomes carrying these mutations were never sequenced to verify this supposition.

CONCLUSION

The seven mutants I have described (including *trus*) illustrate the diversity of genes that, when mutated, can result in late larval lethality and the inability to complete the cell cycle properly.

LITERATURE CITED

Aoyagi, N., Matsuoka, S., Furunobu, A., Matsukage, A. and Sakaguchi, K. (1994). Drosophila DNA polymerase delta. Purification and characterization. *J Biol Chem* **269**, 6045-50.

Baker, B. S., Smith, D. A. and Gatti, M. (1982). Region-specific effects on chromosome integrity of mutations at essential loci in Drosophila melanogaster. *Proc Natl Acad Sci U S A* **79**, 1205-9.

Bueno, A. and Russell, P. (1992). Dual functions of CDC6: a yeast protein required for DNA replication also inhibits nuclear division. *Embo J* **11**, 2167-76.

Clemens, J. C., Worby, C. A., Simonson-Leff, N., Muda, M., Maehama, T., Hemmings, B. A. and Dixon, J. E. (2000). Use of double-stranded RNA interference in Drosophila cell lines to dissect signal transduction pathways. *Proc Natl Acad Sci U S A* **97**, 6499-503.

Diffley, J. F. (1994). Eukaryotic DNA replication. *Curr Opin Cell Biol* **6**, 368-72.

Foe, V. E. and Alberts, B. M. (1983). Studies of nuclear and cytoplasmic behaviour during the five mitotic cycles that precede gastrulation in Drosophila embryogenesis. *J Cell Sci* **61**, 31-70.

Gatti, M. and Goldberg, M. L. (1991). Mutations affecting cell division in Drosophila. *Methods Cell Biol* **35**, 543-86.

Kiger, A. A., Baum, B., Jones, S., Jones, M. R., Coulson, A., Echeverri, C. and Perrimon, N. (2003). A functional genomic analysis of cell morphology using RNA interference. *J Biol* **2**, 27.

Koizumi, K., Nakao, K., Hotta, Y. (1995). no optic lobe, gene that is essential for larval neurogenesis. In *A. Dros. Res. Conf.*, vol. 36 (ed., pp. 333B. Bathesda, MD, USA.

Koundakjian, E. J., Cowan, D. M., Hardy, R. W. and Becker, A. H. (2004). The Zuker collection: a resource for the analysis of autosomal gene function in Drosophila melanogaster. *Genetics* **167**, 203-6.

Lau, E., Zhu, C., Abraham, R. T. and Jiang, W. (2006). The functional role of Cdc6 in S-G2/M in mammalian cells. *EMBO Rep* **7**, 425-30.

Lisziewicz, J., Godany, A., Agoston, D. V. and Kuntzel, H. (1988). Cloning and characterization of the Saccharomyces cerevisiae CDC6 gene. *Nucleic Acids Res* **16**, 11507-20.

Lydall, D. and Weinert, T. (1997). G2/M checkpoint genes of Saccharomyces cerevisiae: further evidence for roles in DNA replication and/or repair. *Mol Gen Genet* **256**, 638-51.

Mimura, S., Seki, T., Tanaka, S. and Diffley, J. F. (2004). Phosphorylation-dependent binding of mitotic cyclins to Cdc6 contributes to DNA replication control. *Nature* **431**, 1118-23.

Riparbelli, M. G., Callaini, G. and Glover, D. M. (2000). Failure of pronuclear migration and repeated divisions of polar body nuclei associated with MTOC defects in polo eggs of Drosophila. *J Cell Sci* **113 (Pt 18)**, 3341-50.

Williams, B. C., Karr, T. L., Montgomery, J. M. and Goldberg, M. L. (1992). The *Drosophila zw10* gene product, required for accurate mitotic chromosome segregation, is redistributed at anaphase onset. *J Cell Biol* **118**, 759-73.

Yu, J., Fleming, S. L., Williams, B., Williams, E. V., Li, Z., Somma, P., Rieder, C. L. and Goldberg, M. L. (2004). Greatwall kinase: a nuclear protein required for proper chromosome condensation and mitotic progression in Drosophila. *J Cell Biol* **164**, 487-92.